POLAROGRAPHIC AND NUCLEAR MAGNETIC RESONANCE

Studies of Some Metal-Amino-polycarboxylic Acid Complexes.

A thesis submitted to the Faculty
of Graduate Studies and Research
of the University of Manitoba
in partial fulfillment of
the requirements for the degree
DOCTOR OF PHILOSOPHY

by

Peter Letkeman B.Sc.(Hons.) '60 M.Sc. '61

August, 1969

c Peter Letkeman 1969

THE UNIVERSITY
LIBRARY
OF MANITOBA

To my Mother

ACKNOWLEDGEMENTS

I wish to thank Dr. J. B. Westmore for his continuous advice and encouragement given during the course of this work. The research topic was suggested by Dr. H. D. Gesser.

I would like to express my gratitude to the National Research Council for financial assistance in the form of summer stipends. I am also indebted to the Brandon University which purchased a Sargent Model XXI Polarograph for this study.

Mr. George Epp is thanked for the construction of a number of H-cells. Mr. R. Fitch and Mr. R. Dickinson are thanked for their assistance in obtaining the N.M.R. spectra. Dr. H. M. Hutton and Dr. B. B. Smith provided helpful discussions on the interpretation of the N.M.R. spectra.

ABSTRACT

ABSTRACT

The polarography of cadmium and lead complexes of diethylenetriaminepentaacetic acid has been studied in an aqueous medium from pH = 2.00 to 9.00 at 25.0°C and with an ionic strength of 0.20 M. Three distinct types of polarographic behavior were noted as the pH range was spanned. The first wave (Wave A) was reversible, i.e. the reduction of the free metal for which the following mechanism was postulated for the lead complex,

$$PbH_2A^- \rightleftharpoons Pb^{++} + H_2A^=$$

and

$$CdH_2A^- + H^+ \rightleftharpoons Cd^{++} + H_3A^=$$

for the cadmium complex. Wave A for both metal complexes was kinetically controlled when its height was small ($i_\ell < 1.0\mu A$) compared to the overall reduction wave height. The second wave (Wave B) was irreversible, not diffusion controlled but kinetically controlled, as indicated by temperature and pressure studies. The reduction mechanism postulated for both complexes was

$$\underset{\text{(reducible)}}{MH_2A^-} \rightleftharpoons \underset{\text{(non-reducible)}}{MHA^=} + H^+$$

where the doubly protonated complexes (CdH_2A^- and PbH_2A^-) were the electroactive species. The third wave (Wave C) was also irre-

versible and kinetically controlled. The mechanism postulated for both metals (same mechanism) was:

$$\underset{\text{(reducible)}}{MHA^{=}} \rightleftharpoons \underset{\text{(non-reducible)}}{MA^{\equiv}} + H^{+}$$

The individual rate constants for the various mechanisms have been calculated. The stability constants for the various metal complexes were calculated from $E_{1/2}$ data and are summarized below:

$\log K_{CdA} = 19.15$	$\log K_{PbA} = 19.10$
$\log K^{H}_{CdHA} = 2.95$	$\log K^{H}_{PbHA} = 4.05$
$\log K^{H}_{CdH_2A} = 2.95$	$\log K^{H}_{PbH_2A} = 3.40$
$\log K^{H}_{CdH_3A} = 2.73$	$\log K^{H}_{PbH_3A} = 2.75$

A nuclear magnetic resonance study of both Cd-DTPA and Pb-DTPA was also undertaken. These studies were carried out in an aqueous medium from pH = 2.00 to 10.00 at 0, 38, and 72°C with an ionic strength of approximately 2.5 M. The protonation of both metal complexes was studied and structures were postulated for each. From the N.M.R. data, the relative life-time was estimated for an individual metal-ligand bond. Both investigations indicated that the doubly and triply protonated complexes play an important role in the co-ordination chemistry of metal-DTPA chelates.

TABLE OF CONTENTS

TABLE OF CONTENTS

LIST OF TABLES

ILLUSTRATIONS

CHAPTER 1

INTRODUCTION

Polyaminopolycarboxylic acids have become one of the most important classes of complex forming agents known to the analytical chemist. Ethylenediaminetetraacetic acid (EDTA) was introduced in 1947 by Schwarzenbach[1], and its applications to analytical methods were clearly documented by Welcher[2], Pribil[3], Flaschka[4], and Schwarzenbach[5]. By now (1969) there are some 1500 papers in the literature on this compound alone.

EDTA

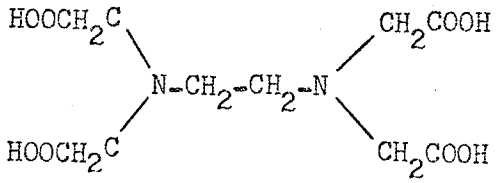

The next higher homologue of EDTA, i.e. diethylenetriaminepentaacetic acid (DTPA) was first examined by Wanninen[6] in 1955. He found that it would complex with the alkaline earths to a larger degree than EDTA. This generated a lot of interest for more research in this field, as evidenced by the papers of Durham[7] et al, Frost[8] et al, and Chaberek[9-11] et al, to mention a few.

DTPA

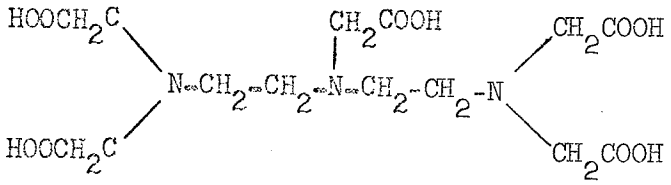

In 1956, Frost[8] reported the synthesis of triethylenetetraaminehexacetic acid (TTHA). Some five years later Pribil[12] used TTHA as a

titrating agent, followed by such workers as Bailar[13] et al, Grimes[14] et al, and Martell[15] et al. It became evident however that the complexing ability of TTHA with transition and rare earth metals was less than that of DTPA.

TTHA

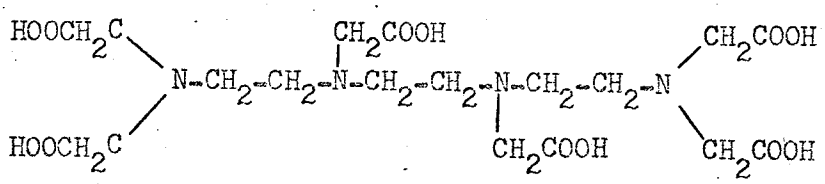

During this time the Geigy Chemical Co. in Basel, Switzerland had prepared a small quantity of tetraethylenepentaaminoheptaacetic acid (TPHA). This compound is extremely difficult to prepare and purify, hence little work has been done with it. Catch[16] and Jordan did complex Ce and Po with it, but found DTPA a better reagent for doing so. Academically, it should be a very interesting ligand because it has twelve co-ordinating positions as compared with ten for TTHA and eight for DTPA.

TPHA

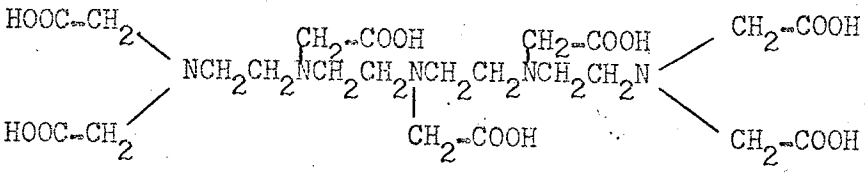

The cadmium EDTA complex has been studied polarographically by Koryta and Koesler[17] and Pecsok[18] who found no reduction wave for the complex. However Heyrovsky and Matyas[19] reported a doublet wave, and Tanaka[20] et al found a single wave. Schmid and Reilley[21] resolved these contradictory observations by studying the kinetic character of the reduction wave.

The cadmium DTPA complex had not been studied polarographically, although cadmium TTHA was investigated by Conradi.[22]

With this background it seemed worthwhile to systematically study the complexes of cadmium with DTPA. A second metal, e.g. lead was studied similarly. The polarographic technique was chosen because of its versatility in obtaining equilibria information and the relatively low concentrations of complexing agents required. The nuclear magnetic resonance technique was also applied to obtain further information on the structures of the metal complexes.

CHAPTER 2

THE POLAROGRAPHIC METHOD

A. Introduction

Voltammetry is a branch of electroanalytical chemistry that deals with the effect of the potential of an electrode in an electrolysis cell on the current flowing through it. The electrode whose potential is varied is the indicator electrode while the reference electrode remains at a constant potential.

Polarography is that branch of voltammetry in which a dropping mercury electrode (D.M.E.) is used as the indicator electrode though a number of modifications of this electrode are in use today. The D.M.E. is described fully in the experimental section. Its main advantage is that the drops of mercury coming out of the capillary tip are identical in size and growth rate with fresh mercury exposed to the solution every few seconds. Consequently the currents are perfectly reproducible from one drop to the next.

The polarographic method of analysis is based on the current-voltage curves arising at a microelectrode when diffusion is the rate-determining stage in the discharge of ions. The voltage necessary for the electrolysis indicates the nature of the reacting substance, while the current observed is a function of its concentration. The method is best applied to solutions having a concentration of electroreducible or electrooxidizable ions in the concentration range of 10^{-6} to 10^{-2} M. An accuracy of $\pm$ 1% may be expected in the range of 10^{-2} to 10^{-4} M, and only $\pm$ 5% below 10^{-4} M. From the current-voltage curves one can often determine unknowns qualitatively and quantitatively, half-wave potentials, equilibria

involved in the discharge process, kinetic rate constants and stability constants of complex ions.

In 1922 Heyrovsky[23] published his first results that led to the invention of a polarograph in 1925 with the help of Shikata. Heyrovsky coined the term "polarograph" to indicate that the instrument graphically records current-voltage curves obtained with a polarized electrode. In 1959 he was presented with the Nobel Prize in Chemistry for his contributions to the field of polarography.

There are well over 10,000 papers published in the field of polarography, along with a number of excellent books. A few of the well known text-books are written by Meites[24], Heyrovsky and Kůta[23], Lingane[25], Kolthoff and Lingane[26], Zuman and Kolthoff[27], Milner[28], Muller[29], Longmuir[30] and Delahay[31]. With this background of available literature the theory section of this paper will be kept to a minimum.

B. Basic Principles

A simple circuit diagram which could serve to obtain current-voltage curves with a dropping mercury electrode is shown in Figure 1. The solution under investigation is placed in the D.M.E. compartment of the H-cell, oxygen removed by bubbling nitrogen through the solution for 15 minutes and the capillary immersed in the test-solution. Figure 2 indicates the general arrangement of the H-cell and D.M.E. assembly. It consists of a mercury reservoir connected with neoprene tubing to the stand-tube, which in turn is connected to a piece of fine glass capillary tubing. The mercury reservoir above the lower end of the capillary is raised until the mercury drops fall into the solution at a rate of about one drop every 4 ± 2 seconds. The reference electrode (S.C.E.) is in electrical contact with the test solution via an agar plug and a sintered glass disc in the connecting arm. The S.C.E. is connected to the positive side of the battery via the slidewire contact. The D.M.E. functions as the cathode in Figure 1 though it may serve as the anode in other determinations. By keeping the D.M.E. quite small and the S.C.E. area relatively large, one keeps the potential of the S.C.E. constant while the D.M.E. is easily polarized, adopting the potential of the applied e.m.f. across the H-cell. A sensitive galvanometer is connected between the negative side of the battery and the D.M.E., and with the aid of the shunt a wide range of currents can be recorded by the galvanometer. Any desired voltage may be applied (0.0 to 3.0 v.) across the H-cell by merely adjusting the slide-wire contact appropriately. The galvanometer records oscillations between maximum and minimum values owing to the periodic change in

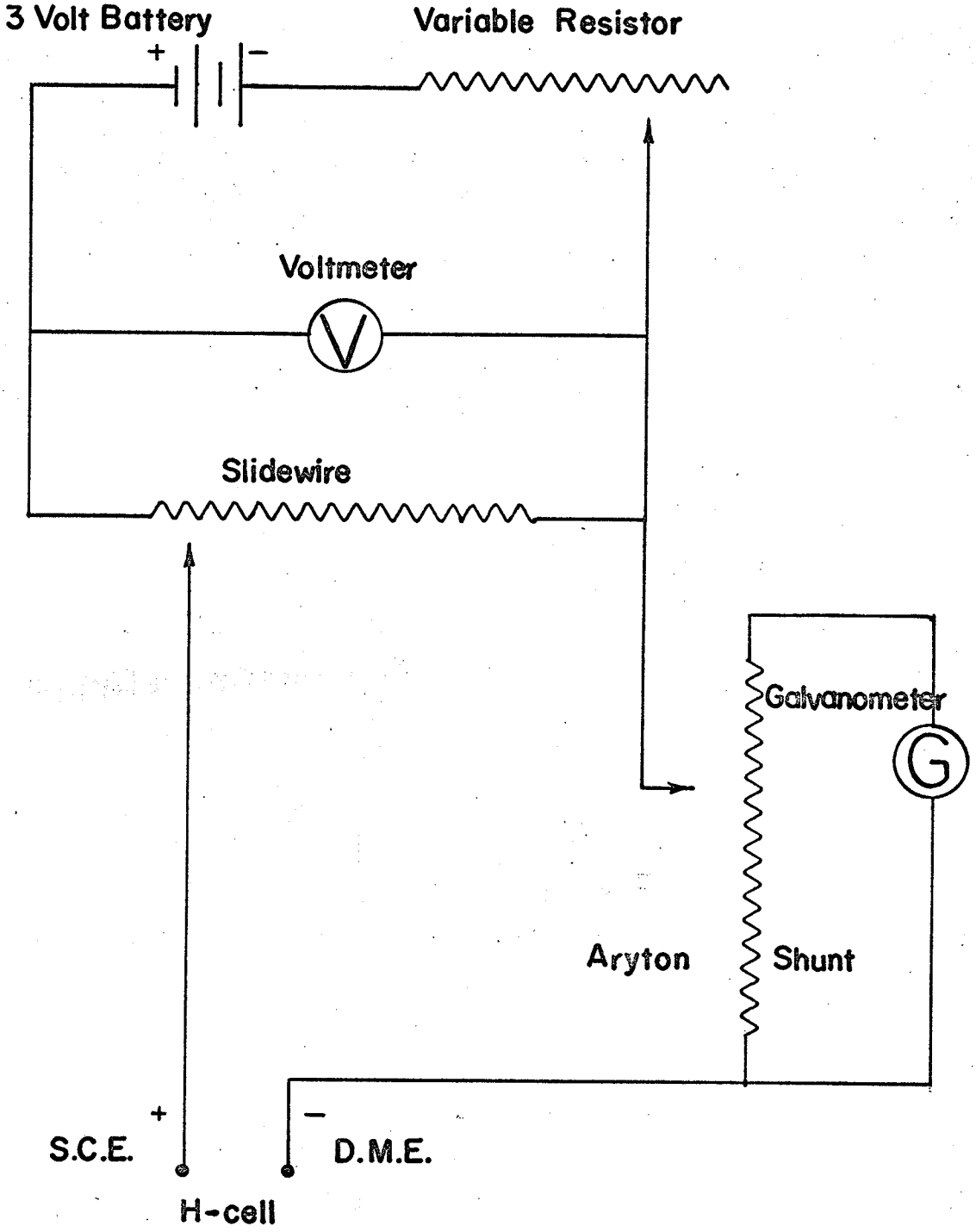

FIGURE 1 BASIC CIRCUIT FOR OBTAINING CURRENT-VOLTAGE CURVES POLAROGRAPHICALLY.

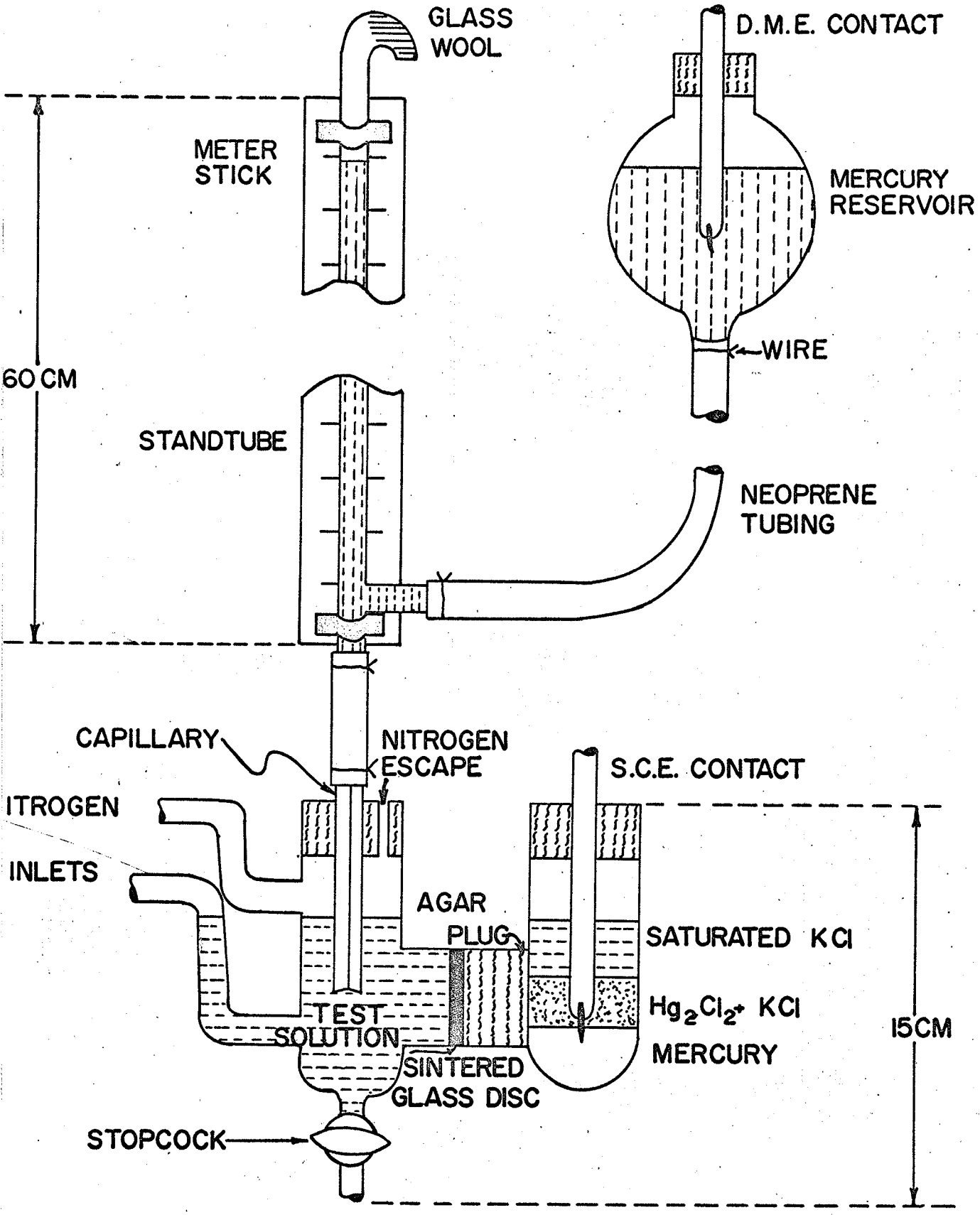

URE 2 THE H-CELL & D.M.E. ASSEMBLY

area of each drop as it grows and falls. In the present investigation a commercial polarograph was employed, in conjunction with a precision potentiometer to check all potentials recorded as shown in Figure 3.

The technique, therefore, is to gradually increase the potential difference across the two electrodes, and measuring small currents, of the order of microamperes, produced by the reduction of ions at the D.M.E. A typical current-voltage curve is shown in Figure 4 which illustrates the result of electrolyzing an oxygen-free solution of cadmium ions in a sodium perchlorate-acetic acid solution. At low potentials (below 0.55 v) from A to B virtually no current is flowing and hence nothing is reducing at the D.M.E. However the current sharply increases from B to D indicating that reduction is taking place. Since the solution is not stirred the current reaches a maximum plateau D to E quickly and a concentration gradient is established between the electrode surface and the bulk of the solution. To keep ions from migrating toward the D.M.E. a large excess of "background electrolyte" ($NaClO_4$) is added to the test solution and serves to conduct current without undergoing any electrode reaction. Hence the currents observed are due to the diffusion of Cd^{++} ions into the electrode layer. According to Fick's law the rate of diffusion of a particular ionic species is directly proportional to the concentration gradient of the solution. This is a characteristic property of a completely polarized electrode, and serves as the basis for quantitative analyses.

The conditions leading to the production of this limiting current plateau DE are explained as follows. At B cadmium ions in the D.M.E. layer

FIG. 3

THE EXPERIMENTAL SETUP

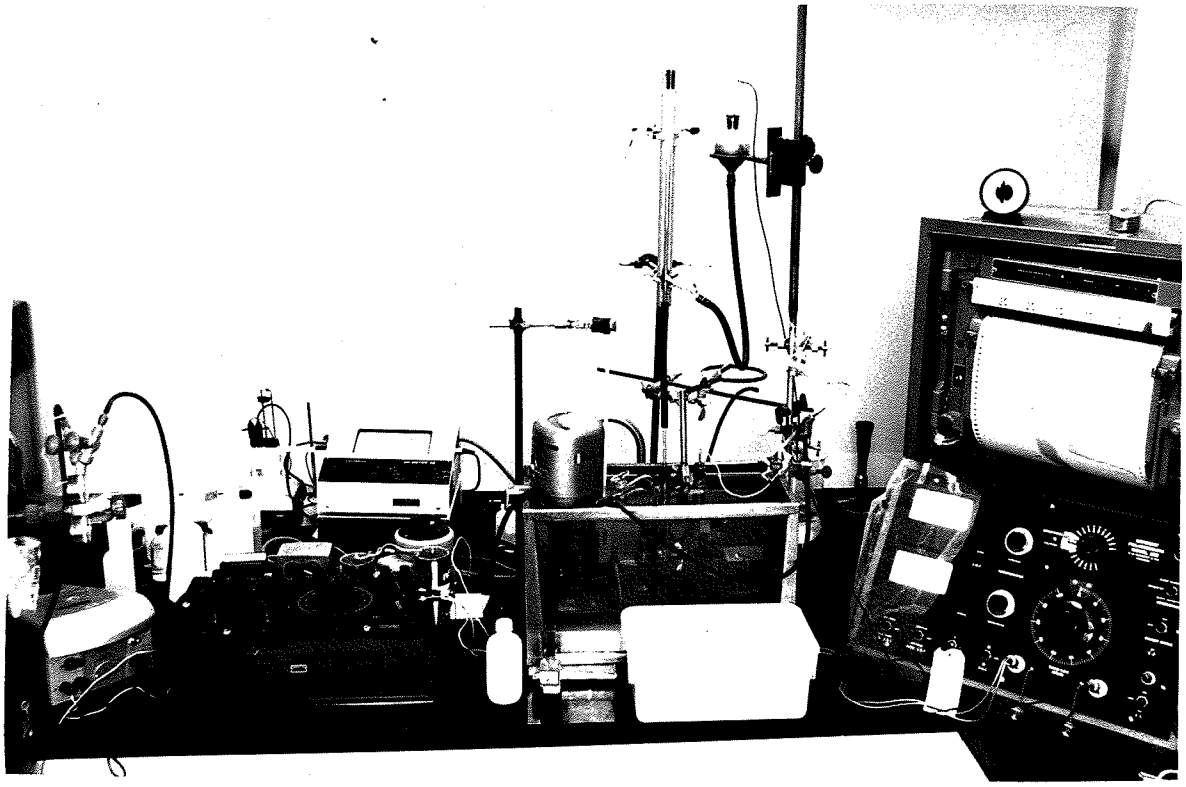

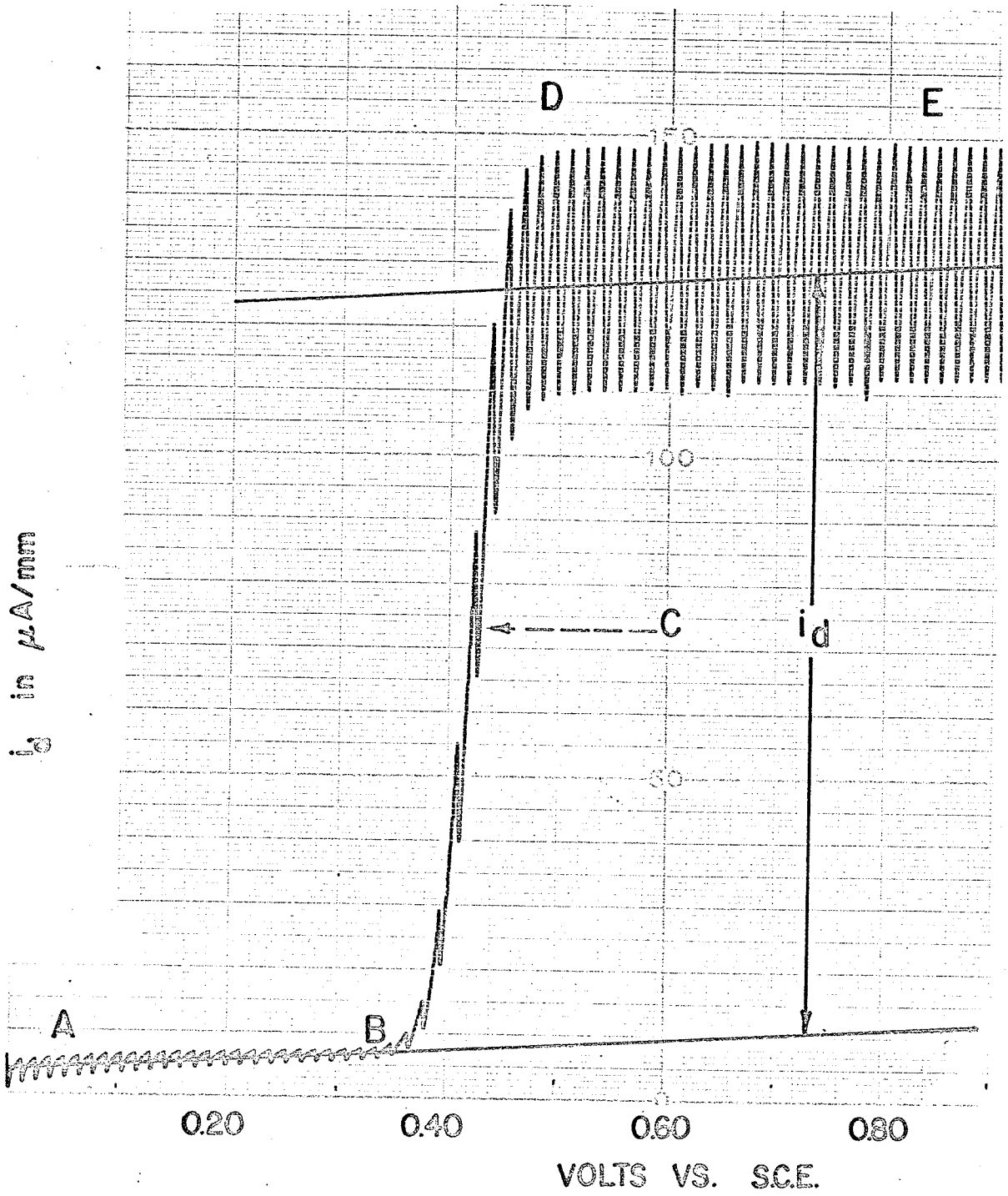

FIG. 4 A CURRENT - VOLTAGE CURVE

are reduced and dissolve in the mercury according to the expression

$$Cd^{++} + 2\bar{e} + Hg^{\circ} \longrightarrow Cd(Hg)$$

When the mercury drop falls away from the cathode the cadmium is removed as a weak amalgam. The cadmium thus lost is replenished by the diffusion of fresh ions from the bulk of the solution. At the anode the following reaction is occuring at the same time:

$$2Hg^{\circ} + 2Cl^{-} \longrightarrow 2\bar{e} + Hg_2Cl_2$$

As the applied e.m.f. is increased further the current quickly approaches a limiting value and becomes constant (apart from a slight increase due to the residual current) and independent of further e.m.f. increases. Under these circumstances a steady rate of diffusion is set up giving rise to the "diffusion current", i_d, as shown in Figure 4.

The potential of the point C on the current voltage curve at which the current is one-half of its limiting value is known as the half-wave potential, $E_{1/2}$, which in most instances is characteristic of an element, given the background electrolyte used. $E_{1/2}$ values are independent of the concentration of the reacting ions in solution, the size of the mercury drops and galvanometer sensitivity. Each species (electroreducible or electro-oxidizable) gives rise to a current voltage curve having its own particular half-wave potential and charts have been drawn up for a large number of substances in various background electrolytes by many different authors[23-25].

The choice of a background electrolyte is quite important for it may change the value of the half-wave potential substantially, as well as

the general nature of a polarogram. Essentially the background electrolyte should be one that does not interfere with the ions under investigation. Thus it should not cause any precipitation or absorption of the ions being studied, its cations should have a very negative $E_{1/2}$ value to avoid overlapping with the ions under observation, it should provide a medium where the observed ions are in one definite chemical form and in general provide well-defined and well-separated waves for all constituents. In practise very often a compromise must be reached between these desirable features and the chemical nature of the ions studied. The salts of the alkali, alkaline earth metals and of the mineral acids are used as background electrolytes because their decomposition potentials are about -1.6 to -2.2 volts with respect to the S.C.E., sufficiently negative not to interfere with most determinations. Various other electrolytes are used to eliminate the migration current and one example of such a collection is given by Meites[24].

A current voltage curve as shown in Figure 4 has a limiting current plateau DE made up of the residual current AB and the diffusion current i_d. Generally speaking the limiting current which is caused by an extreme state of concentration polarization by the depletion of electroactive substances at the D.M.E. may also contain contributions such as the migration current, kinetic currents, catalytic and absorption currents. Apart from these, "maxima" may occur as well as interference from dissolved oxygen in the solution under investigation. The cause and effect of each contributing current is briefly explained.

The residual current AB (see Figure 4) may be regarded as the sum

of a "condenser" current and a "faradaic" current. When a D.M.E. is placed in an "inert" electrolyte eg. (KCl) its potential can be varied from the oxidation of mercury (+.4v vs S.C.E.) to the discharge of potassium ions (-1.8v vs S.C.E.). This change of the potential of the mercury relative to the solution results only in a change in the charge density of the "electrical double layer" at the D.M.E. solution interface. The layer of negative charge at the surface of the electrode and the layer of positively charged solution adjacent to it constitute the so-called electrical double layer. There is no transfer of charge across it such as occurs in an electrochemical reaction. The interface thus behaves as an electrical condenser, the charge on one side being provided by an excess or deficit of electrons in the mercury, and on the other by an excess of cations or anions in the adjacent solution. At -0.46 volts vs S.C.E. mercury in a 1 molar potassium chloride solution has a "null potential" where the charge on either side of the double layer is zero, corresponding to a maximum in the interfacial tension. Hence this point is called the "electrocapillary maximum" of mercury in that solution. The presence of anions that tend to be absorbed on the mercury surface shifts the null point in a negative direction and absorbed cations cause an opposite shift. Whenever the D.M.E. has a potential different from this null potential a current must flow through the external circuit. This is required in order to provide the charge on the two sides of the interface, remembering that in the absence of any electrochemical process as the electrode, no charge can cross the interface. The average value

of the condenser or charging current is quite small, dependent on capillary characteristics and potential, with a slope of about 0.15 microamps per volt in the region of AB (see Figure 4). If one examines a complete polarogram of an inert electrolyte, there is an initial rise (oxidation of mercury) and a final rise (discharge of cation) apart from the region just examined, where even at the electrocapillary maximum the current is not zero. These phenoma are due to the occurrence of faradaic processes, which are quite independent of double layer charging. Traces of impurities in the background electrolyte account for the faradaic contribution at the electro capillary maximum. Hence one must be careful to use the best grade of chemicals available, or if necessary purify the chemicals as the determination requires. In practise the residual currents may be extrapolated and then subtracted from the limiting current, as shown in Figure 4, to yield the diffusion current.

The rate of diffusive transfer to the electrode depends directly on the concentration gradient at the surface of the electrode, or on the difference in concentration between the bulk of the solution and the electrode surface. As the applied potential is increased above the decomposition potential and the current rises from B to D (see Figure 4), the demand for the cadmium ions at the electrode increases, but its concentration at the electrode surface decreases. Consequently, the rate of diffusive transfer increases. Ultimately a condition is reached in which the cadmium ions are reduced as rapidly as they diffuse to the electrode surface, and its concentration at the D.M.E. sinks to a minimal value which remains

practically constant with further increase in potential. The rate of diffusive transfer, dependent on the difference in concentration between D.M.E. surface and the bulk solution, thus becomes constant, and correspondingly a diffusion-controlled limiting current results. In 1934, Ilkovic[3], in collaboration with Heyrovsky, succeeded in deriving the now famous equation which is the foundation of quantitative polarography. The relation is:

$$i_d = 607\ n\ D^{1/2}\ C\ m^{2/3}\ t^{1/6}$$

where n is the number of faradays of electricity per molar unit of electrode reaction, D the diffusion coefficient of electroactive substance, C is the concentration in millimoles per liter, m is the rate of mercury flow (mg/sec) and t is the drop time in seconds. The great virtue of the Ilkovic equation is that it accounts quantitatively for the influence of all the many factors which influence the diffusion current.

The migration current is known as that portion of the total current which is due to an electrical force that affects the rate at which electroactive ions reach the electrode surface. This increases as the transference number of the ion responsible for a wave increases, and it also depends on the charge carried by that ion. Cations are attracted to a negatively charged electrode, and thus the electrical force under these conditions leads to an increase of the limiting current, so that the migration current is positive. Exactly the opposite is true when the electroactive species is anionic. In either case the transference number can be reduced to a negligible value by addition of a background electrolyte, whose ions assist in conducting electricity through the solution. Hence

it is customary to carry out all polarographic measurements in the presence of a supporting electrolyte whose concentration is 0.1M or higher. The supporting electrolyte serves an additional purpose of decreasing the H-cell resistance to only a few hundred ohms, reducing the iR drop through the solution to a negligible value, thereby permitting one to equate the voltage applied from the external circuit to the potential difference between the D.M.E. and S.C.E.

The kinetic contribution to the limiting current may arise when an electroactive substance is formed from an inert species at a rate comparable to the diffusion rate. The classic example of a kinetic current is found for the reduction of pyruvic acid, $CH_3CO\ COOH$, which can be abbreviated to HA. The reaction is as follows:

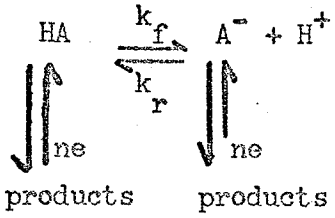

Only one wave is observed in strongly acidic medium, corresponding to the reduction of HA, two waves occur at intermediate pH values and only one wave for the basic region, corresponding to the reduction of the anion A^-. In general, the two waves in the intermediate pH range do not reflect the relative equilibrium concentrations of the undissociated acid HA or the anion A^- in the bulk of the solution. Instead, the first wave (due to HA) is relatively larger than the concentration of HA would warrant and yet not large enough to account for the equilibrium being completely shifted to the left. Hence it is concluded that this first wave is not

due to diffusion alone, but also affected by the rate at which H^+ combines with A^- to form HA. The second wave is affected by the rate of dissocation of the acid in a similar manner. Since rates of reaction are highly temperature dependent, more so than diffusion, these kinetic contributions may be identified by a temperature study. Secondly, kinetic currents are virtually independent of mercury pressure, quite different from a diffusion-controlled current, and lastly, they are dependent on pH and ionic strength. An example of a kinetic current is illustrated by the first wave in Figure 5. A thorough account of this situation will be given later because kinetic currents were observed in this study.

An example of a catalytic contribution to the limiting current is the reduction of ferric ions in presence of hydrogen peroxide. Hydrogen peroxide is only reduced at a very negative potential so that the iron reduction wave is well separated from it. However, with hydrogen peroxide present the ferric iron wave is much larger than in the absence of hydrogen peroxide. The explanation is obvious, i.e. the ferrous ions formed by reduction of ferric ion are oxidized back to the ferric ion by the hydrogen peroxide at the surface of the D.M.E., and so the freshly produced ferric ion is reduced again. Thus the limiting current of ferric ion is much greater than corresponds to the concentration of ferric ion in the bulk of the solution. If the rate constant of oxidizing ferrous to ferric ions were small, then the limiting current would be essentially diffusion controlled, and if the rate constant were large the limiting current would be proportional to the concentration of hydrogen peroxide in solution. For

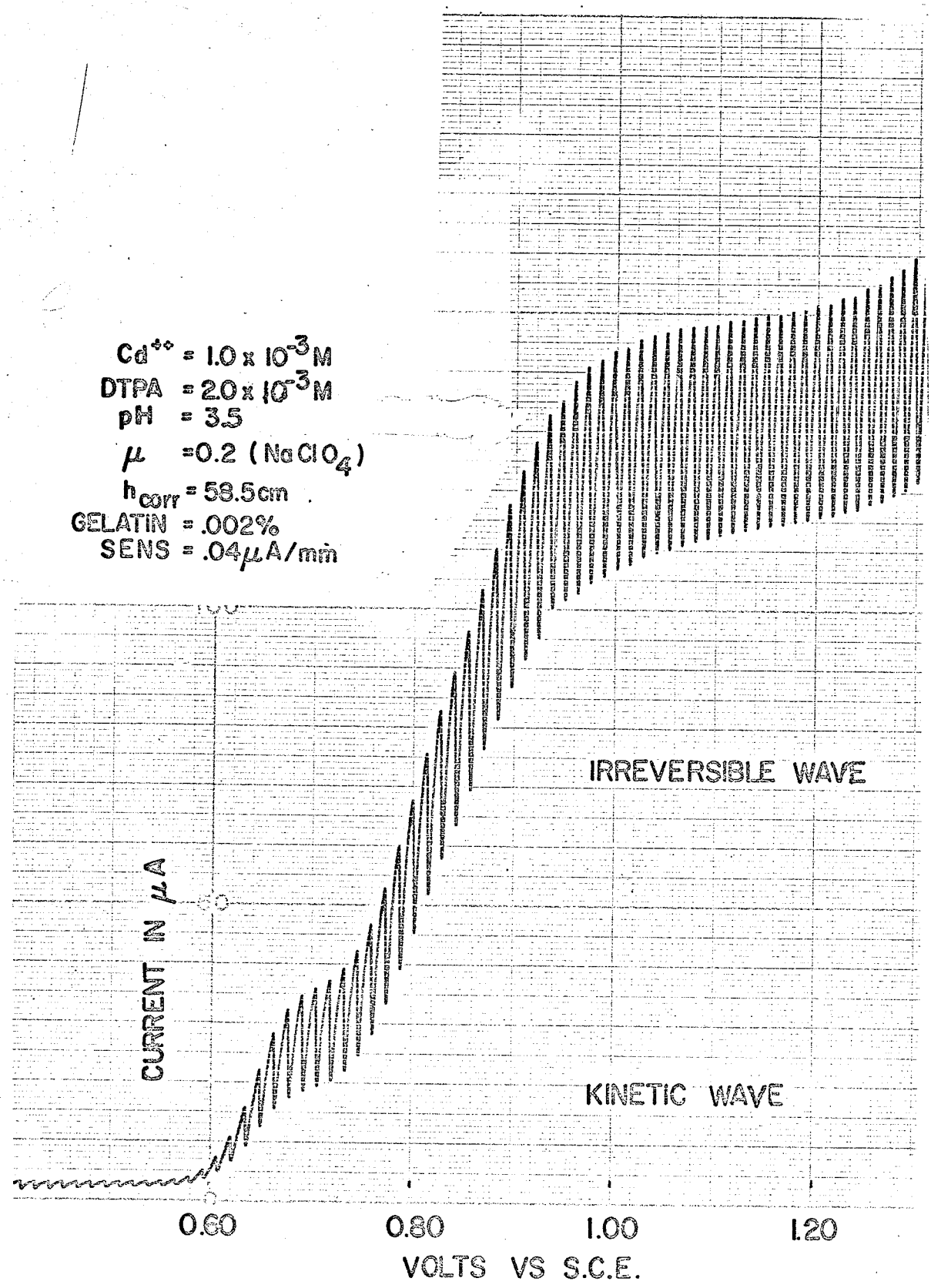

FIG. 5 A KINETIC WAVE AND AN IRREVERSIBLE WAVE

this Fe^{++} -Fe^{+++} case, the rate is intermediate and one can not relate wave height to ferric concentration directly. Though the heights of catalytic waves are sensitive to variations in pH, temperature and other experimental conditions, the use of a catalytic wave for analytical purposes may often be advantageous because of the high sensitivity that can be attained. Actually catalytic waves are useful especially in the determination of trace amounts of molybdate, vanadates and tungstates.

Absorption waves may be due either to the reactant electroactive species absorbed on the electrode (post-wave) or to the absorption of the product of the electrode reaction (pre-wave). If the reduced form is absorbed a small prewave of constant height which is independent of concentration will be followed by a "normal" reduction wave. The total diffusion current (sum of the prewave and the normal one) is proportional to the concentration of species in solution. The second wave decreases with a decrease in concentration, until finally, (5×10^{-4} M) only the prewave remains. The $E_{1/2}$ of the prewave is slightly more positive than the true redox potential of the system. This difference corresponds to the energy involved in the absorption of the reduced form on the D.M.E., and disappears at high temperature (90°C) because of a decrease in absorption with a rise in temperature. Similarly an increase of pH very often causes the two waves to coalesce into one wave. The postwave has similar characteristics. In either case the absorption wave is proportional to the number of molecules absorbed on the mercury drop during its life-time (5 sec). Hence the absorption current is dependent on temperature,

mercury height, and concentration of electroactive species. The fundamental criterion for absorption waves is the direct proportionality on the corrected height of the mercury column. Absorption waves have been observed in solutions of methylene blue, riboflavin and other organic compounds.

Not all current-voltage curves are as symmetrically S shaped and well defined as the lead wave in Figure 4. In fact one of the general characteristics of current-voltage curves obtained with a D.M.E. are the "maxima" present unless measures have been taken to eliminate their occurrence. There are two types of maxima, i.e. "maxima of the first kind" and "maxima of the second kind". In the first kind the current increases linearly with an increase of voltage (Ohm's Law) to a value much larger than the true diffusion current then suddenly falls to a steady normal diffusion current. One finds that the height of the maximum is greatly dependent on the concentration of the reducible substance. In general, metal ion solutions do not yield maxima below 0.1mM. As a rule there is no simple relation between maxima heights and concentration. The magnitudes of the maxima also depend on the drop time, becoming smaller the slower the drop time, and also smaller with a decrease in concentration of electroactive species. Maxima are especially prevalent when the $E_{1/2}$ is considerably removed from the electrocapillary zero of mercury. Upon examination of maxima one must conclude that the supply of reducible ion at the D.M.E. is abnormally high. Now two explanations have been proposed, the first by Heyrovsky and Ilkovic and the second by Antweiler and von

Stackelberg, both of whose theories are reviewed by Kolthoff and Lingane[26].

Heyrovsky attributes the increased supply of reducible ions at the D.M.E. to absorption on the mercury drop similar to the condenser current case mentioned previously. This interpretation explains some simple cases, but faces certain difficulties in other circumstances. For instance, the direction of the electric field responsible for absorption must change at the electrocapillary maximum, and so reducible ions of a given sign only should be absorbed, by electrical attraction, on one side of the electrocapillary maximum, but not on both. Hence cations which are absorbed on the negative side of the electrocapillary maximum would be repelled on the other side. Actually, it is found, in contradiction to the Heyrovsky-Ilkovic theory that the discharge of cations gives rise to maxima on <u>both</u> sides of the electrocapillary maximum, e.g. lead ($E_{1/2}$ = .45 v) and nickel ($E_{1/2}$ = 1.0 v).

Some rather ingenious experiments of Antweiler have shown that pronounced "streaming" of the liquid around the D.M.E. does account for the maxima. He made diffusion layers and stirring visible microphotographically by applying a "Schlierenmethod"[26]. In this view, due to the shielding effect of the capillary tip, the current density is greater at the bottom of the drop than at the top, and so causes a potential difference between the top and bottom of the drop and hence a difference of interfacial tension. Electrical double layers can migrate under the influence of a potential gradient and so cause streaming of the diffusion layer. This streaming could provide a mechanism for allowing an increased supply

of the reducible ions to reach the mercury drop. On this basis, one can explain why cadmium has no maximum, because its half-wave potential is close to the null point of mercury. In general, Antweiler's theory can account for most of the maxima characteristics encountered.

Fortunately, maxima can be suppressed by the addition of surface active substances to the aqueous solution under investigation. These compounds (gelatin, dyes, TX100, etc.) are called maximum suppressors. The function of any such suppressor is to form an absorbed layer on the aqueous side of the mercury solution interface which in turn prevents streaming of the diffusion layer. Care is needed in this method because even small concentrations e.g. as low as (0.01%) can alter the shape of a polarographic wave markedly, along with the value of the diffusion current. A detailed study of these effects is given in a later section.

Maxima of the second kind were discovered by Kryukova[23] in 1940 and named by her as such. They occur on both cathodic and anodic diffusion currents in concentrated solutions of supporting electrolyte of about 0.1M. These maxima do not decrease abruptly but rather slowly decrease in a straight line toward the true diffusion current height. They are caused by a turbulence arising inside the drop because of a high flow rate of mercury. Hence the effect increases with an increase of drop time, and in addition it is most efficiently transmitted to the surrounding layer of solution at the electrocapillary maximum, where the interfacial tension between drop and solution is greater. Moreover, the effect depends on the concentration of the supporting electrolyte, being more pronounced for more

concentrated solutions. These maxima are directly proportional to the height of the mercury column. Again these maxima may be eliminated by stationary electrodes, reducing flow rates, using a streaming mercury electrode or adding a suppressor.

Another important feature of a current-voltage curve is the half-wave potential $E_{1/2}$, mentioned already in previous pages. Under any defined set of experimental conditions, each substance has its own characteristic half-wave potential and this is the basis of qualitative polarographic analyses. $E_{1/2}$ values are dependent on the concentration of supporting electrolyte, damping of the polarograph, resistance of the H-cell, pH, temperature, structure of the electroactive ions, maximum suppressor and the electrical double layer and reversibility of polarographic waves. To have any meaning this $E_{1/2}$ parameter must be carefully determined under controlled conditions which are reproducible. There are numerous ways of measuring the $E_{1/2}$ of which a few will be mentioned. The most common method is illustrated in Figure 6. Parallel lines are drawn through the average residual and limiting currents. Then a line is drawn through the average oscillations on the steep rising part of the wave. Where the mid-point of the diffusion currents, measured perpendicular to the residual current, coincides with line drawn on the rising wave, that point is the half-wave potential, $E_{1/2}$. To gain accuracy the $E_{1/2}$ area is scanned with a low voltage span to spread out the wave as much as possible.

A more accurate method and one which was used extensively in this study is illustrated in Figure 7. This is the so called "logarithmic plot"

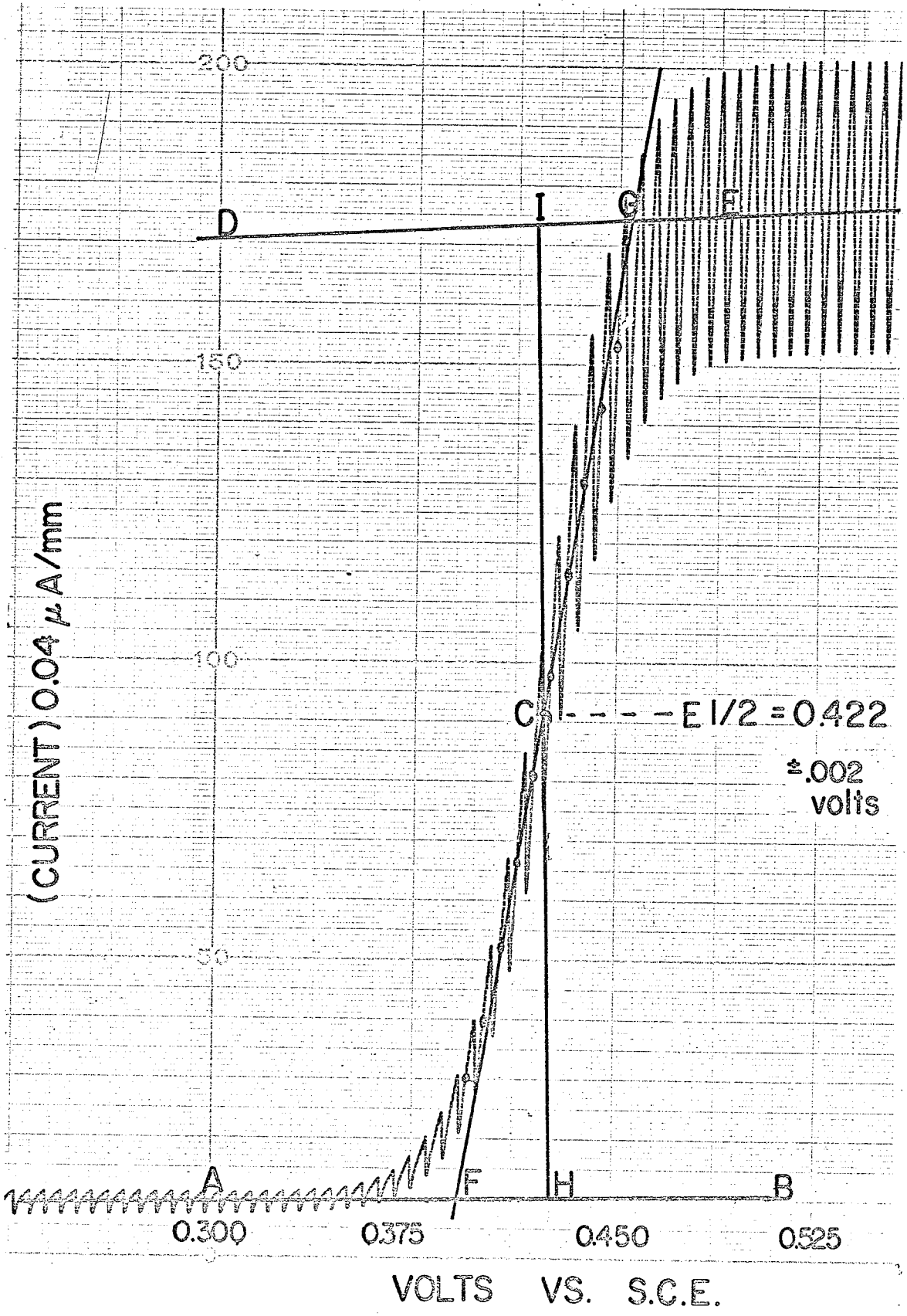

FIG.6 DIRECT MEASUREMENT OF E 1/2

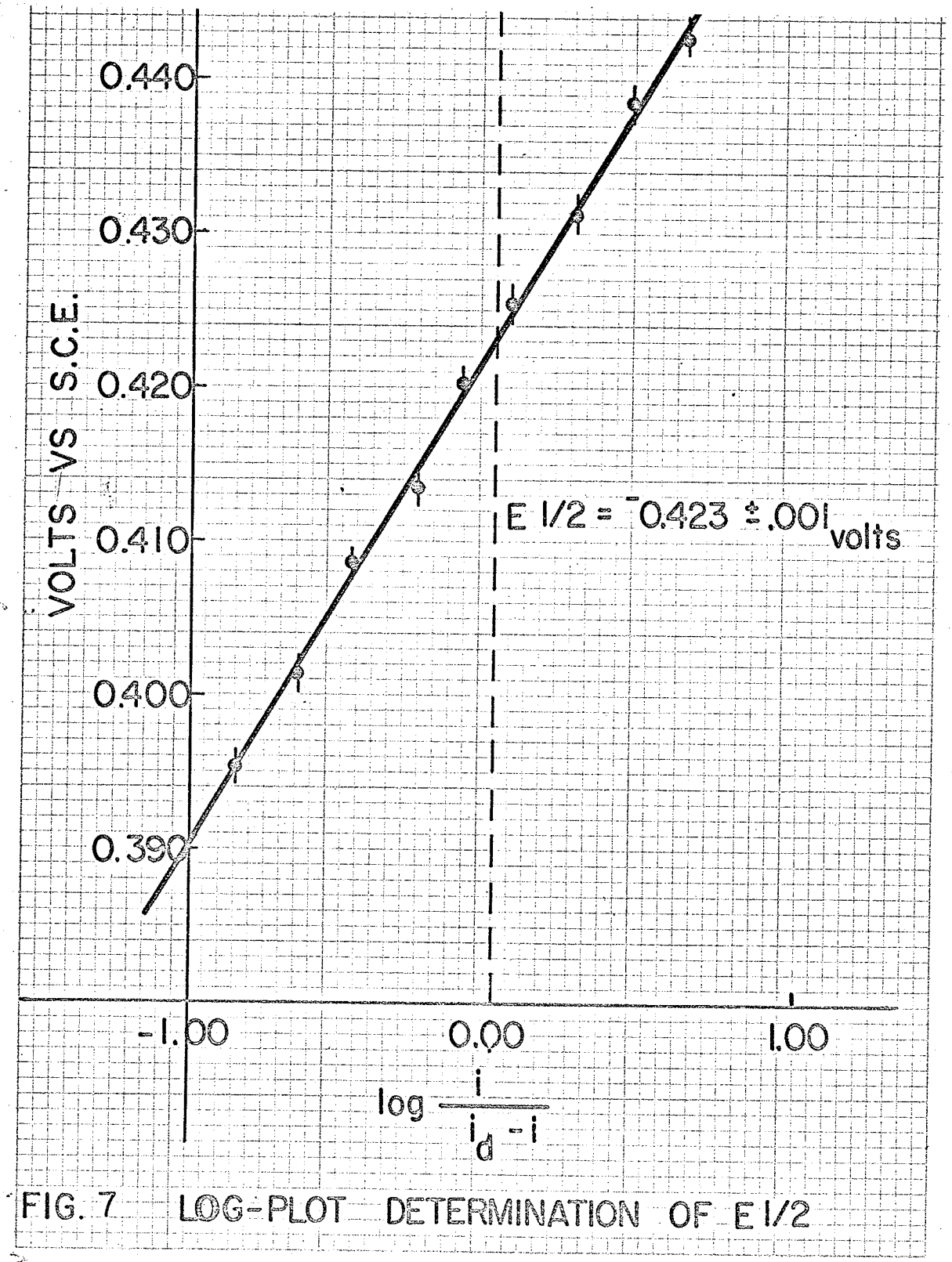

FIG. 7 LOG-PLOT DETERMINATION OF E 1/2

method. A polarogram must be obtained with a long drop time, no damping and a drawn out wave spread to minimize errors in the measurement of the potential as well as individual diffusion currents. At about ten points equally spaced along the potential axis on the rising part of the wave, an oscillation is picked and the average height of a growing drop oscillation is marked. The vertical distance between each such point and the extrapolated residual-current line is proportional to the value of (i) at the corresponding potential. This value is subtracted from the average diffusion current (i_d) to obtain ($i_d - i$). Then the $\log \frac{i}{(i_d - i)}$ vs applied potential is plotted. Where the $\log \frac{i}{(i_d - i)}$ becomes zero the half-wave potential must be located. This method then is based on ten readings and the best straight line drawn through these points, with the added advantage of using any convenient scale on the graph paper. This $E_{1/2}$ need not be corrected for an iR drop if the resistance through the polarograph and H-cell is under 1000 ohms. At high sensitivity the polarograph may have a resistance of several thousand ohms., at which point a correction is necessary when the current is above luA. The reason being that the iR drop now is of the order of several millivolts. In this study the largest iR drop was under one millivolt which made any corrections unnecessary.

CHAPTER 3

POLAROGRAPHIC THEORY

A detailed treatment of polarographic theory may be found in a number of text-books[23,24,26,28] thus only a brief review will be given here. In the preceeding chapter various contributions to the limiting current were discussed and the diffusion-controlled current was singled out as the most important parameter in polarography. In order to see the significance of the diffusion current, a closer look at the process of diffusion is necessary.

A. The Diffusion Current

Diffusion may be described as a spontaneous process leading to equilibration of concentration differences in solution, where solute starts to move from areas of high to those of lower concentration. The rate of diffusion is proportional to the concentration gradient, but also depends on the properties of the diffusing particles. If diffusion occurs in one direction only the process is called "linear diffusion". Consider a cylinder with a cross-sectional area, A, and a plane electrode at one end. The concentration of electroactive species decreases in the direction perpendicular to the electrode owing to an electrochemical change at the electrode. The number of moles dN of the substance that diffused across the area A at a distance x is proportional to A, to the concentration gradient dC/dx and the time interval dt in the following manner:

$$dN = DA \frac{dC}{dx} dt \quad \ldots\ldots\ldots\ldots\ldots\ldots\ldots\ldots\ldots\ldots (1)$$

This is known as Fick's First Law, which was derived in 1855. The proportionality constant, D, (diffusion coefficient) indicates the number of

moles of the substance that passes by diffusion through unit area at a unit concentration gradient in unit time. The magnitude of D is of the order, 10^{-5} cm^2/sec. The number of moles of substance that diffuse through unit area in unit time is called the unit flow or flux. It is given by the following expression:

$$\frac{dN}{Adt} = D \frac{\partial C}{\partial x} \quad \text{.....(2)}$$

As the diffusion proceeds, the concentration gradient decreases and hence the flux decreases accordingly. Therefore equation (2) is valid at a given instant of time only. To calculate the amount of material diffusing across a given plane in a finite interval of time one must know how a change in concentration varies with time, at a given plane at a given instant. This concentration gradient may be calculated from Fick's Second Law:

$$\frac{\partial C}{\partial t} = D \frac{\partial^2 C}{\partial x^2} \quad \text{.....(3)}$$

This is the fundamental equation for linear diffusion. The diffusion current is determined by the concentration gradient at the surface of the electrode, i.e.:

$$i = nF \frac{dN}{dt} = nFDA \left(\frac{\partial C}{\partial x}\right) \quad \text{.....(4)}$$

where n is the number of electrons involved in the electrode process, F is a faraday (96,500 coulombs) and D, A, and C and x have their usual significance. From equation (4) it can be shown that the current at a plane stationary electrode is

$$i = nFDA \frac{C^* - C_o}{\sqrt{\pi Dt}} \quad \text{.....(5)}$$

or for the limiting diffusion current ($C_o = 0$)

$$i_l = nFDA \frac{C^*}{\sqrt{\pi Dt}} \quad \text{.....(6)}$$

where C* is the concentration of electroactive material in the bulk of the solution, C_o is the concentration at the electrode surface and the square-root term is the differential thickness of the diffusion layer which is a function of time.

In symmetrical spherical diffusion the electroactive species diffuses toward the centre of a sphere along its radius. In this case the diffusion field could be a spherical shell surrounding the electrode. The radius of the electrode is designated by r_o and the distance of the diffusion shell by r. It is assumed that the diffusion shell is infinitesimally thin, the thickness being dr. Fick's First Law would take on the following form:

$$dN = 4\pi r^2 D \frac{\partial C}{\partial r} dt \quad \text{.....(7)}$$

When determining the concentration gradient towards a stationary spherical electrode the derivation must follow Fick's Second Law, which is given in spherical co-ordinates:

$$\frac{dC}{dt} = D\left[\frac{\partial^2 C}{\partial r^2} + \frac{2}{r}\frac{\partial C}{\partial r}\right] \quad \text{.....(8)}$$

From the solution of equation (8), with appropriate initial and boundary conditions, it follows that where r approaches r_o, the solution of the equation resembles that for diffusion towards a plane electrode. Thus diffusion within a short distance from the surface of spherical electrode may be regarded as linear. Hence it can be shown that:

$$i = nFDAC^* \left(\frac{1}{\sqrt{\pi Dt}} + \frac{1}{r_o}\right) \quad \text{.....(9)}$$

The first term on the right-hand side corresponds to the expression for diffusion towards a plane electrode (eg. 6) and its magnitude is a function of time. The second term is a time-independent constant. If the thickness of the diffusion layer $\sqrt{\pi Dt}$, (for small t) is considerably less than r_o, it follows that the value of the first term exceeds that of the second term and that the diffusion towards a spherical drop (DME) is governed by the laws of linear diffusion. Verifying eqn. (9) experimentally is quite difficult because at longer drop-times (t), convection occurs in the vicinity of the electrode giving rise to streaming that disturbs the diffusion layer.

Diffusion at a D.M.E. is spherically symmetrical, but due to the periodic growth and fall of the mercury drops the area of the diffusion field changes continuously during the life of a drop. The diffusion then takes place in a medium which is moving with respect to the centre of the drop in a direction opposing the direction of diffusion. Calculation of the concentration gradient towards a growing dropping electrode is quite complicated. The problem was first solved by Ilkovic[32] in 1934 with the assumption that the dropping electrode behaves as a plane electrode with an area equal to that of the surface of the drop i.e., an area increasing with time. The derivation of the famous Ilkovic equation was suggested actually by experimental work which showed that capillaries with equal flow rates give equal limiting currents and the dependence of the diffusion currents on the height of the mercury column is parabolic. By applying Fick's laws of diffusion and considering the area of a growing

mercury drop Ilkovic obtained an expression for the mean diffusion current:

$$i_d = 0.627\ nFCD^{\frac{1}{2}}\ m^{2/3}\ t^{1/6} \quad \text{.....(10)}$$

The mean diffusion current is considered because with the ordinary D'Arsonval galvanometer used in polarography, the complete current time curves are not observed, because the inertia of the moving coil is so large that it is unable to follow the complete periodic change in the current. Thus the average diffusion current, incorporating F into a numerical constant is;

$$i_d = 607\ nCD^{1/2}\ m^{2/3}\ t^{1/6} \quad \text{.....(11)}$$

where C is expressed in millimoles (mM) per liter, m, in mg. per second, t, the drop time in seconds, and i_d in microamperes, μA. It is evident from the above equation that for given values of m and t, i.e. if the same capillary is used with a constant height of mercury, the diffusion current is directly proportional to the analytical concentration of the electroactive species in solution:

$$i_d = kC \quad \text{.....(12)}$$

where $k = 607\ nD^{1/2}\ m^{2/3}\ t^{1/6}$.

In practical work the average of the galvanometer oscillations is measured, corresponding very closely to the true average current. The diffusion currents obtained with a D.M.E. are perfectly reproducible for reasons that have been discussed already. Antweiler[33] showed that the thickness of the normal diffusion layer was only of the order of 0.05 mm. The diffusion layer is thus so thin that there is no appreciable stirring effect due to density gradients, which accounts for the perfect repro-

ducibility of the D.M.E. current. If the diffusion current values of electroactive ions are plotted against concentration, a straight line passing through the origin is obtained, which may be used as a calibration curve for determining the concentration of the ion in unknown samples. When the Ilkovic equation is rearranged as

$$I_d = 607\ n\ D^{1/2} = \frac{i_d}{C\ m^{2/3}\ t^{1/6}} \quad \text{.....(13)}$$

we have an expression for the diffusion current constant, I_d. This immediately leads to an absolute method for the determination of unknown concentration once a known sample is run, i.e. once I_d is known. Similarily unknown concentrations may be obtained by direct comparison, of heights, standard addition and internal standard methods. Thus the Ilkovic equation is of paramount importance and the very foundation of quantitative polarographic analysis.

On the whole, the validity of the Ilkovic equation has been proved satisfactorily by many investigators. Thus the linear dependence of the diffusion current, i_d, on concentration is satisfied with $\pm$ 1%, the dependence on $m^{2/3}\ t^{1/6}$ within $\pm$ 3% and the constancy of the diffusion current constant I_d, as given in equation (13) within $\pm$ 5%. It was this big change in I_d with m and t that led to corrections on the original Ilkovic equation.

In deriving the Ilkovic equation the curvature of the electrode was neglected and only linear diffusion was considered. The first derivation that accounted for the curvature of the electrode was presented by

Lingane and Loveridge[34]. Essentially they multiplied the second term on the r.h.s. of equation (9) by $\sqrt{7}/3$. Their final result was that:

$$i_d = 607\ nCD^{1/2}\ m^{2/3}\ t^{1/6}\ (1 + B\ \frac{D^{1/2}\ t^{1/6}}{m^{1/3}}) \quad \ldots\ldots\ldots(14)$$

where B is a numerical coefficient. Various authors attempted the same task and in all cases obtained an equation similar to the one above differing only in the value of B. Lingane and Loveridge[34] set B equal to 39. Strehlow and von Stackelberg[35] chose 17. A rigorous treatment by Koutecky[27] gave a complex equation as follows:

$$i_d = 607\ nCD^{1/2}\ m^{2/3}\ t^{1/6}\ (1 + \frac{3.4\ D^{1/2}t^{1/6}}{m^{1/3}} + \left[\frac{D^{1/2}t^{1/6}}{m^{1/3}}\right]^2) \quad \ldots\ldots(15)$$

On the basis of Koutecky's equation, the diffusion currents for the normal capillaries should exceed those calculated from the simple Ilkovic equation by 5-10%. However the variations in flow rate with time and transfer of concentration polarization upset the theoretical prediction. Years of research have shown that the correction for spherical diffusion is approximately counterbalanced by the transfer of concentration polarization and that the variation in flow rate is within the experimental error of the recording polarograph. Hence the mean currents measured with a normal polargraph i.e. vertical capillary and serial drops, are in satisfactory agreement with the Ilkovic equation. Reinmuth[36], Markowitz and Elving[37] and Meites[38] have all compared the corrected equations to that of the original Ilkovic and come to the conclusion that there is no significant advantage of using one or the other for describing the current-potential curve.

B. Electrochemical and Theoretical Principles

The last section discussed the behavior of the current at the plateau of the wave, where it is virtually independent of the potential of the D.M.E., i.e., the condition of complete concentration polarization. It is now appropriate to consider the manner in which the current is affected by the electrode potential on the rising part of the wave. In order to explain the shape of the current-potential curve, one must know the relationship between the concentration of electroactive species at the electrode surface and the potential at any given point on the wave. For reversible processes this relationship can be obtained from the Nernst equation:

$$E = E^{o} - \frac{RT}{nF} \ln \frac{[Red]}{[Ox]} \quad \text{.....(16)}$$

Red and Ox denote the concentrations of reduced and oxidized forms of the depolarizer, E^{o} is the standard oxidation-reduction potential of the system, E the potential of the D.M.E., R is the gas constant, T is the absolute temperature and nF has its usual significance.

The Nernst equation holds only for reversible thermodynamic equilibrium, i.e. under conditions when no current is flowing. In fact a small current does flow for the electrode process in polarography. Hence the question arises, when is a reaction reversible? Thermodynamically a reaction is reversible when equilibrium is attained at any and every instant of time. In polarography this would mean that thermodynamic equilibrium would have to be very nearly attained at every instant during the life of a drop at any potential. For such reversible reactions the variation

of current with potential reflects the changing position of the equilibrium, slightly disturbed in favour of the reduced form due to the small current flowing during the reaction. At the other extreme is the class of totally irreversible reactions which are so slow that they proceed only a fraction of the way toward equilibrium during the life of each drop. For these reactions it is the rate of electron-transfer process that governs the relationship between current and the potential. Between these two extremes is an intermediate class of reactions that are fast enough to approach equilibrium during the drop life, but not detectible as irreversible within experimental measurements. Hence a reaction is said to be reversible if, within the limits of experimental error, its behaviour cannot be distinguished from an infinitely fast reaction. However, valuable information can be obtained from both reactions using the polarographic technique, though it is no simple task to positively identify, a "reversible wave".

There are four possibilities to consider in the reduction and oxidation of simple metal ions at the D.M.E. First, reduction of cations to the metallic state forming an amalgam, i.e., the metal is soluble in mercury. Secondly, reduction to the metallic state where the metal is insoluble in mercury. Third, reduction or oxidation from one soluble oxidation state to another, e.g. Fe^{+++} to Fe^{++}. Lastly a combination of case three with either the first or second, so that a stepwise reduction occurs and a polarogram is obtained with two, or more waves.

To illustrate the theory, case one will be examined. The treat-

ment here is a summary based on the reviews given by Meites[24], Kolthoff and Lingane[26] and Heyrovsky and Kuta[23]. The electrode reaction corresponds to:

$$M^{n+} + ne + Hg^{o} = M(Hg) \quad \text{.....(17)}$$

where M^{n+} represents the metal cation, and M(Hg) is the amalgam formed at the D.M.E. If the reaction is reversible and very fast when compared to the diffusion of ions to the electrode surface, the D.M.E. will be subject only to concentration polarization. The concentration of metal atoms to metal ions at the D.M.E. must conform to the Nernst equation:

$$E_{d.m.e.} = E_s^o - \frac{RT}{nF} \ln \frac{f\,[M(Hg)]}{a_{Hg^o}\; f_s\,[M^{n+}]} \quad \text{.....(18)}$$

(a denotes activity) where f denotes the activity coefficient, E_s^o is the standard potential of the simple metal ion and a_{Hg^o} is unity because the amalgam formed is very dilute and hence it is regarded as pure mercury. Equation 18 may then be written:

$$E_{d.m.e.} = E_s^o - \frac{RT}{nf} \ln \frac{f\,[M(Hg)]}{f_s\,[M^{n+}]} \quad \text{.....(19)}$$

If the electrode reaction is diffusion controlled, the current, i, is proportional to the difference between the concentration of M^{n+} in the bulk of the solution and that at the electrode surface, i.e. Fick's Law. Since the concentration of ions at the electrode surface at any potential on the plateau of the wave is virtually zero for a reversible process, because the ions are reduced as rapidly as they reach the electrode the current is equal, by definition, to the diffusion current as stated in equation 12:

$$i_d = k_s C_s$$

where s denotes simple metal ion. The concentration of the metal atoms

in the amalgam at the drop surface is also proportional to the current:

$$i = - k_{am} C_{am} \quad \text{.....(20)}$$

where subscript am refers to the atoms instead of ions as in equation 12. The negative k_{am} appears because a negative current is obtained when metal atoms are being oxidized at the drop surface, as for a dropping metal-amalgam electrode in a solution of the supporting-electrolyte alone.

Combining the above equations for the condition when $i = i_{\frac{d}{2}}$ namely the half-wave potential:

$$E_{d.m.e.} = E_{\frac{1}{2}} - \frac{RT}{nF} \ln \frac{i}{i_d - i} \quad \text{.....(21)}$$

or at 25°C equation 21 simplifies to

$$E_{d.m.e.} = E_{\frac{1}{2}} - \frac{.05915}{n} \log \frac{i}{i_d - i} \quad \text{.....(22)}$$

In the above equation i is the cathode current resulting from the reduction of M^{n+}. Similarly equations can be derived for anodic currents or a "composite" condition of an anodic-cathodic wave. On examining equation 22 one realizes that a plot of $\log \frac{i}{i_d - i}$ vs. $E_{d.m.e.}$ should yield a straight line having a slope of $\frac{.05915}{n}$ from which n can be determined. As has been mentioned previously such a plot is extremely useful to find $E_{\frac{1}{2}}$ values, i.e. where the log term is zero. The log term of equation 22 can be transformed to include diffusion coefficients instead of currents if so desired. The Ilkovic equation then predicts:

$$E_{\frac{1}{2}} = E^{o}_{s} - \frac{.05915}{n} \log \frac{f_{am} D_s^{\frac{1}{2}}}{f_s D_{am}^{\frac{1}{2}}} \quad \text{.....(23)}$$

The various uses and implications of equation 22 will be discussed later.

If the solution contains a complexing agent, so that the metal ion is present as a complex rather than as the simple ion, the half reaction can be described by the equation

$$MX_p^{(n-pb)+} + ne + Hg^o = M(Hg) + p\,X^{-b} \quad \text{.....(24)}$$

where X is the complexing agent, p is the number of ligands attached to the metal ion and b is the charge of the ligand. It is convenient to imagine that the reduction proceeds in two steps:

$$MX_p^{(n-pb)+} = M^{n+} + p\,X^{-b} \quad \text{.....(25)}$$

$$M^{n+} + ne + Hg^o = M(Hg) \quad \text{.....(26)}$$

This may not be the actual kinetic mechanism involved, but it serves to facilitate an explanation of the thermodynamic relationships involved. If the foregoing reactions are rapid and reversible at the D.M.E. then the potential of the latter at any point on the wave is given by equation 19

$$E_{d.m.e.} = E_s^o - \frac{RT}{nF} \ln f_{am} \frac{[M(Hg)]}{f_s [M^{n+}]}$$

When the dissocation of the complex ion is very fast so that equilibrium with respect to reaction 25 is maintained at the electrode surface then M^{n+} can be replaced by:

$$M^{n+} = K_c \frac{[MX] f_{mx}}{[X]^p f_x^p f_m} \quad \text{.....(27)}$$

where K_c is the dissociation constant of the metal ion complex. If one assumes that the complexing agent is in large excess over the complex then the liberation of X^{-b} at the D.M.E. has a negligible effect on the

bulk concentration X^{-b}. Secondly, K_c is normally so small that the free M^{n+} in the bulk of the solution is also negligible.

With these assumptions the Nernst equation predicts that

$$E_{d.m.e.} = E_a^o + \frac{RT}{nF} \ln \frac{K_c f_{mx}}{f_a f_x^p} - \frac{RT}{nF} \ln \frac{[M^{n+}][X]^p}{[MX]} \quad \text{.....(28)}$$

Upon substituting in the relationships of currents to concentrations one gets an expression for the half-wave potential:

$$E_{1/2_c} = E_a^o + \frac{0.05915}{n} \log \frac{K_c f_{mx} k_a}{f_a k_c} - p \frac{0.05915}{n} \log f_x [X] \quad \text{....(29)}$$

at 25°C, where $\frac{k_s}{k_c} = \frac{\sqrt{D_s}}{\sqrt{D_c}}$. It is evident from equation 29 that the concentration of the metal ion complex does not enter into the $E_{1/2_c}$ expression. It has been verified experimentally that the $E_{1/2_c}$ is constant and independent of the concentration of the complex metal ion. Hence the half wave potential of a complex metal ion should shift to more negative values of potential with changing activity of the ligand as follows:

$$\frac{E_{1/2_c}}{\log [X] f_x} = - p \frac{0.05915}{n} \quad \text{.....(30)}$$

From this relationship one can determine the coordination number, p, of the complex, and thus its formula. From equation 29 it is clear that the $E_{1/2_c}$ depends on the logarithm of K_c and it is more negative the smaller the value of K_c, i.e., the more stable the complex ion. This is reasonable thermodynamically; that is, it would take a more negative potential to reduce a more inert or non-labile complex. The most accurate method of determining K_c in practice is to measure the difference between $E_{1/2_c}$ and $E_{1/2_s}$ under similar conditions, where c and s denote complex

and free metal ion respectively. It follows from the above equations that:

$$E_{\frac{1}{2}c} - E_{\frac{1}{2}s} = \frac{0.05915}{n} \log \frac{K_c f_c k_s}{f_s k_c} - p \frac{0.05915}{n} \log [X] f_x \quad \ldots\ldots(31)$$

For approximate purposes most textbooks simplify the above expression to

$$E_{\frac{1}{2}c} - E_{\frac{1}{2}s} = \frac{0.05915}{n} \log K_c - p \frac{0.05915}{n} \log [X] \quad \ldots\ldots\ldots\ldots(32)$$

For exact work the ratio of k_s/k_c can be determined experimentally from the ratio of the observed diffusion currents of the simple and complex metal ions at the same polarographic conditions according to the Ilkovic equation:

$$\frac{k_c}{k_s} = \frac{D_c^{\frac{1}{2}}}{D_s^{\frac{1}{2}}} = \frac{I_c}{I_s} \quad \ldots\ldots\ldots\ldots\ldots\ldots\ldots\ldots\ldots(33)$$

Hence knowing the diffusion current constants, I_c and I_s, one can calculate the ratio of k_c to k_s. An error of $\pm$ 10% in this ratio corresponds to only $\pm \frac{2.4}{n}$ mv in the difference between $E_{\frac{1}{2}c}$ and $E_{\frac{1}{2}s}$. More care must be exercised however when the ligands are large, e.g. EDTA and DTPA, for here the diffusion coefficient of the complex will be significantly different from that of the simple metal ion. Activity coefficients are difficult to estimate but fortunately they may be omitted in many cases. When the concentrations are kept low (as in polarography) and the metal ion and the complex have comparable charges e.g. $Cu(C_2O_4)_2^{=}$ and $Cd(EDTA)^{=}$ the error introduced by neglecting activities is no greater than the uncertaintity in liquid junction potentials, especially in solutions of equal ionic strength. Hence equation 32 yields remarkably good values of K_c in most cases.

A log plot based on equation 30 often gives p a non integral value. If the plot is a straight line only one complex exists over the range of ligand concentration studied, and a curved line is obtained when a number of different complexes exist in the same solution. If p is 1.5, this does not mean one has an equimolar mixture of complexes with p = 1 and p = 2. The mathematical treatment of data on such systems has been worked out by Hume and Deford (39).

When all the factors in equation 31 are considered, a value of K_c from polarographic data should not be assigned an accuracy better than $\pm$ 50%, though better accuracy very often is obtained. When n is 2 this error corresponds to $\pm$ 5 mv. error in the measured difference between $E_{1/2_c}$ and $E_{1/2_s}$. Usually activity coefficients and liquid-junction potentials contribute an uncertainty of several millivolts so one can expect a variation of $\pm$ 5 mv. The polarographic method then compares favourably with other techniques of measuring thermodynamic dissociation constants.

The difference between the diffusion coefficients of a free and complexed metal ion may be used to evaluate the proportions in which these are present in a mixture. For a 1:1 complex, MX, if the concentration of free ligand X, is much larger than the total concentration of metal ion one can show that: [23]

$$\bar{D} = \frac{D_M + D_{MX} K_c [X]}{1 + K_c [X]} \qquad \text{..............................(34)}$$

where $\bar{D}$ is the apparent diffusion coefficient corresponding to the total wave height for the simultaneous reduction of M and MX in the mixture D_m and D_{mx} (diffusion coefficients of metal and complex) are evaluated from

The Ilkovic equation (see equation 33). The equilibrium should be rapid and the concentration of M (roughly) should be equal to the concentration of MX. This method is suitable for chelons where $D_M \approx D_{MX}$ and the dissociation constants are relatively small ($\geq 10^{-15}$). Some complex ions cannot be reduced directly but must dissociate first. This is true of many metal chelonates, which have been extensively investigated and the mechanism elucidated by Koryta[27,40]. One reason, among others, is probably that the metal ion cannot "bridge" to the electrode as it does for simple complexes of Cl^-, $SO_4^=$, etc. If the dissociation is slow, a kinetic wave is obtained, and if the resulting free metal ion is reversibly reduced it can be shown that:

$$E_{1/2_c} = E_{1/2_k} - \frac{0.05915}{n} \log \frac{i_d}{i_k} \quad \text{.....(35)}$$

where $E_{1/2_c}$ is the half wave potential and i_d the average diffusion current of the hypothetical reversible wave that would be obtained for instaneous dissociation, while $E_{1/2_k}$ and i_k refer to the actual kinetic wave. The value of i_d is estimated from data on similar complexes that do yield diffusion controlled waves, and so $E_{1/2_c}$ can be obtained for further use in calculations of K_c. Such kinetic behavior was observed for Cd (EDTA) by Schmid and Reilly[41], for Cd (HEDTA)* by Koike and Hamaguchi[42] and for Cd (TTHA) by Conradi, Kopanica and Koryta[22]. In this study similar observations were made with respect to Cd (DTPA). Thus the next section will be devoted to kinetic current phenomena.

---

* hydroxyethylethylenediaminetriacetic acid (HEDTA)
sometimes written (HEEDTA)

C. Kinetic Wave Theory

There are an appreciable number of electrode processes where the current is controlled by a homogeneous chemical reaction taking place in the vicinity of the electrode. These currents, which have certain characteristic properties, are called kinetic currents. The quantitative investigation of these currents was initiated by Wiesner[43] in 1943. He found a kinetic current arising from the transformation of a non-reducible species, X, into a reducible one, Y, at potentials at which Y is reduced as rapidly as it is formed. These kinetic currents have two distinguishing polarographic characteristics; first, their value is less than that predicted for the reduction of all of the X present, but larger than the value predicted for the reduction of the equilibrium concentration of Y, and secondly, the current depends only on the rate of transformation of X into Y and therefore independent of m and t, so that i is independent of the mercury height. The latter characteristic is the fundamental criterion of a kinetic wave. Pronounced deviations from this idealized pattern will be observed if the equilibrium concentration of Y in the bulk of the solution is appreciable compared to that of X, or if the rate constant for the transformation of X into Y is large; in either case the current will display properties intermediate between those just described and those of a true diffusion current.

Chemical reactions may be combined with electrode processes in three ways; (a) the reaction precedes the electrode process proper, (preceding reaction) where the electrode-active form of the depolarizer is produced

by a chemical reaction from a polarographically inactive form with which it is in mobile equilibrium, (b) the reaction runs parallel to the electrode process, which involves a chemical regeneration of the original depolarizer from the product of the electrode process, and (c) the reaction follows the electrode process (subsequent reaction) where the primary product of a reversible depolarization process is transformed to a polarographically less active or inactive form. A theoretical analysis of the currents produced in the above reactions permits the determination of the rate constant of the chemical reaction. This may be done by an approximate method or a rigorous approach.

The approximate method, worked out by Brdicka and Wiesner[44], assumes the existence of a thin reaction layer at the electrode surface, where the electrode process and the associated chemical reaction proceed under steady state conditions. The thickness of the reaction layer (for large reaction rates) is very small compared to the diffusion layer, and thus the thickness of the reaction layer is related to the rate constant for the corresponding reaction. The decrease in concentration of the reaction components within the reaction layer is counterbalanced by diffusion from the bulk of the solution. This method yields satisfactory results for very fast chemical reactions and is described fully by Brdicka, et al[27,30], and Koryta[27,30,40].

The problem was approached in a rigorous fashion by Koutecky[45-48] and finally solved in 1953. He expressed the changes in concentration at the electrode caused by diffusion and chemical reaction by a system of

differential equations, in the first instance for a planar electrode and finally including a correction factor for the growth of the mercury drops. He attempted to use $\sqrt{\frac{7}{3}}$ as a correction factor from Ukovic's theory, but found that for kinetic currents the factor approached unity rather than $\sqrt{\frac{7}{3}}$. A brief account of both methods for a preceding reaction follows as summarized from references 23,24,27, and 49. The method for a preceding reaction is derived because it is applicable to the data in this investigation.

In this type of reaction, form Y of the depolarizer is produced by a chemical reaction from form X, which is inactive in the given range of potentials. In the electrode process Y is transformed into the amalgam product Z. The reaction scheme may be written:

$$X \underset{k_r}{\overset{k_f}{\rightleftharpoons}} Y \rightleftharpoons Z \qquad \text{.....36}$$

where k_f is the rate constant for the formation of Y; it may depend on the concentration of other substances participating in excess in the chemical reaction. The rate constant for the reverse reaction is k_r, and the ratio of the two constants may be given by an equilibrium constant σ. Hence:

$$\sigma = \frac{k_r}{k_f} = \frac{[X]}{[Y]} = \frac{1}{K} \qquad \text{.....37}$$

and if the ratio $\frac{[Y]}{[X]}$ is very small, the limiting current is controlled almost entirely by the rate of the chemical reaction; at large values of this ratio, the diffusion of Y from the bulk of the solution makes a significant contribution to the current. The kinetic component of the current is favored by increasing k_f, e.g. by temperature increase and by

a change in pH.

The rate of formation (v) of Y is given by a first order reaction relationship:

$$v = k_f [X]_o \qquad \text{.....38}$$

where the subscript o denotes the concentration at the electrode surface. Let us assume that only those particles of Y are reduced which are formed in the reaction-layer of thickness μ, surrounding the electrode, according to equation 36. Then the current is proportional to the concentration of Y formed in a volume $\Delta V = \mu\bar{q}$, where $\bar{q}$ is the mean area of the electrode expressed in cm^2 and μ is the thickness of the reaction layer in cm. The mean current is given by:

$$\bar{i} = n F \frac{dN}{dt}$$

according to equation 4, where dN/dt is the number of moles of depolarizer reaching the D.M.E. per second. This can be set equal to the number of moles of Y produced in a reaction volume ΔV per second as follows:

$$\frac{dN}{dt} = \Delta V \frac{d[Y]}{dt} = \mu\bar{q} \cdot 10^{-3} k_f [X]_o \qquad \text{.....39}$$

consequently, for the mean limiting kinetic current we have

$$\bar{i}_k = nF \bar{q} \cdot 10^{-3} \mu k_f [X]_o \qquad \text{.....40}$$

where the factor 10^{-3} changes the reaction volume ($\mu\bar{q}$) to liters. $[X]_o$ represents the concentration of non-reducible X in the reaction layer and is taken to be constant due to the thinness of the reaction layer. Since X is the only species transported to the reaction layer by diffusion, the kinetic currents may be expressed, in an approximation:

$$\bar{i}_k = \frac{\frac{n F \bar{q} \mu k_f}{10^3 \bar{K}}}{1 + \frac{n F \bar{q} \mu k_f}{10^3 \bar{K}}} i_{d_x} \quad \ldots\ldots\ldots\ldots\ldots 41$$

From this equation, the properties of a limiting current controlled by the rate of a preceding chemical reaction can be formulated. From the Ilkovic equation $i_d = \bar{K}C$, and if the reaction is slow ($n F \bar{q} \mu k_f << 10^3 \bar{K}$), the second term in the denominator of equation 41 may be neglected. Then:

$$\bar{i}_k = n F \bar{q} \cdot 10^{-3} \mu k_f C \quad \ldots\ldots\ldots\ldots\ldots 42$$

where $i_k << i_d$ and there is no significant depletion of X in the reaction volume. Since the mean surface area $\bar{q}$ is independent of the height of the mercury column (mt = constant), the kinetic current is likewise independent of h_{Hg}. Unless the condition $i_k << i_d$ is valid, the second term in the denominator in equation 41 cannot be neglected. In this case the current is controlled partially by the diffusion rate of X, the inactive form, and such currents depend on the mercury head (semi-kinetic currents). If the rate of reaction is greater than the rate of diffusion ($n F \bar{q} \mu k_f >> 10^3 \bar{K}$), unity may be neglected in equation 41 relative to the second term and the limiting current is controlled entirely by diffusion:

$$\bar{i}_k = \bar{K}C = \bar{i}_d \quad \ldots\ldots\ldots\ldots\ldots 43$$

In order to calculate the rate constant k_f, the thickness of the reaction layer μ must be known. The reducible form Y produced in a chemical reaction at a certain distance from the D.M.E. must reach the electrode during its life-time if it is to be subject to an electrochemical change.

The differing life-times of individual particles of Y may be replaced by the mean life-time $\bar{\tau}$. Hence, the distance, within which the reaction product is within range of the electrode is equal to its mean displacement in one dimension during its mean lifetime $\bar{\tau}$. This displacement is given by the Einstein-Smoluchowski formula:

$$s = (2d\bar{\tau})^{1/2} \qquad \text{.....44}$$

where D is the diffusion coefficient of the depolarizer Y. Koutecky and Brdicka showed that the correct relationship for μ was:

$$\mu = (D\bar{\tau})^{1/2} \qquad \text{.....45}$$

The mean life-time of Y for a monomolecular reaction is given by the reciprocal of the rate constant k_r. If $K = \frac{k_f}{k_r}$, then $\bar{\tau} = \frac{K}{k_f}$ and equation 45 becomes:

$$\mu = \left(\frac{DK}{k_f}\right)^{1/2} \qquad \text{.....46}$$

Substituting this relationship into equation 41 and setting $\bar{q} = 0.51\ m^{2/3} t^{2/3}$ and $\bar{K} = 0.627\ n\ F \cdot 10^{-3}\ D^{1/2}\ m^{2/3}\ t^{1/6}$, the final formula is obtained:

$$\frac{i_k}{i_{d_x}} = \frac{0.81\ (K\ k_f\ t)^{1/2}}{1 + 0.81\ (K\ k_f\ t)^{1/2}} \qquad \text{.....47}$$

Koutecky's rigorous solution for the current at a growing D.M.E., controlled by a preceding chemical reaction, uses differential equations and dimensionless parameters. He obtained an equation for $\bar{i}_k$ quite similar to the equation above:

$$\frac{i_k}{i_d} = \frac{0.886\ (K\ k_f\ t)^{1/2}}{1 + 0.886\ (K\ k_f\ t)^{1/2}} \qquad \text{.....48}$$

or

$$\frac{\bar{i}_k}{\bar{i}_d - \bar{i}_k} = 0.886\ (K\ k_f\ t)^{1/2} \qquad \text{.....49}$$

The above theory can explain the currents observed during the reduction of certain metallic complexes, which are limited by the rate of dissociation to a more easily reducible, free cation. These kinetic currents were discovered by Koryta[50], in 1951, for cadmium and lead complexed with nitrilotriacetic acid (NTA). Later Koryta[50] and Schmid and Reilley[41] examined Cd-EDTA which showed a similar behaviour to the NTA complex. These systems give a double wave, the first corresponding to the reduction of free cations with an important kinetic component and the second to an irreversible reduction of the complex itself. For the Cd-NTA system the following equilibria are involved:

$$Cd\ X^{-} \underset{k_r}{\overset{k_d}{\rightleftharpoons}} Cd^{++} + X^{-3}$$

$$X^{-3} + H^{+} \rightleftharpoons H\ X^{=}$$

where X is anion of NTA. Provided that the concentration of NTA is in excess so that the preceding chemical reaction is first-order, equation 49 can be used to calculate the dissociation rate constant, k_d. For this system k_d is a function of the hydrogen ion concentration; and

$$\frac{1}{K} = \frac{Cd\ X^{-}}{Cd^{++}} = K_{CdX}\left[X^{-3}\right] = \frac{k_r}{k_f} = \sigma$$

and $\left[X^{-3}\right]$ is related to the analytical concentration of NTA, $C_X = \left[X^{-3}\right] + \left[HX^{=}\right]$ and its dissociation constant $K_3 = \dfrac{\left[H^{+}\right]\left[X^{-3}\right]}{\left[HX^{=}\right]}$.

Then:

$$[X^{-3}] = \frac{K_3 C_X}{[H^+] + K_3}$$

and in a buffered medium at pH4-6, the value of K_3 is negligible with respect to $[H^+]$ and can be neglected, accordingly;

$$[X^{-3}] = \frac{K_3 C_X}{[H^+]}$$

Substitution into equation 49 results in:

$$\frac{i_k}{i_d - i_k} = 0.886 \left(\frac{k_d\, t\, [H^+]}{K_{CdX}\, K_3\, C_X}\right)^{1/2} \qquad \text{.....50}$$

Koryta[50] also presented a general solution of the problem for dissociation rates in systems comprising of a series of complexes, MX, MX_2, ...MX_n. The assumption being that there is only one slow conversion $MX_k \rightarrow MX_{k-1}$, the complexes of higher and lower order being in rapid equilibrium with each of these species, respectively. The system is buffered and the complexing agent is in excess. The free cation and the complexes from MX to MX_{k-1} are assumed to be reducible, whereas the other complexes from MX_k to MX_n are not reducible. If these conditions are applied to equation 49, a general formula

$$\frac{i_k}{i_d - i_k} = 0.886 \frac{(k_d k_0 \cdots k_k [X]^k \sum_{i=0}^{k-1} k_0 \cdots k_i [X]^j\, t)^{1/2}}{\sum_{j=k}^{n} k_0 \cdots k_j [X]^j} \qquad \text{....51}$$

where k_0-k_j are the equilibrium constants for consecutive complex formation of the cation with the ligand X. If, moreover, the formation of reducible complexes with the ligand Y takes place with the corresponding rate con-

stants for consecutive complex formation $k_0' \ldots k_j'$, then the above formula becomes:

$$\frac{i_k}{i_d - i_k} = 0.886 \frac{(k_d \sum_{j=0}^{p} k_0' \ldots k_j' [Y]^j t)^{1/2}}{1 + \sum_{j=0}^{n} k_2 \ldots k_j [X]^j (k_1 [X])^{1/2}} \quad \ldots\ldots 52$$

The above equations can be modified to satisfactorily treat systems which are not buffered and also where the complexing agent is not in excess.

The stability constants of metal complexes (Cd-NTA, Cd-EDTA, etc.) can also be determined from the half-wave potentials of kinetic currents, as demonstrated by Koryta[50]. He found that the kinetic wave had the same form mathematically as a reversible diffusion-controlled wave. For the half-wave potential of the complex, he obtained:

$$E_{\frac{1}{2}c} = E_{\frac{1}{2}s} - \frac{0.05915}{n} \log K_{mx} [X] + \frac{0.05915}{n} \log \frac{i_d}{i_k} \quad \ldots\ldots 53$$

If consecutive complex formation takes place and the slow step governing the kinetic wave is

$$MX_k \underset{k_r}{\overset{k_d}{\rightleftharpoons}} MX_{k-1} + X,$$

a general equation for the shift in the $E_{1/2}$ can be shown to be:

$$\Delta E_{1/2} = \frac{-0.05915}{n} \log \sum_{j=k}^{n} k_0 \ldots k_j [X]^j + \frac{0.05915}{n} \log \frac{i_d}{i_k} \quad \ldots\ldots 54$$

where the concentration of electroactive complexes is much less than the electro-inactive complexes. This expression also assumes the diffusion coefficients of metal and complex to be the same. Taking into account the formation of reducible complexes with ligand Y equation 54 becomes:

$$\Delta E_{1/2} = \frac{-0.05915}{n} \log \left\{ \sum_{j=0}^{n} k_0 \cdots k_j [X]^j + \sum_{j=1}^{p} k'_1 \cdots k'_j [Y]^j \right\}$$

$$+ \frac{0.05915}{n} \log \frac{i_d}{i_k} \qquad \text{.....55}$$

where the last term of equations 53-55 makes a kinetic current correction to the diffusion controlled equation. Equations 48-55 will be applied to the data obtained in this investigation in a later section, with slight modifications.

CHAPTER 4

EXPERIMENTAL

A. Materials

DTPA was obtained from the J.T. Baker Chemical Co. It was recrystallized from hot water, dried at 110°C overnight and dissolved in distilled water by the addition of sodium hydroxide to make up the stock solutions. Except for DTPA, all chemicals used were of reagent grade and hence not further purified. Chloroacetic acid and sodium hydroxide were used to buffer the solution from pH = 2.00 to pH = 4.00. From pH = 4.00 to 7.00 acetic acid and sodium acetate were used as buffers. Cadmium acetate (J.T. Baker Chem. Co.) was used to prepare stock solutions of cadmium. Lead nitrate (Fisher Scientific Co.) was used to prepare stock solutions of lead. Sodium perchlorate was used to adjust the ionic strength. The maximum suppressors used were TX100 (Rohm and Haas Co.) and gelatin (BDH).

Triply distilled mercury (Shawinigan Chem. Co.) was used for the dropping mercury electrode. Neoprene tubing was used to connect the various parts of the electrode assembly as shown in Figure 2. The best grade of commercial nitrogen was used to remove oxygen from the solutions under investigation. All solutions were stored in polyethylene bottles because DTPA does slowly attack glass given enough time.

B. Solutions

3.9335 gm. of DTPA was weighed out and dissolved in distilled water to a volume of one liter. Since the solubility of DTPA is only 0.5 gm. per 100 ml. of water at 20°C some sodium hydroxide had to be added to make it soluble. This 0.01 M stock solution of DTPA was used to make up the various solutions under study.

0.10 M and 0.01 M stock solutions of cadmium were prepared by weighing out the appropriate amount of cadmium acetate and dissolving in distilled water. 1.00 M stock solutions of chloroacetic acid and acetic acid were used as buffers in the pH ranges of 2.0 - 4.0 and 4.0 - 7.0 respectively. The pH of individual solutions was adjusted by addition of either sodium hydroxide or perchloric acid solutions.

0.5 gm. of gelatin was dissolved in 100 ml. of distilled water to make a 0.5% stock solution. This had to be warmed at 65°C for at least a half an hour to be completely soluble. Furthermore the gelatin solution was prepared frequently to avoid using a "stale" solution. A 0.2% TX100 stock solution was prepared similarly. This solution was stable during the time of the study (3 yrs.), in fact Meites[24] claims TX100 is stable for at least 10 years.

C. Equipment

A Sargent Model XXI Polarograph was used for this study. The polarograms were recorded by a Brown strip chart recorder and all potentials recorded were checked by a Rubicon type B precision potentiometer, in conjunction with a Leeds and Northrup type E galvanometer.

An H-cell as shown in Figure 2 similar to the one described by Lingane and Laitinen[24] was employed. One compartment of the H-cell contained a saturated calomel reference electrode. This electrode was prepared by adding pure mercury to the reference compartment to give a layer 2 cm. deep. The mercury was then covered with an equally thick layer of a paste made by mixing equal weights of mercurous and potassium chlorides in a few milliliters of saturated potassium chloride. Finally the compartment was filled with a saturated solution of potassium chloride containing a large excess of solid salt. Electrical connection to the calomel compartment was made in the usual fashion with a platinum wire sealed in a glass tube as shown in Figure 1. The second compartment contained the solution under investigation and the dropping mercury electrode (d.m.e.). The two compartments were separated by a sintered glass disc fused into the middle of the connecting arm. To avoid any mixing of solution into the calomel compartment or vice versa, an agar plug was inserted on the reference side before the calomel electrode was prepared. The plug consisted of a 4% solution of agar in saturated potassium chloride.

The dropping electrode assembly as shown in Figure 2 consisted of a capillary and column of mercury above it. Marine barometer tubing obtained from E.H. Sargent Co. (#S - 29417) was used. The capillary

tubing used was 18.5 cm. long. It was connected to the stand-tube with neoprene tubing which is less likely to contaminate mercury than rubber tubing. The stand-tube and mercury reservoir were of the standard type as shown in Figure 2. A shortened meter stick was fastened to the glass tubing in such a way that it read the height of mercury directly. The mercury reservoir could be raised and lowered to any desired position. This was facilitated by a home-made rack and pinion welded to the reservoir holder. All neoprene tubing connections were tightened by wire to prevent breaks and the spilling of mercury. The electrical connection to the mercury reservoir was similar to the calomel connection.

The water thermostat bath (18"L, 10"W, 12"D) was controlled at 25°C and other specified temperatures by a commercial Tecam temperature control. Effective circulation of the water was maintained by having a stirrer housed within the heating-coil unit. The temperature was maintained within $\pm$.1°C, sufficiently accurate for polarographic work since the diffusion currents usually vary only by 1.5%/°C. The water bath was grounded and the stirrer turned off for all polarographic runs. The latter precaution was necessary because the electrode assembly experienced small vibrations from the stirring action. The D.M.E. is very sensitive to vibrations and hence all precautions were taken to avoid them.

D. Procedure

To illustrate the general technique in detail a typical example is given for a solution of Cd: DTPA in the ratio of 2:1. 25.00 ± .05 ml. of 0.01M DTPA stock solution and 50.00 ± .05 ml. of 0.01M cadmium stock solution were delivered into a 400 ml. beaker. Then 25 ml. each of 1.00 M sodium perchlorate stock solution and 1.00 M acetic acid buffer were added to the solution. This brought the ionic strength μ = 0.2 as seen later. Distilled water was added to make approximately 200 ml. Then the solution was checked for its exact pH value, and sodium hydroxide or perchloric acid added as needed. These additions were negligible in concentration when compared to μ = 0.2. After the pH adjustment enough distilled water was added to make exactly 250 ml. Hence, the concentration of cadmium and DTPA were 0.002M and 0.001M respectively. This solution was allowed to come to equilibrium overnight though this seemed to be instantaneous.

From this prepared solution 25 ml. were placed in the H-cell. The H-cell when not in use contained saturated potassium chloride solution. The solution compartment was cleaned before and after each run by flushing with distilled water, spraying the inside with dilute nitric acid and finally rinsing with five 20 ml. portions of distilled water.

Next the H-cell was lowered into the water bath as shown in Figure 3. Then 0.10 ml. (2 drops) of 0.5% gelatin stock solution was added to give a 0.002% gelatin concentration. This was necessary especially in the pH range from 2.00 - 4.00 where "maxima" were located. Then nitrogen was slowly bubbled through a wash bottle containing a 0.2M solution of

sodium perchlorate and then passed through the test solution. This was done to saturate the nitrogen gas with water vapor to prevent the evaporating of an appreciable quantity of the test solution during the oxygen removal period. Fifteen minutes was sufficient time to remove the oxygen. After this the nitrogen was passed over the top of the solution to prevent oxygen from redissolving into the solution during the time of a polarographic run.

The next step was to lower the d.m.e. into the solution compartment and raise the level of the mercury reservoir to 60 cm. above the tip of the capillary as indicated by the attached meter stick on the stand-tube. This was done with an accuracy of better than $\pm$ 1 mm.

Then the polarograph, which was on "stand-by" at all times was adjusted. A sensitivity of 0.04 μA/mm was most frequently used in order to obtain diffusion currents of the order of a few microamps (μA). A voltage span of 0.00 - 2.00 volts was necessary for the investigation due to the reduction potential value of the metals and their complexes. Finally the instrument was turned "on" and a typical polarogram obtained as shown in Figure 8. The potential at various intervals was checked by a Rubicon potentiometer. This was achieved by stopping the recorder and turning the e.m.f. to "constant". The exact potential to $\pm$ .2 millivolt (mV) was marked on the chart paper and proper corrections made during the analysis of the data. Most solutions were run a number of times in order to check reproducibility. The solutions were also run at mercury heights of 50, and of 70 cm., except for the pressure studies where the intermediate heights of 55,65 and 75 cm. were also used.

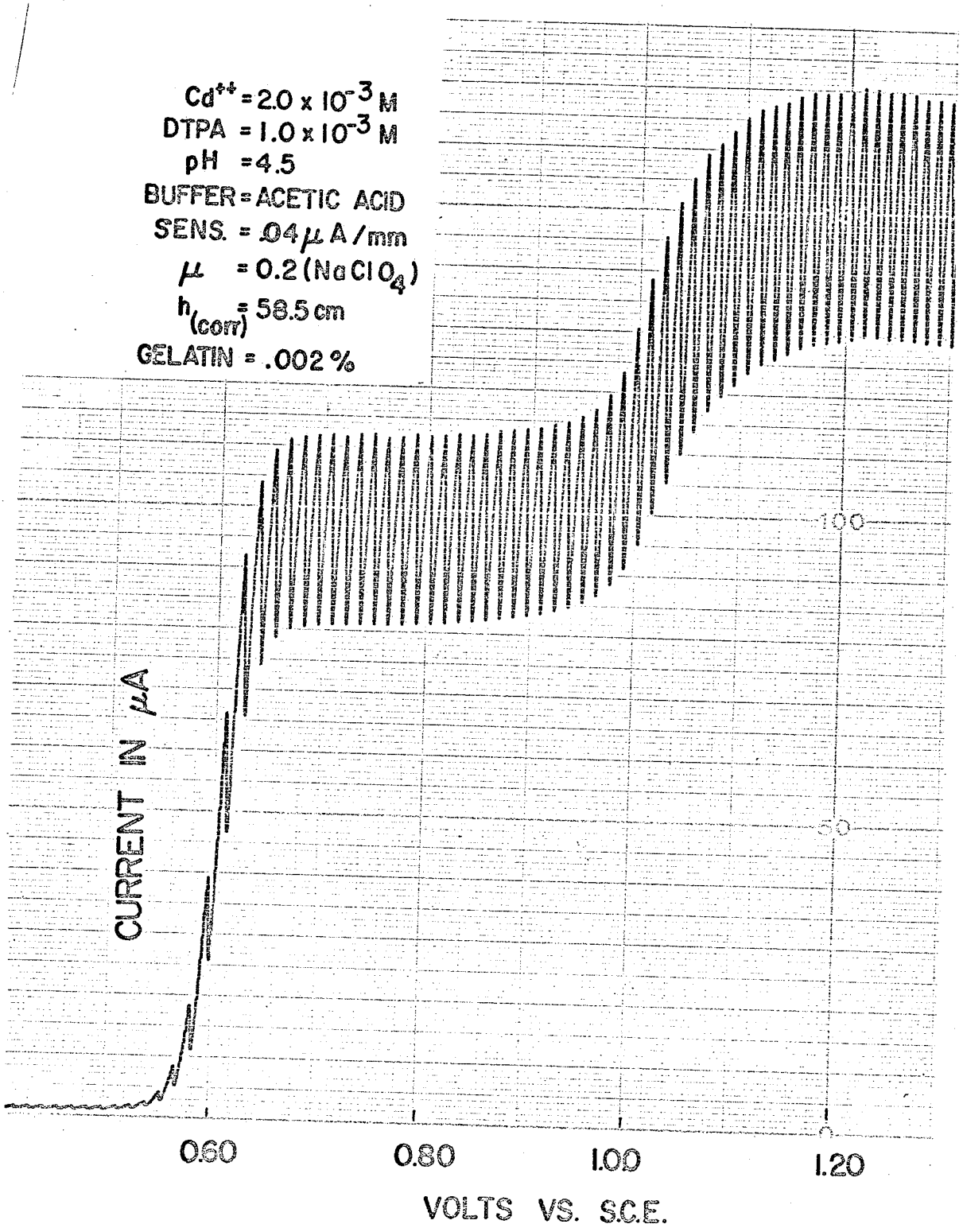

FIG. 8 POLAROGRAM OF Cd - DTPA

RESULTS

A. DROP-TIME STUDIES - Capillary Characteristics

The Ilkovic equation predicts that the diffusion current of a reversible wave depends directly on $m^{2/3} t^{1/6}$, (see Eq'n 12) termed the capillary characteristics. Thus the capillary characteristics must be given in order to be able to compare the polarographic results with similar work being done by other investigators. The variation of m and t with mercury pressure has been discussed by Los and Murray[30]. They refer to the Poiseuille equation, which points out the fact that m depends on the "effective pressure" of mercury. The effective pressure, or usually called "corrected pressure" of mercury, can be obtained by correcting for the interfacial tension between mercury and solution and by subtracting the back hydrostatic pressure of the solution. By taking an average value of 400 dynes/cm for the interfacial tension and combining the numerical constants for 25° C, they obtained an equation for the corrected mercury pressure (h_{corr}):

$$h_{corr} = h_{Hg} - \frac{h \text{ sol'n } d \text{ sol'n}}{13.5} - \frac{3.1}{mt^{1/3}} \quad \ldots\ldots\ldots 56$$

where h_{Hg} is the direct reading of the mercury height. The last term on the r.h.s. gives the back pressure due to interfacial tension at the drop surface. The second term is due to hydrostatic back pressure of the solution, and usually is only 1 or 2 mm.

In this investigation the capillary tip was immersed in the

test solution to a depth of approximately 15 mm. Hence the hydrostatic pressure correction was slightly over 1 mm. The product of mt for the capillary used was 8.698, which gave an interfacial tension correction of 1.508 cm. Therefore

$$h_{corr} = h_{Hg} - (.10) - 1.508$$

with an approximate correction value of 1.60 cm used throughout this work due to the fact that the mercury height on the meter stick could only be read with an accuracy of $\pm$ 1 mm. The capillary characteristics are given below for the heights of mercury most often used.

h_{Hg} cm	h_{corr} cm	m mg/sec	t sec	mt	$m^{2/3} t^{1/6}$
50	48.4	1.733	5.02	8.699	1.8867
60	58.4	2.071	4.20	8.698	2.0640
70	68.4	2.396	3.63	8.697	2.2171

The above measurements of m and t were made with an open circuit and the capillary dipped into a solution of Cd-DTPA, where $Cd^{++} = 1.0 \times 10^{-3}$ M, DTPA = 2.0×10^{-3} M. This was done to obtain the capillary characteristics in a medium similar to the experimental conditions used later. The time was recorded for 50 drops of mercury to fall from the capillary, the mercury dried and weighed to obtain m in the table above.

The effects of the corrected mercury pressure, h_{corr}, on m and t are such that $m^{2/3}\ t^{1/6}$ is proportional to $h_{corr}^{1/2}$ [23]. It follows from the Ilkovic equation

$$i_d = 607\ n\ D^{1/2}\ C\ m^{2/3}\ t^{1/6}$$

that the diffusion current (i_d) is proportional to $h_{corr}^{1/2}$. Hence the ratio of $i_d/h_{corr}^{1/2}$ must be constant for a given concentration of reducible species. The ratio of $i_d/h_{corr}^{1/2}$ provides a convenient check as to whether or not a particular wave is diffusion controlled and was used frequently in later sections.

To determine how many electrons are involved in a particular reduction step one can employ equation 22 :

$$E_{d.m.e.} = E_{1/2} - \frac{.05915}{n} \log \frac{i}{(i_d - i)}$$

A plot of $\log \frac{i}{(i_d - i)}$ vs. $E_{d.m.e.}$ should yield a straight line having a slope of $\frac{0.05915}{n}$, from which n can be calculated. Secondly if the ratio $\frac{0.05915}{n}$ is not approximately 60, 30 or 20 mV, i.e. integral values of n = 1, 2 or 3, the reduction step is irreversible and likely controlled by chemical reactions preceding reduction. Hence the plot of $\log i/(i_d - i)$ vs. $E_{d.m.e.}$ is a a standard check for reversibility of a reduction step in polarography.

B. SUPPRESSOR STUDIES

Polarograms of Cd-DTPA and Pb-DTPA solutions exhibited a maximum from pH = 2.00 to pH = 4.00. This maximum could easily be suppressed by the addition of gelatin or TX-100. After a close study of suppressor effects on the polarographic waves, gelatin was chosen for the Cd-DTPA and TX-100 for Pb-DTPA solutions, because one suppressor seemed to perform better than the other for the two metal-ligand solutions involved. A detailed suppressor study is shown in Figures 9 and 10 for Cd-DTPA.

Free cadmium was virtually unaffected by gelatin concentations below 0.003%, whereas the Cd-DTPA wave was lowered substantially by that amount of suppressor. The maximum concentration of gelatin was needed around pH = 3.0 and here 0.002% was sufficient. This amount of gelatin caused no distortion in the overall wave nor on the current-voltage wave of any individual drop. It was discovered that an excess of suppressor deformed the top (maximum value) of an oscillation, while too little suppressor would cause erratic behavior on the bottom (minimum value) of an oscillation. Hence it was relatively simple to add just enough suppressor at any given pH to obtain well defined waves. Most solutions were also run

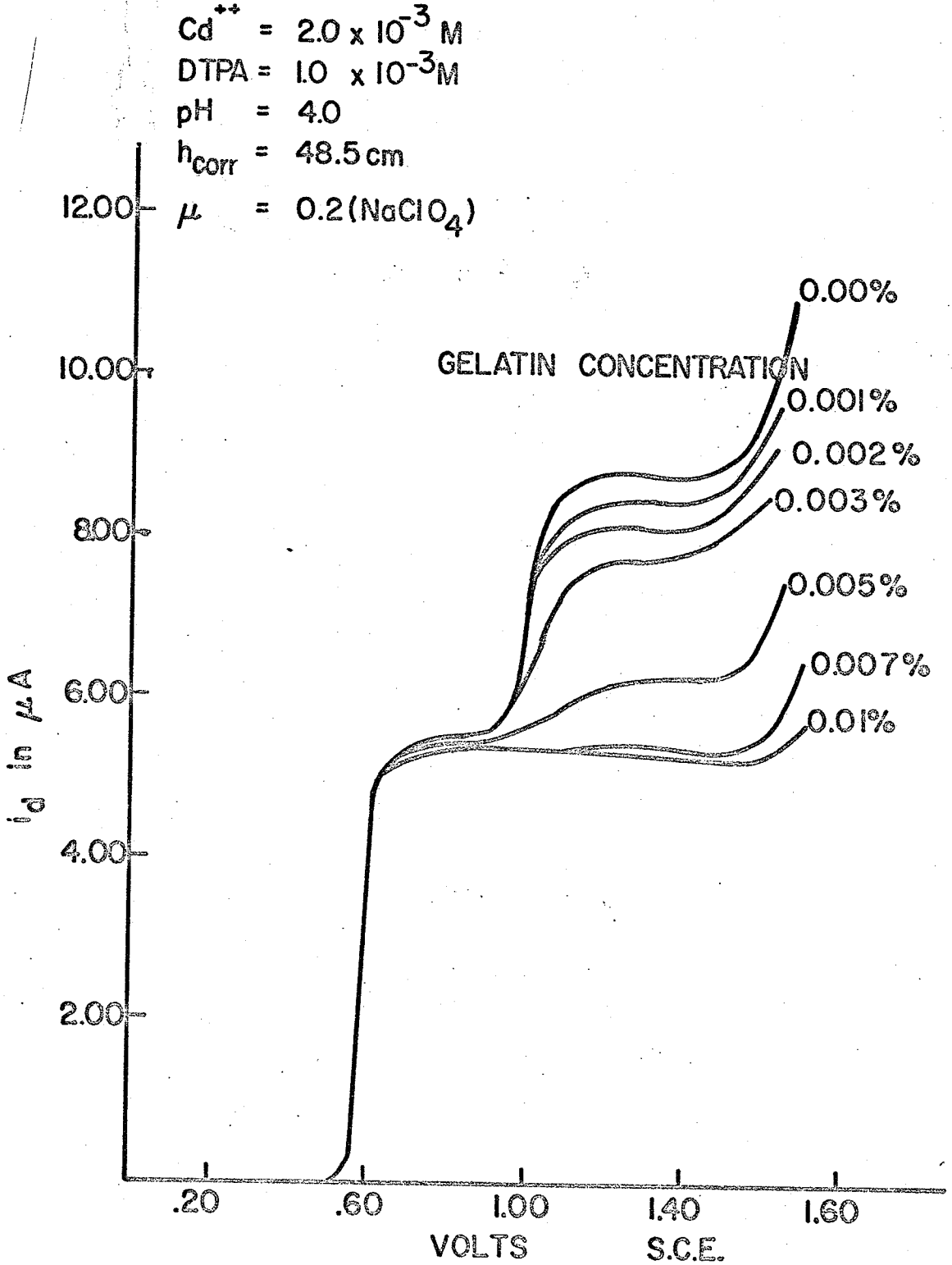

FIG. 9 SUPPRESSOR EFFECT ON Cd - DTPA

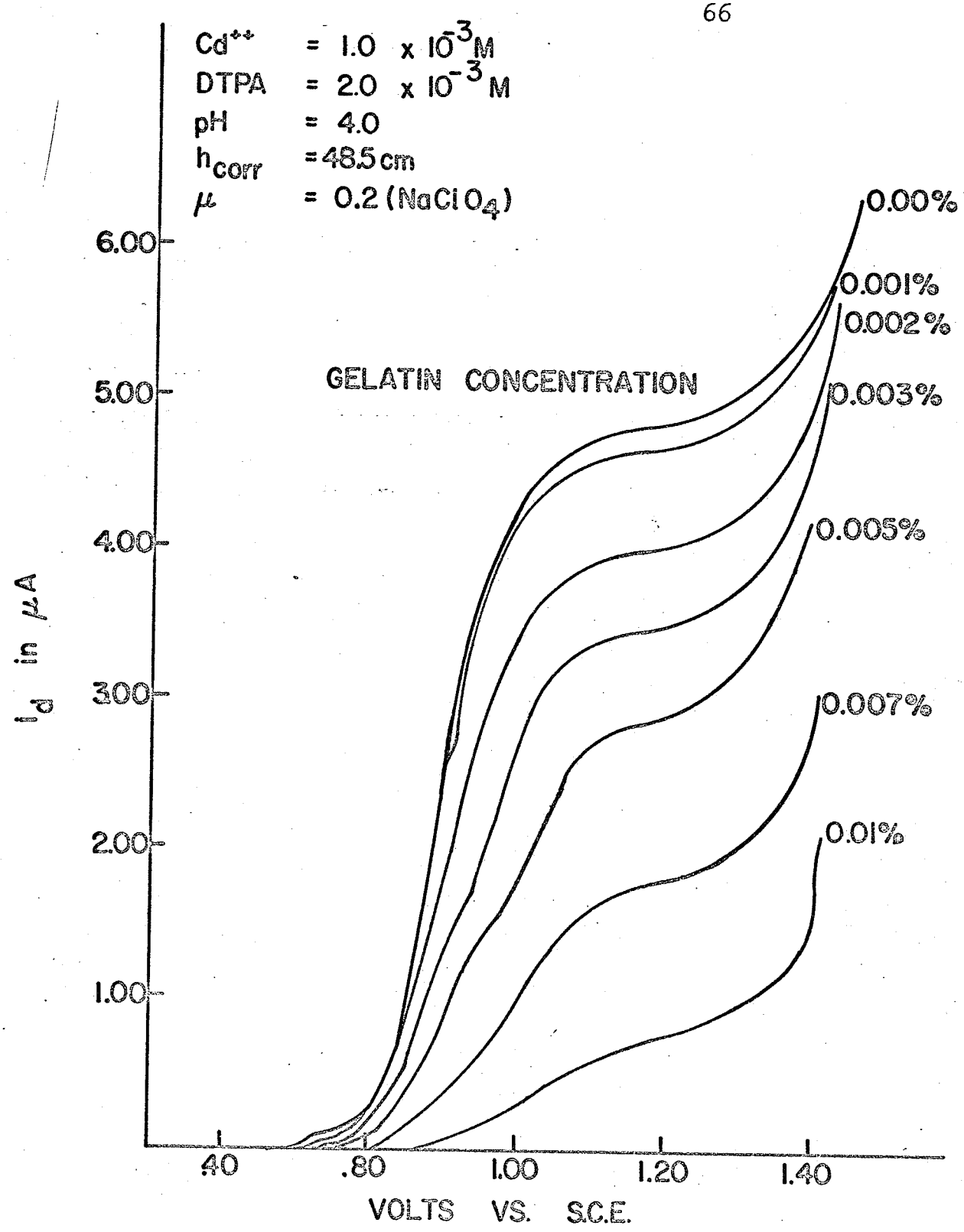

FIG. 10 SUPPRESSOR EFFECT ON Cd - DTPA

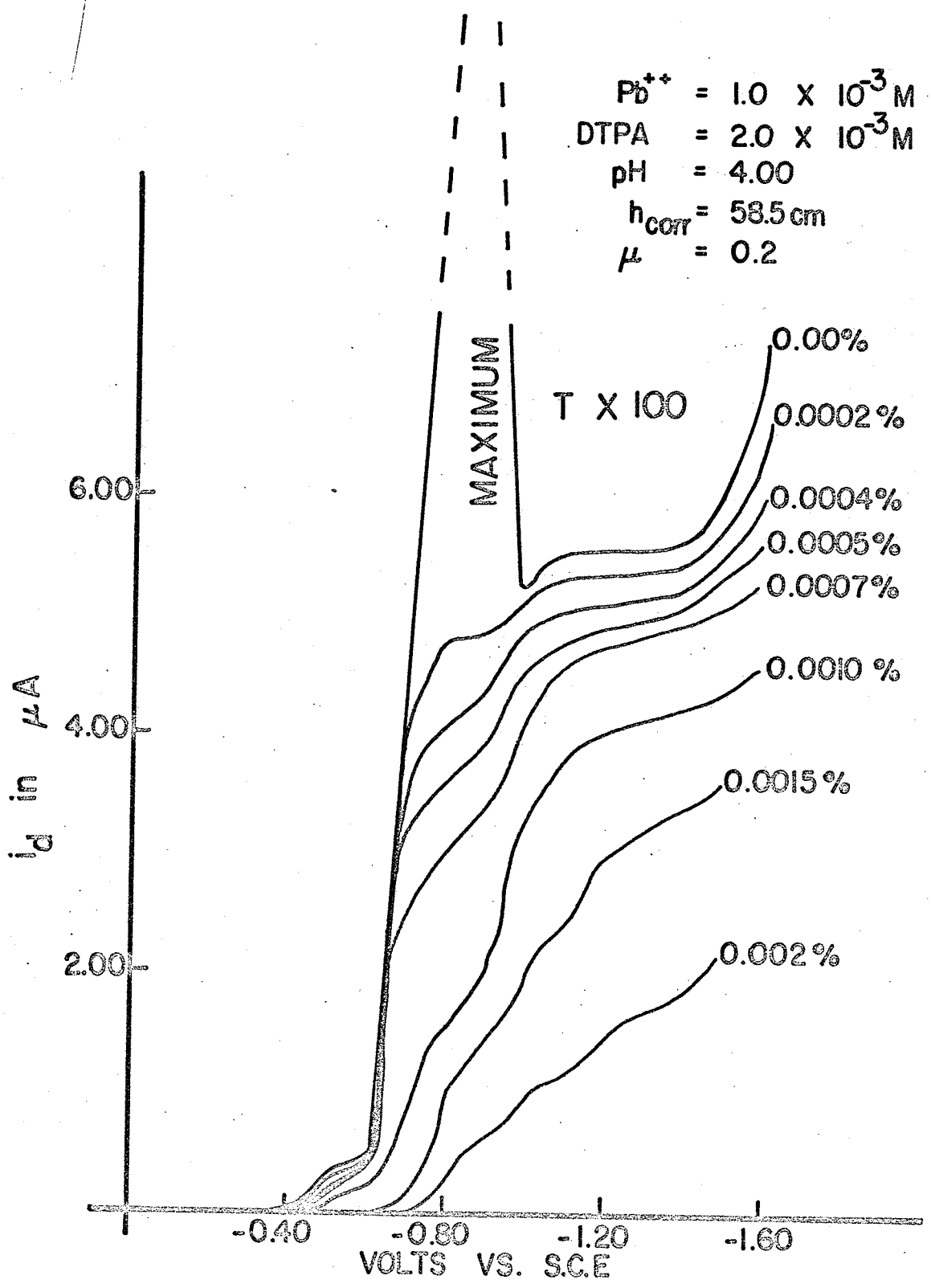

FIG. II SUPPRESSOR EFFECT ON Pb - DTPA

with a constant amount of gelatin (.002%) to compare the behavior of both techniques.

TX-100 (TX-100 < 0.003%) had little effect on free lead but suppressed the complex wave significantly. A study of the suppressor effect on Pb-DTPA is given in Figure 11. These solutions proved to be quite different from the Cd-DTPA solutions, in that the lead complex waves could not be uniformly suppressed by TX-100. There were two sensitive areas in the maximum, one at -0.60v and the second around -0.75v. The first maximum could be suppressed with 0.0006% TX-100 and the second with 0.0014% TX-100. Hence a compromise was taken, that of 0.001%. This controlled the second area at the expense of suppressing the first, yet the polarograms were not distorted.

C. DIFFUSION CURRENT CONSTANTS

Polarograms were run of various concentrations for free metal ion against constant pH, h_{Hg}, suppressor and temperature. The diffusion current constants were calculated according to equation 13,

$$I_d = \frac{i_d}{C\, m^{2/3}\, t^{1/6}}$$

The results and experimental conditions are given below.

TABLE 1 Diffusion Current Constant of Cd^{++}

$[Cd^{++}]$ moles/liter	i_d μA	$C\, m^{2/3}\, t^{1/6}$	$I_d = \frac{i_d}{C\, m^{2/3}\, t^{1/6}}$
1.0×10^{-4} M	0.68	0.2064	3.29
4.0×10^{-4} M	2.71	0.8256	3.27
5.0×10^{-4} M	3.40	1.0320	3.29
8.0×10^{-4} M	5.52	1.6512	3.34
1.0×10^{-4} M	7.03	2.0640	3.40

Average $I_d = 3.33 \pm .07$

Experimental conditions: pH = 3.00, μ = 0.2, gelatin = 0.002%, h_{corr} = 58.4 cm and $m^{2/3}\, t^{1/6}$ = 2.064

When the concentration of cadmium was kept constant and the pH varied from 2.0 to 6.0, a similar value for I_d was obtained. At low pH the I_d value was higher (3.45) than the average value (3.35) and at high pH the opposite was true (I_d = 3.25).

The diffusion current constants for Cd-DTPA complexes vary from zero to a maximum value of 2.5, depending on pH and metal to ligand concentration ratio. The reason being that various complexes form at certain pH intervals and some complexes do not reduce under the experimental conditions used.

Free lead exhibited a similar diffusion current constant I_d, when compared to cadmium under identical experimental conditions. The results are tabulated below.

TABLE 2 Diffusion Current Constant of Pb^{++}

$[Pb^{++}]$ moles/liter	i_d in μA	$C\, m^{2/3}\, t^{1/6}$	$I_d = \frac{i_d}{C\, m^{2/3}\, t^{1/6}}$
1.0×10^{-4} M	0.73	0.2064	3.53
2.0×10^{-4} M	1.45	0.4128	3.51
4.0×10^{-4} M	2.88	0.8256	3.48
8.0×10^{-6} M	6.00	1.6512	3.63
1.0×10^{-3} M	7.44	2.0640	3.60

Average $I_d = 3.55 \pm .08$

Experimental conditions: pH = 3.00, μ = 0.2, TX-100 = 0.001%, h_{corr} = 58.4 cm and $m^{2/3}\, t^{1/6}$ = 2.064.

D. METAL-LIGAND CONCENTRATION STUDY

Polarograms were run for metal to ligand concentration ratios ranging from 5:1 to 1:10 as shown in figures 12 and 13. These solutions were prepared by keeping the metal concentration constant and increasing the DTPA concentration. The first wave (later called wave A) in figure 12 had an $E_{1/2}$ value of $^{-}0.62$ v. vs. S.C.E., i.e. a free Cd^{++} wave. The $E_{1/2}$ of this wave was virtually independent of DTPA concentration which was further evidence that the Cd^{++} ions were not coming from a complex, such as Cd_2 (DTPA), [22] for if this were the case the $E_{1/2}$ would shift toward more negative values with an increase of DTPA. The cadmium wave was found to be reversible, diffusion controlled and slightly dependent on pH. The cadmium wave height decreased with an increase of DTPA until it disappeared at the 1:1 concentration ratio. The second wave increased as the DTPA concentration increased reaching a maximum at the 1:1 concentration ratio. This second wave (later called wave C) was poorly shaped or "ill defined" and showed evidence of a third wave (later called wave B) at its base. The $E_{1/2}$ of the second wave was $^{-}1.05$v vs. S.C.E. at the 1:1 ratio and increased to $^{-}1.10$ v at the 1:10 ratio. The $E_{1/2}$ of the third wave was $^{-}0.88 \pm .01$ v vs. S.C.E. Each of the above waves will be examined in detail later.

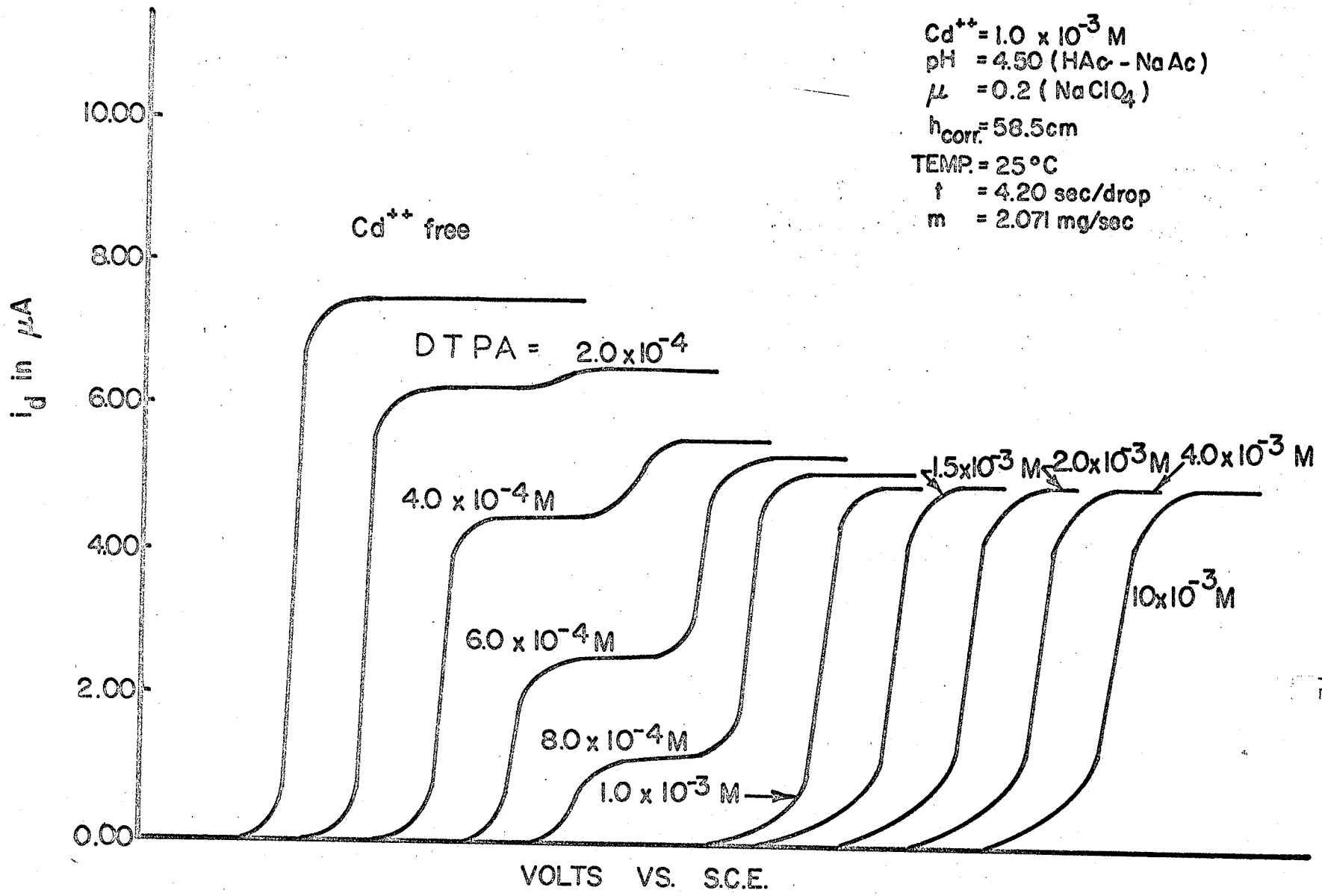

FIG. 12 Cd-DTPA CONCENTRATION STUDY

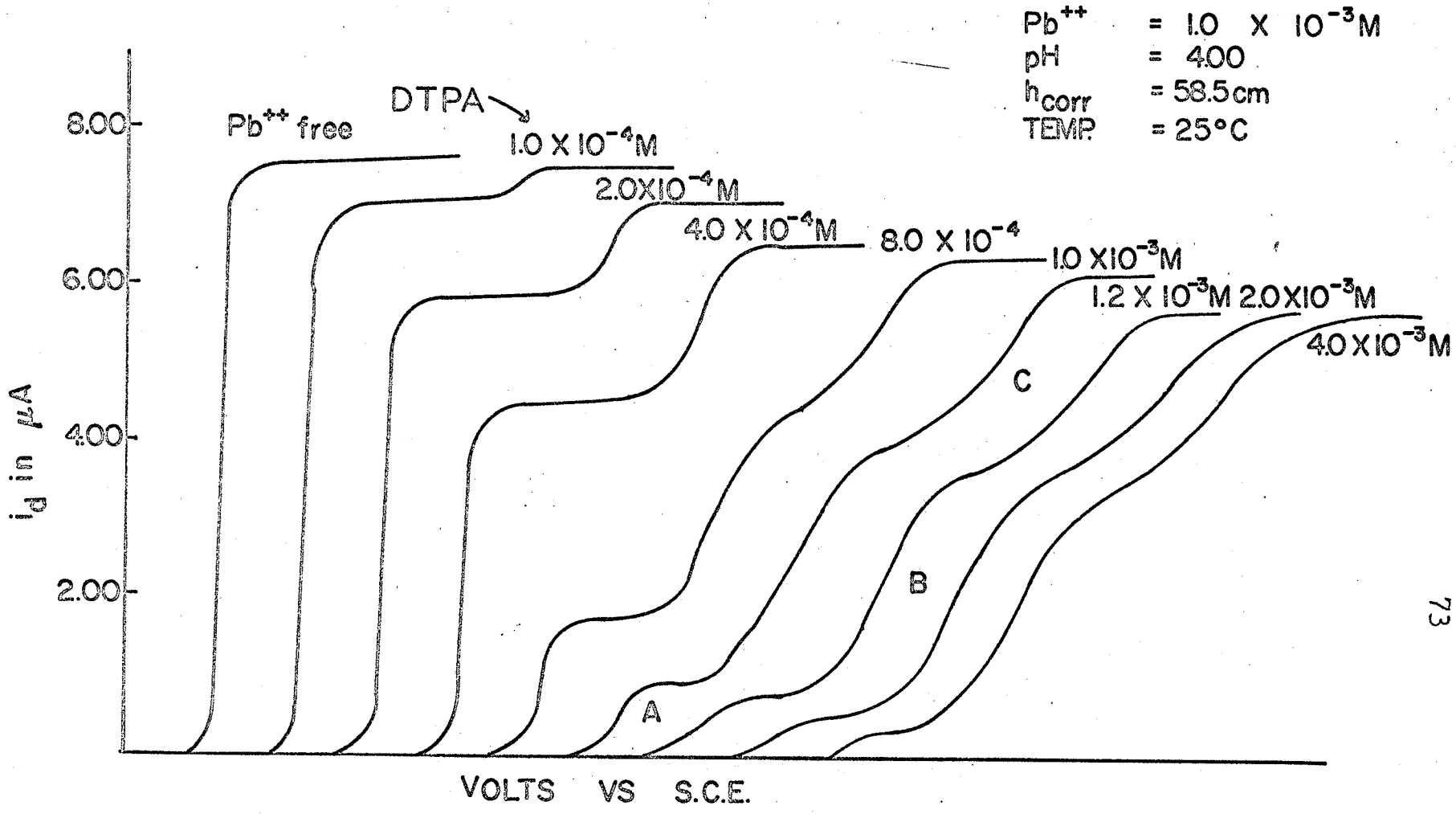

FIG. 13 Pb - DTPA CONCENTRATION STUDY

Figure 13 shows a similar set of polarograms for Pb-DTPA solutions. Again the first wave (wave A) was due to free lead and it slowly diminished as the DTPA concentration was increased to a 1:1 ratio, where virtually all of the lead was complexed by DTPA. The Pb-DTPA complexes formed only reduced at higher negative potentials just as the Cd-DTPA complexes showed in figure 12. Thus for Pb-DTPA (at a 1:1 ratio) at pH = 4.00, three distinct reduction waves were observed at approximately $^{-}$0.50, $^{-}$0.70 and $^{-}$0.90v respectively. Since the behavior of these metal-ligand solutions was highly pH dependent, these solutions (ratio 1:1, 1:2, etc.) will be discussed individually in the following sections.

E. VARIOUS pH STUDIES

a) Free Metal Solutions

Polarograms were obtained from cadmium and lead solutions of varying concentration while the pH, ionic strength, buffer and suppressor were kept constant. The $E_{1/2}$ values were obtained by a log-plot method as shown in figure 1. The results are tabulated below.

Table 3 $E_{1/2}$ of Cadmium and Lead.

M^{++} moles/liter	$-E_{1/2}$, Cd^{++}	$-E_{1/2}$, Pb^{++}
2.0×10^{-4}	$0.607 \pm .002$V	$0.434 \pm .002$V
4.0×10^{-4}	0.610 "	0.437 "
6.0×10^{-4}	0.608 "	0.435 "
8.0×10^{-4}	0.611 "	0.433 "
1.0×10^{-3}	0.609 "	0.436 "
Average	$0.609 \pm .004$V	$0.435 \pm .004$V

Experimental conditions: pH = 4.0, μ = 0.2, acetate buffer, Suppressor; gelatin = 0.002% for Cd^{++}, TX-100 = 0.001% for Pb^{++} Temp = 25°C and h_{Hg} = 60 cm.

Next the concentration of the metal was kept constant and the pH varied from 2.0 to 6.0. These results are tabulated in table 4 and shown in figure 14.

Table 4 $E_{1/2}$ of free metal vs. pH.

pH	$-E_{1/2}$ vs. S.C.E. - Cd^{++}	$-E_{1/2}$ vs. S.C.E. - Pb^{++}
2.00	0.602 ± .002V	0.417 ± .002V
2.50	0.604 "	0.420 "
3.00	0.606 "	0.424 "
3.50	0.607 "	0.429 "
4.00	0.609 "	0.435 "
4.50	0.611 "	0.440 "
5.00	0.613 "	0.446 "
5.50	0.615 "	0.448 "
6.00	0.617 "	0.452 "

Experimental Conditions: μ = 0.2 ($NaClO_4$), acetate buffer, gelatin = 0.002% for Cd^{++}, TX-100 = 0.001% for Pb^{++}, Temp = 25°C, and h_{Hg} = 60 cm.

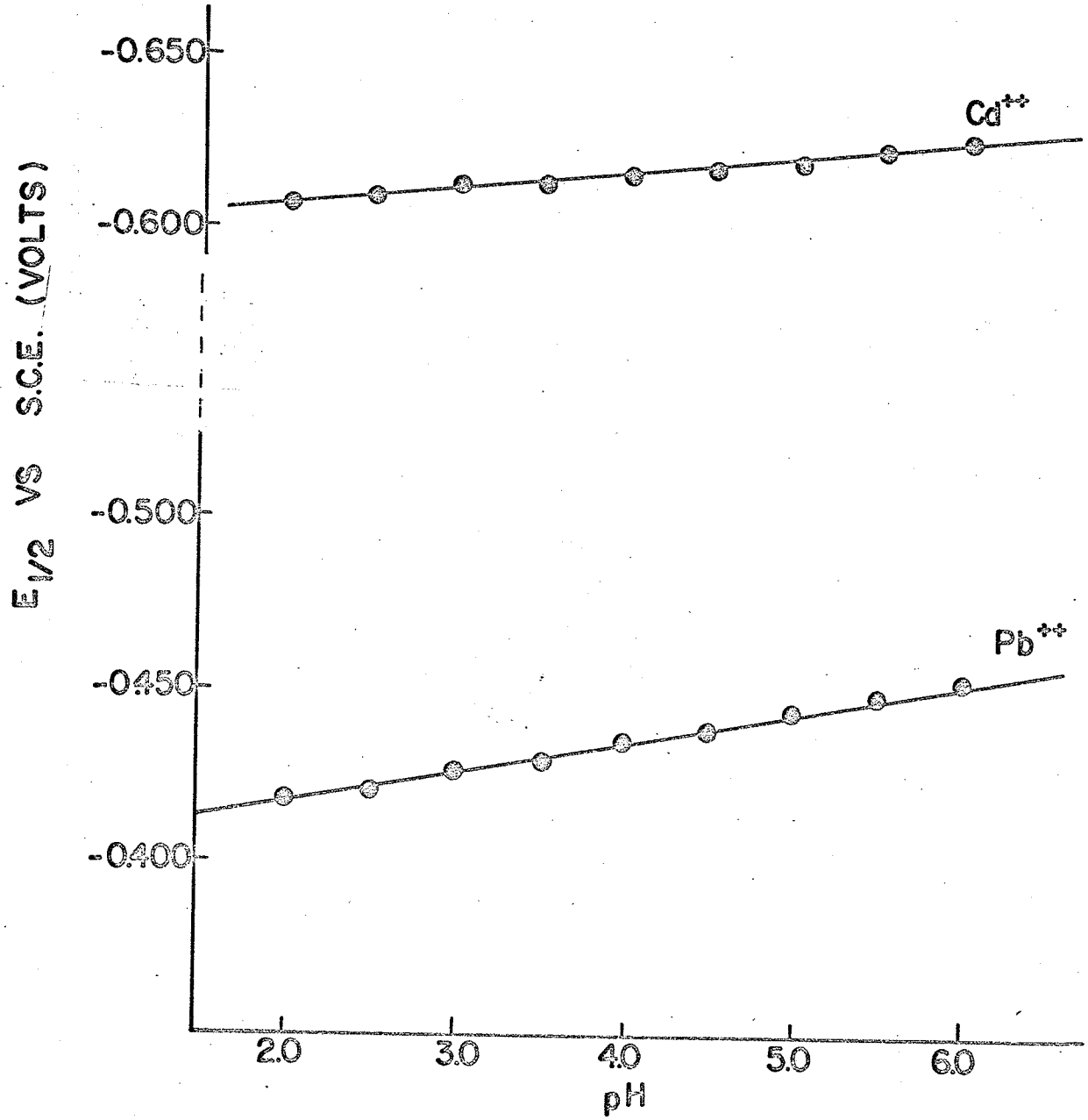

FIG. 14 $E_{1/2}$ OF FREE METAL VS pH

(b) Cd-DTPA ratio of 2:1

An excess of ligand to metal concentration is required for the usual polarographic calculations (reaction rates, mechanisms and stability constants) involving complex equilibria. Hence this part of the investigation, with an excess of metal to ligand, is recorded for general information only. Figure 15 shows a number of Cd-DTPA polarograms for a metal to ligand ratio of 2:1. The first reduction wave ($E_{1/2} \approx -0.62$v) is due to free cadmium and the second wave ($E_{1/2} \approx -1.10$v) is presumably due to a Cd-DTPA complex. From the heights of the two reduction waves it can be concluded that one half of the cadmium is free and the other half complexed to DTPA. If a 2:1 complex formed (there was no evidence for a 2:1 complex in this study) under these conditions it would have to dissociate readily (unstable or labile complex) into free cadmium ions and a 1:1 complex to fit the experimental data.

An increase of pH shifts the half-wave potential of the second wave to larger negative values (figure 15). This indicates an increase in the stability of the complex with an increase in pH which is expected for metal-aminopolycarboxylic acid complexes. With an increase in pH the reducible Cd-DTPA complex slowly changed into a non-reducible complex, which in turn caused the complex wave height to diminish (figure 15) until finally at pH = 6.5 no complex reduction could be observed at all.

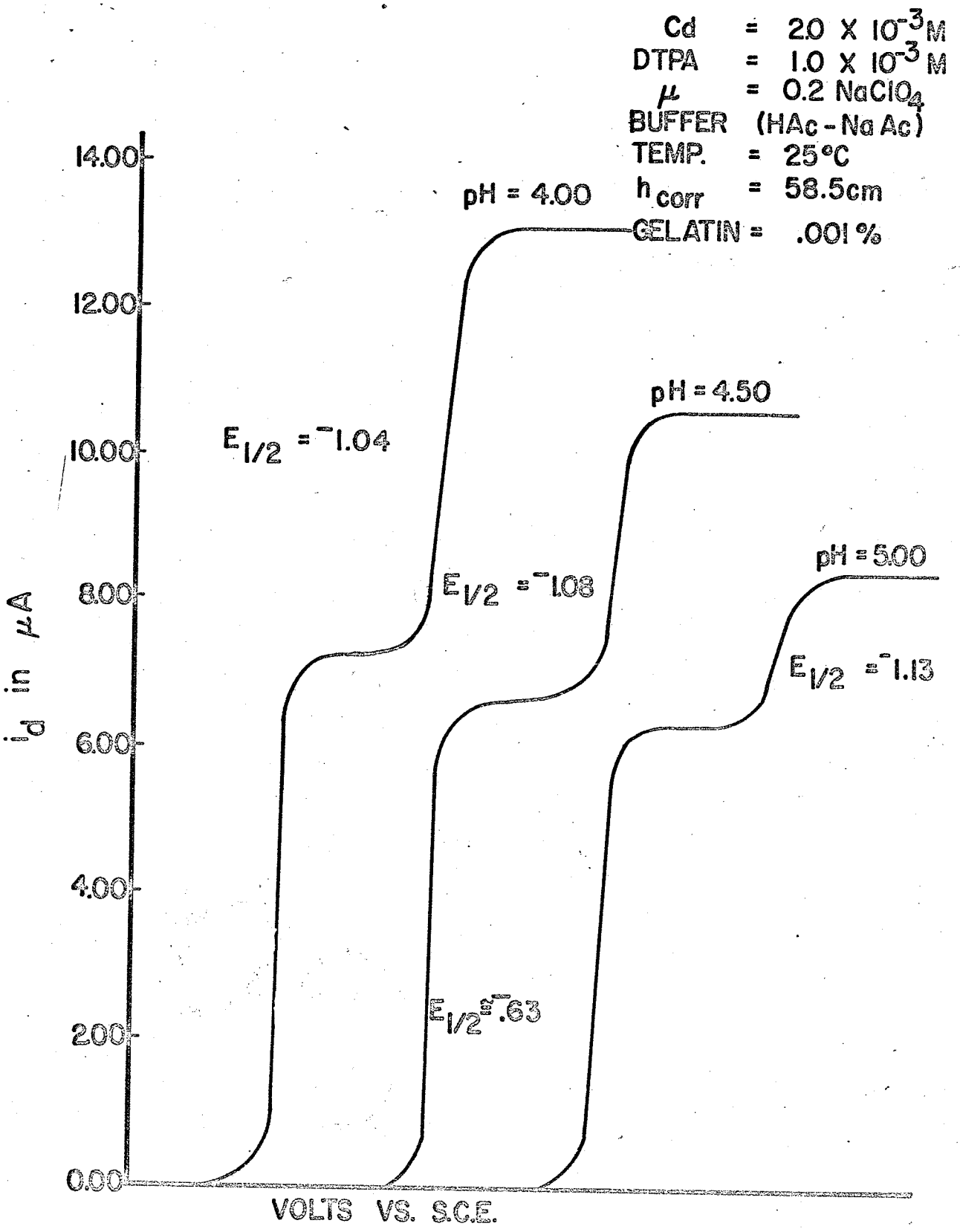

FIG. 15 A pH STUDY OF Cd-DTPA (2:1).

(c) Cd-DTPA ratio of 1:1

Figure 16 illustrates a pH study of the equimolar Cd-DTPA solutions. At low pH (pH < 2.0) essentially free cadmium exhibited a reduction wave A. Wave A was reversible and diffusion controlled at average wave height (i_d > 1.0μA). At a pH = 2.50 it split into two reduction waves, the second wave, labelled B, was presumably due to a protonated Cd-DTPA complex. Later at pH = 3.50, wave A had decreased considerably in height, and wave B was separating into two different reduction steps as shown in figure 16. The third reduction wave, labelled C, being due to a second Cd-DTPA complex, was more stable than the first complex judging from the larger negative half-wave potential. Wave C slowly decreased in height with an increase of pH until finally it disappeared at pH = 6.50, indicating that the reducible complex had slowly changed into a non-reducible complex.

Except for wave A the reduction waves were ill-defined making accurate measurements ($E_{1/2}$ and i_l) extremely difficult. The individual wave heights were difficult to measure especially in the pH range from 3.00 to 5.00. In general the half-wave potentials (for metal-ligand solutions) were measured with a precision ± .005 volts, and the wave heights (i_l, limiting currents which include both diffusion controlled and kinetic controlled currents) to approximately ± 2%. The halfwave potentials and wave heights are recorded in table 5.

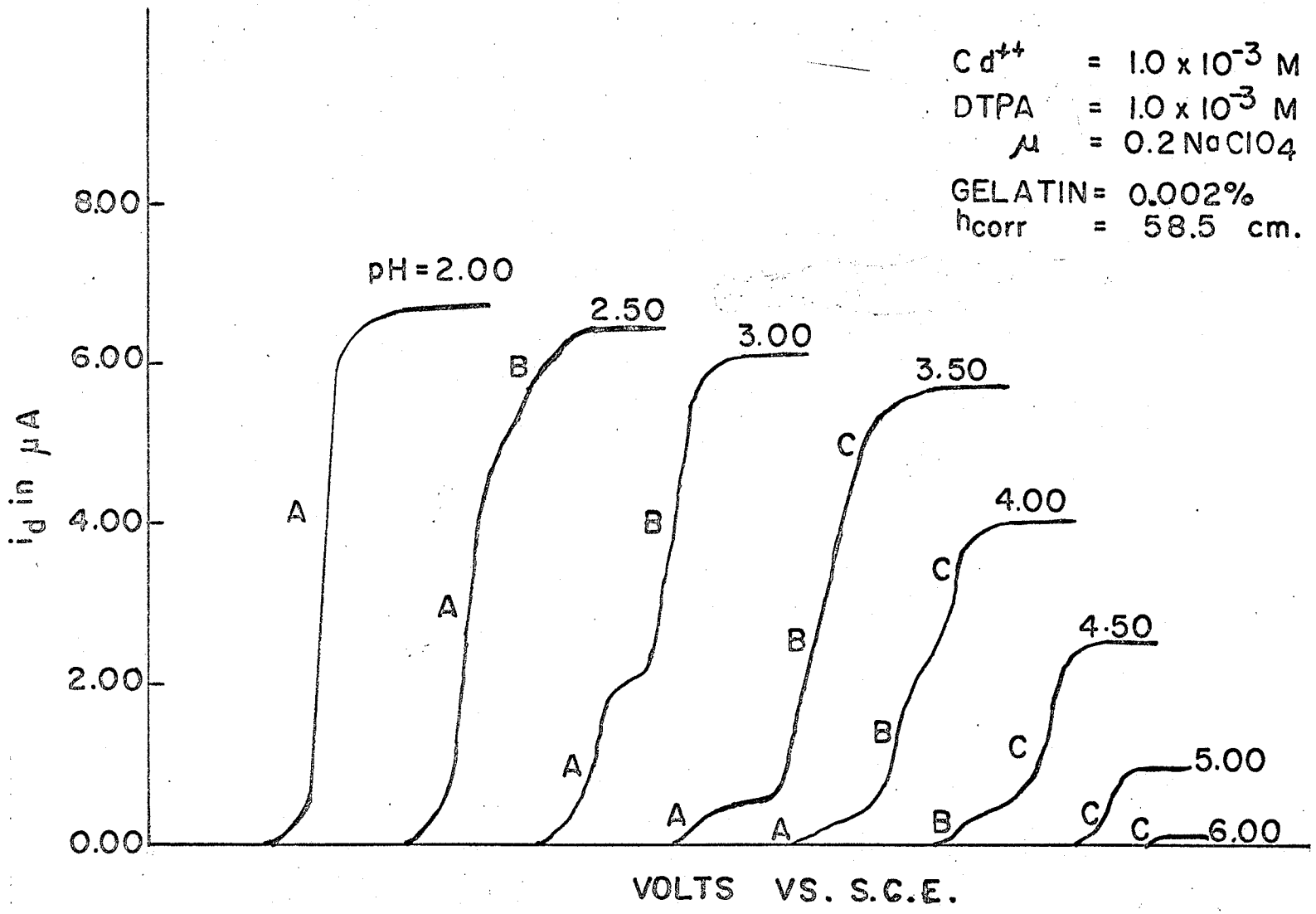

FIG. 16.

A pH STUDY OF Cd-DTPA (1:1).

Table 5 $E_{1/2}$ and i_l for Cd-DTPA (1:1)

	Wave A		Wave B		Wave C	
pH	$-E_{1/2}$	i_l	$-E_{1/2}$	i_l	$-E_{1/2}$	i_l
2.00	0.63 V	6.0 μA				
2.25	0.64	4.8				
2.50	0.65	4.0		poorly defined waves		
2.75	0.65	2.9				
3.00	0.66	1.65				
3.25	0.66	0.80				
3.50	0.66	0.40	0.80 V	2.5 μA	0.90 V	2.0 μA
3.75	0.67	0.10	0.82	2.0	0.94	2.6
4.00	0.67	0.05	0.84	1.35	0.98	3.1
4.50	-	0.00	0.88	0.20	1.05	2.7
5.00			-	0.00	1.12	1.4
5.50					1.14	0.75
6.00					1.17	0.20
6.50					-	0.00

Experimental conditions: Cd^{++} = 1.0 x 10^{-3} M, DTPA = 1.0 x 10^{-3} M, μ = 0.2, h_{Hg} = 60 cm., temp = 25°C and Gelatin = 0.002%.

(d) Cd-DTPA ratio of 1:2

The Cd-DTPA solutions with an excess of DTPA to metal concentration (ratio 1:2) exhibited reduction waves that were better defined compared to the equimolar solutions. In table 6 are recorded the half wave potentials and wave-heights for the pH range of 2.00 to 6.50. The wave heights are compared and illustrated in figure 17. The half-wave potentials are plotted in figure 18. Figure 19 clearly depicts three waves, i.e. three different reduction steps labelled A, B and C. The three waves will be discussed in sequence.

Wave A, at average heights ($i_d > 2.0\mu A$), was a reversible, diffusion controlled two electron reduction step of free cadmium ions. This was determined from a plot of $\log(\frac{i}{i_d - i})$ vs. E (slope 31 ± 2 mV and n = 2) and the dependence of the wave height on the mercury pressure ($\frac{i}{\sqrt{h_{corr}}}$ = constant). However, when wave A was small ($i < 0.50\mu A$) compared to wave B, there were indications that wave A was a kinetically controlled, reversible reduction of cadmium ions. In table 7 the temperature study showed the wave height of A to increase 2.0% / °C which is above the normal diffusion controlled value of 1.5% / °C. Secondly, a pressure study (table 8) revealed that the wave A height no longer was directly proportional to mercury pressure

Table 6 $E_{1/2}$ and i_l for Cd-DTPA (1:2).

	Wave A		Wave B		Wave C	
pH	$-E_{1/2}$	i_l	$-E_{1/2}$	i_l	$-E_{1/2}$	i_l
2.00	0.62 V	6.2 μA				
2.25	0.62	5.6				
2.50	0.63	4.8	0.75 V	0.75 μA		
2.75	0.64	3.7	0.76	1.6		
3.00	0.65	2.5	0.77	2.0	0.87 V	0.3 μA
3.25	0.66	1.65	0.78	2.3	0.89	0.6
3.50	0.66	0.40	0.81	2.5	0.92	1.4
3.75	0.67	0.12	0.83	2.2	0.96	2.0
4.00	0.68	0.05	0.85	1.70	1.00	2.5
4.25	-	0.00	0.86	1.05	1.03	2.7
4.50			0.87	0.28	1.05	2.8
4.75			0.88	0.10	1.08	2.6
5.00			0.89	0.05	1.12	2.1
5.25			-	0.00	1.13	1.50
5.50					1.14	1.13
5.75					1.15	0.54
6.00					1.16	0.22
6.25					1.17	0.10
6.50					1.18	0.04

Experimental conditions: Cd^{++} = 1.0 x 10^{-3} M, DTPA = 2.0 x 10^{-3} M, μ = 0.2, h_{Hg} = 60 cm., temp = 25°C and Gelatin = 0.002%.

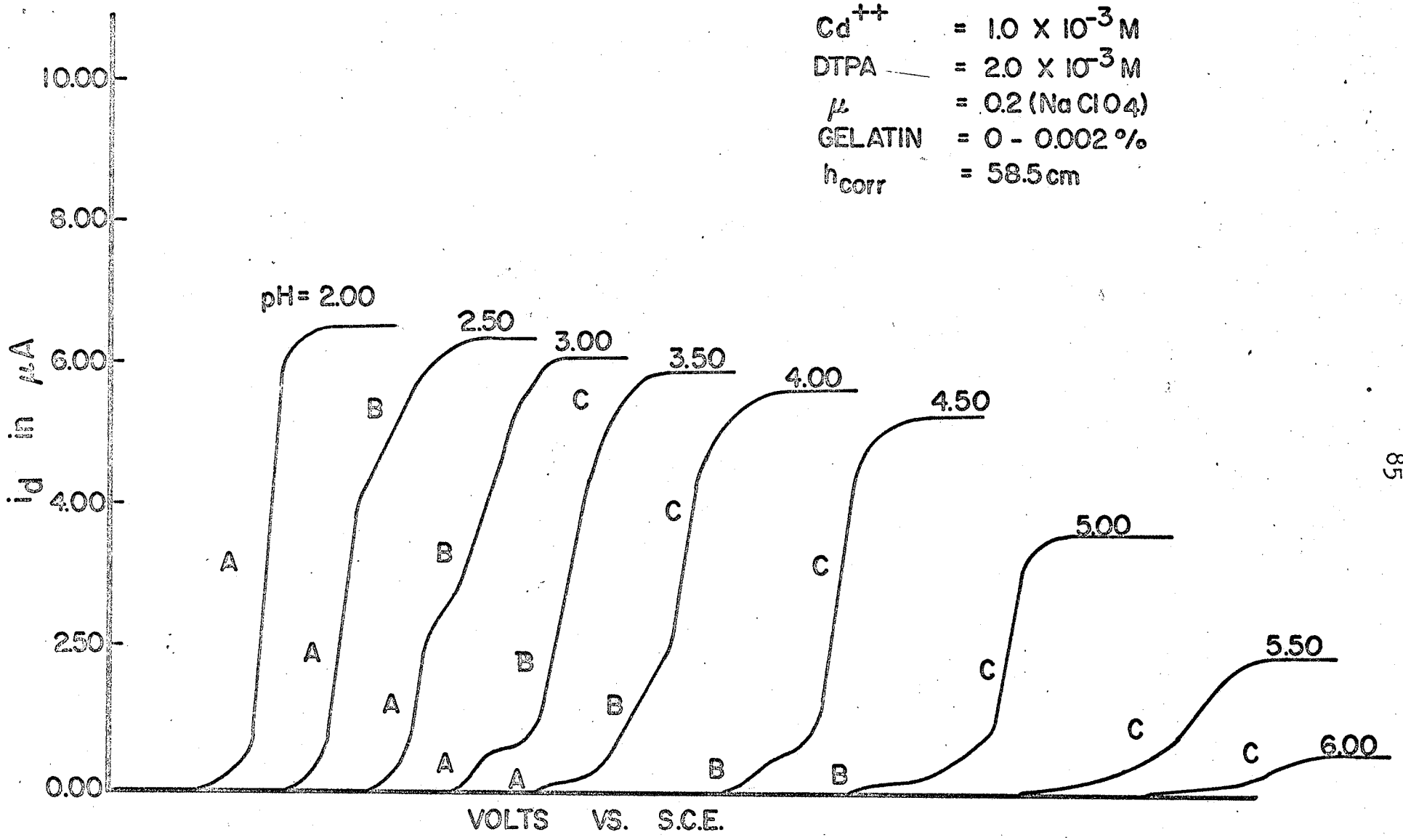

FIG. 17 A pH STUDY OF Cd - DTPA (1:2)

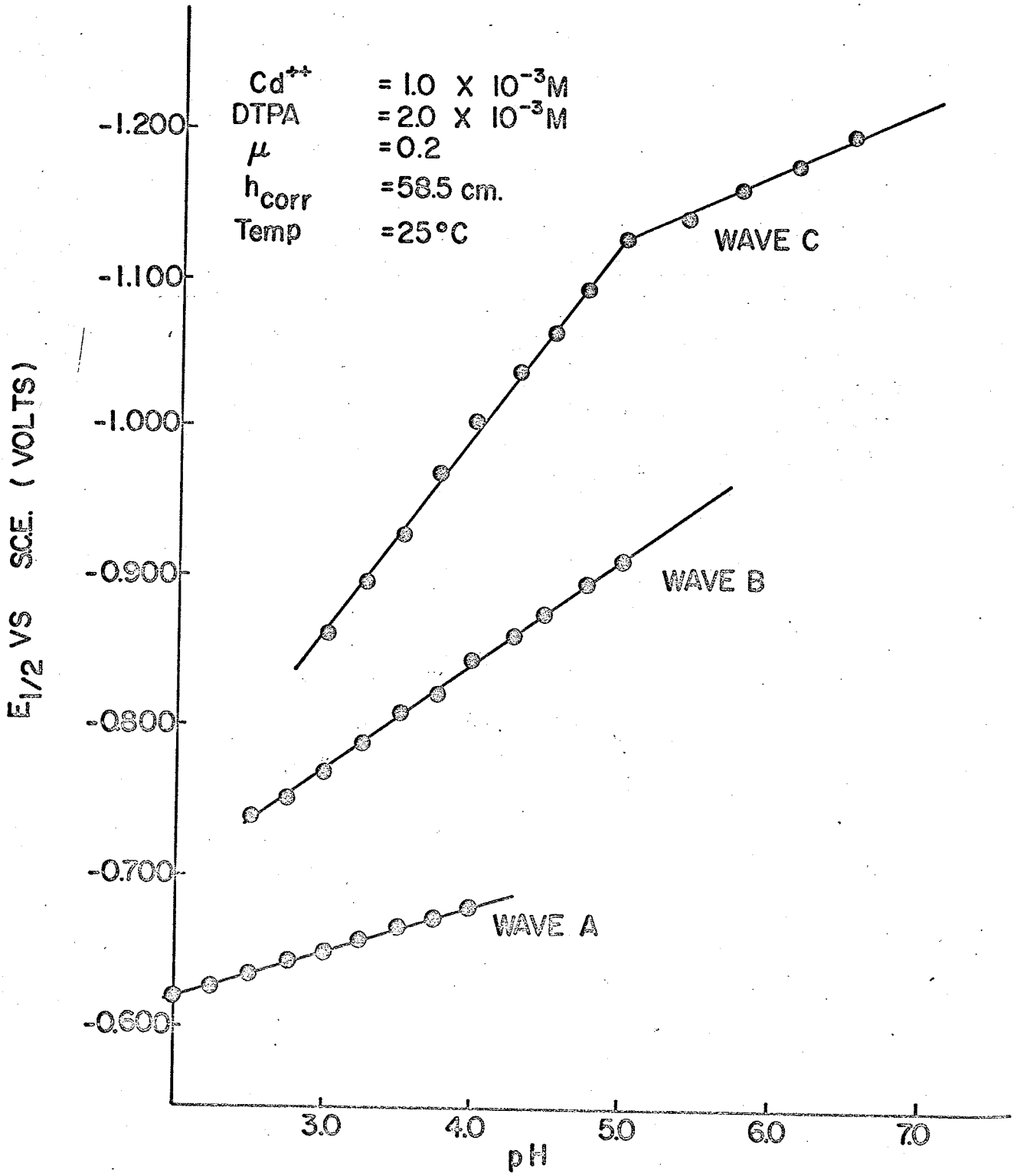

FIG.18 $E_{1/2}$ OF Cd-DTPA VS pH

Cd^{++} = 1.0×10^{-3} M
DTPA = 2.0×10^{-3} M
μ = 0.2
h_{corr} = 58.5cm
GELATIN = 0 -0.002%

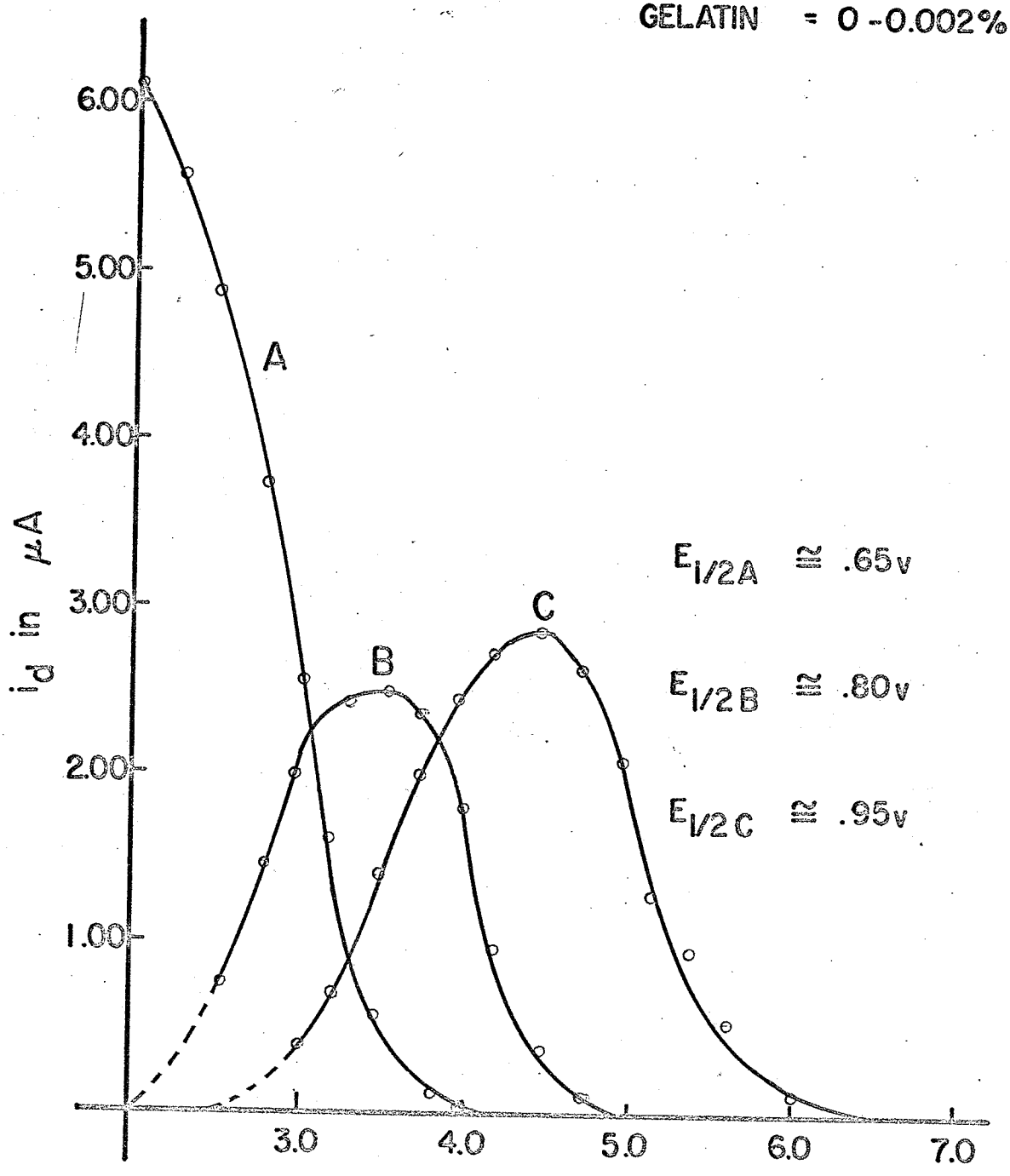

FIG.19 DIFFUSION CURRENTS OF VARIOUS WAVES AS A FUNCTION OF pH

Table 7 Temperature Study of Cd-DTPA (1:2)

	Wave A height at pH = 3.50	Wave B height at pH = 4.50	Wave C height at pH = 5.75
20°C	0.36 ± .01μA	0.26 ± .01μA	0.50 ± .01μA
25	0.40	0.28	0.54
30	0.45	0.30	0.58
35	0.50	0.33	0.61
40	0.56	0.36	0.66
45	0.62	0.39	0.69
50	0.68	0.42	0.75
$\Delta i_d/\Delta T$	2.0% /°C	1.8% /°C	1.9% /°C

Experimental conditions: Cd^{++} = 1.0 x 10^{-3} M, DTPA = 2.0 x 10^{-3}M, μ = 0.2, h_{Hg} = 60 cm, and Gelatin 0.002% (used only for pH = 3.50).

Table 8 Pressure Studies of Cd-DTPA (1:2)

		Wave A at pH = 3.50	Wave B at pH = 4.50	Wave C at pH = 5.75
h_{corr}	$\sqrt{h}_{corr}$	$\frac{i}{\sqrt{h}_{corr}} \times 10^{-2}$	$\frac{i}{\sqrt{h}_{corr}} \times 10^{-2}$	$\frac{i}{\sqrt{h}_{corr}} \times 10^{-2}$
48.4 cm	6.957	$\frac{0.380}{6.957} = 5.46$	$\frac{0.285}{6.957} = 4.09$	$\frac{0.540}{6.957} = 7.76$
53.4	7.307	$\frac{0.390}{7.307} = 5.34$	$\frac{0.280}{7.307} = 3.83$	$\frac{0.545}{7.307} = 7.46$
58.4	7.642	$\frac{0.400}{7.642} = 5.23$	$\frac{0.280}{7.642} = 3.66$	$\frac{0.550}{7.642} = 7.20$
63.4	7.962	$\frac{0.410}{7.962} = 5.15$	$\frac{0.280}{7.962} = 3.52$	$\frac{0.555}{7.962} = 6.97$
68.4	8.270	$\frac{0.420}{8.270} = 5.08$	$\frac{0.280}{8.270} = 3.39$	$\frac{0.560}{8.270} = 6.77$
73.4	8.567	$\frac{0.430}{8.567} = 5.02$	$\frac{0.280}{8.567} = 3.27$	$\frac{0.565}{8.567} = 6.60$
78.4	8.854	$\frac{0.440}{8.856} = 4.97$	$\frac{0.285}{8.854} = 3.22$	$\frac{0.570}{8.854} = 6.43$
$\frac{i}{\sqrt{h}_{corr}}$ uncertainty		$\pm$ 2%	$\pm$ 2%	$\pm$ 2%

Experimental conditions: $Cd^{++} = 1.0 \times 10^{-3}$M, DTPA = 2.0×10^{-3}M, $\pi = 0.2$ and Gelatin = 0.002% (for pH = 3.50 only).

($i/\sqrt{h}_{corr} \neq$ constant). Both of these checks indicate a kinetic wave. A plot of $E_{1/2}$ vs. pH (figure 18) gave a slope of 30 ± 2 mV / pH.

Wave B was throughly examined at small wave heights due to the difficulty of obtaining accurate measurements at intermediate heights where wave A interfered. A plot of $\log \frac{i}{(i_d - i)}$ vs. E gave a slope of 60 ± 2 mV. This meant a one electron reduction step (n = 1) or an irreversible two electron reduction. Most investigators agree that the reduction of a metal complex ion occurs by a stepwise unwrapping of the ligand from the metal, where finally the metal ion reduces to free metal. Since cadmium has no stable + 1 oxidation state it was concluded that wave B was an irreversible reduction step. A pressure study (table 8) showed that wave B was not diffusion controlled ($i/\sqrt{h}_{corr} \neq$ constant). The temperature coefficient ($\Delta i/\Delta T$) from table 7 was slightly above the normal diffusion controlled value also pointing to a semikinetic reduction wave. The slope of $E_{1/2}$ vs. pH (figure 18) was 75 ± 5 mV / pH.

The characteristics of wave C were similar to Wave B. A plot of $\log i/(i_d - i)$ vs. E gave 75 ± 2 mV. Hence wave C was an irreversible reduction step. Both temperature (table 7) and pressure (table 8) studies pointed toward a kinetically controlled reduction wave.

(e) Cd-DTPA ratio of 1:4 and 1:10

The Cd-DTPA solutions with a metal to ligand ratio of 1:4 were briefly studied. The half-wave potentials and wave heights were recorded in table 9. A brief check with table 6 shows that the Cd-DTPA (1:2) case was quite similar. Hence no new information was obtained from the 1:4 ratio except that the $E_{1/2}$ values of all three waves became slightly more negative ($\Delta E_{1/2} \simeq 0.01$ V). Since most of the theoretical calculations of metal complexes in polarography[23] require a large excess of ligand, the 1:10 ratio was studied next.

Table 10 shows the half wave potentials and wave heights for Cd-DTPA (1:10). Again a comparison with table 9 revealed that the $E_{1/2}$ values moved to more negative values. However the polarograms in general were not as well defined as for the 1:2 or 1:4 series, thus making accurate measurements difficult. Therefore it was decided to study the 1:8 ratio of metal to ligand which seemed to be a good compromise between well defined waves and a large excess of ligand.

Table 9 $E_{1/2}$ and i_ℓ for Cd-DTPA (1:4)

	Wave A		Wave B		Wave C	
pH	$-E_{1/2}$	i_ℓ	$-E_{1/2}$	i_ℓ	$-E_{1/2}$	i_ℓ
2.00	0.63 V	5.4 μA				
2.25	0.64	5.0				
2.50	0.65	4.5				
2.75	0.65	4.5				
2.75	0.65	3.7				
3.00	0.66	2.5	0.78 V	1.6 μA	0.85 V	1.3 μA
3.25	0.67	1.20	0.80	2.0	0.89	2.0
3.50	0.68	0.55	0.82	2.2	0.94	2.3
3.75	0.68	0.20	0.83	2.0	0.98	2.4
4.00	0.69	0.05	0.85	1.60	1.02	2.5
4.50	-	0.00	0.88	0.50	1.06	2.3
5.00			0.92	0.10	1.13	1.20
5.50			-	0.00	1.14	0.50
6.00					1.15	0.10
6.50					-	0.00

Experimental conditions: Cd^{++} = 1.0 x 10^{-3} M, DTPA = 4.0 x 10^{-3} M, h_{Hg} = 60 cm., Gelatin = 0.002%, μ = 0.2 and temp. = 25 C.

Table 10 $E_{1/2}$ and i_ℓ for Cd-DTPA (1:10).

	Wave A		Wave B		Wave C	
pH	$-E_{1/2}$	i_ℓ	$-E_{1/2}$	i_ℓ	$-E_{1/2}$	i_ℓ
2.00	0.64 V	4.6 μA				
2.25	0.65	4.4				
2.50	0.66	4.1				
2.75	0.67	3.5				
3.00	0.68	2.0	0.78 V	1.3 μA	0.84 V	1.2 μA
3.25	0.68	1.20	0.79	1.9	0.88	1.6
3.50	0.69	0.55	0.80	2.3	0.93	2.0
3.75	0.70	0.15	0.82	2.4	0.98	2.3
4.00	-	0.00	0.85	1.60	1.02	2.4
4.50			0.89	0.50	1.10	2.4
5.00				0.00	1.17	1.20
5.50					1.19	0.25
6.00					1.20	0.05
6.50					-	0.00

Experimental conditions: Cd^{++} = 1.0 x 10^{-3} M, DTPA = 1.0 x 10^{-2} M, μ = 0.2, Gelatin = 0.002%, h_{Hg} = 60 cm., and temp = 25°C.

(f) Cd-DTPA ratio of 1:8

The half-wave potentials and individual wave heights for Cd-DTPA (1:8) are recorded in table 11. The data is similar to the 1:2 ratio study (table 6). When wave A was small ($i < 0.50\mu A$), compared to wave B, it was reversible but not diffusion controlled (table 13). Table 12 shows wave A to have a temperature coefficient of 2.5% / °C indicating a kinetic contribution to the reduction step. The plot of $E_{1/2}$ vs. pH had a slope of 40 ± 2 mV / pH.

Wave B was irreversible from a plot of log $i/(i_d - i)$ vs. E(slope = 40 ± 2 mV) and not diffusion controlled (table 13) according to pressure studies. However wave B had a temperature coefficient of 1.5% / °C similar to that of a diffusion controlled wave.

Wave C had a slope of 70 ± 2 mV for the plot of log $\frac{i}{(i_d - i)}$ vs. E and thus was determined to be an irreversible reduction step. It was not diffusion controlled according to the pressure studies given in table 13. The temperature coefficient (1.8% / °C) was slightly above the normal diffusion controlled process, which might point to a kinetic contribution in the reduction step.

Table 11 $E_{1/2}$ and i_ℓ for Cd-DTPA (1:8)

	Wave A		Wave B		Wave C	
pH	$-E_{1/2}$	i_ℓ	$-E_{1/2}$	i_ℓ	$-E_{1/2}$	i_ℓ
2.00	0.63 V	4.9 μA				
2.25	0.64	4.5				
2.50	0.65	4.2				
2.75	0.66	3.3				
3.00	0.67	2.0	0.77 V	1.6 μA	0.83 V	1.7 μA
3.25	0.68	0.80	0.78	2.0	0.87	2.4
3.50	0.69	0.30	0.79	2.1	0.90	2.8
3.75	0.70	0.10	0.81	1.8	0.93	3.2
4.00	-	0.00	0.84	1.4	0.96	3.4
4.25			0.86	0.95	1.01	3.5
4.50			0.87	0.25	1.07	3.6
4.75			0.88	0.12	1.10	3.0
5.00			0.90	0.04	1.13	2.3
5.25			-	0.00	1.14	1.50
5.50					1.15	1.10
5.75					1.16	0.64
6.00					1.17	0.25
6.25					1.18	0.10
6.50					1.19	0.05
6.75					-	0.00

Experimental conditions: $Cd^{++} = 1.0 \times 10^{-3}$ M, DTPA = 8.0×10^{-3} M, $\mu = 0.2$, $h_{Hg} = 60$ cm, Gelatin 0.002% and temp. = 25°C.

Table 12 Temperature Study of Cd-DTPA (1:8)

Temp	Wave A height at pH = 3.50	Wave B height at pH = 4.50	Wave C height at pH = 5.75
20°C	0.27 ± 0.01μA	0.23 ± .01μA	0.60 ± .01μA
25	0.30 "	0.25 "	0.64 "
30	0.34 "	0.27 "	0.72 "
35	0.38 "	0.29 "	0.76 "
40	0.43 "	0.31 "	0.84 "
45	0.49 "	0.33 "	0.92 "
50	0.56 "	0.36 "	0.99 "
$\Delta i_d/\Delta T$	2.5 %/°C	1.5 %/°C	1.8 %/°C

Experimental conditions: $Cd^{++} = 1.0 \times 10^{-3}$ M, DTPA = 8.0×10^{-3} M, $\mu = 0.2$, $h_{Hg} = 60$ cm, and Gelatin = 0.002% (used only for pH = 3.50).

Table 13 Pressure Studies of Cd-DTPA (1:8)

		Wave A at pH = 3.50	Wave B at pH = 4.50	Wave C at pH = 5.75
h_{corr}	$\sqrt{h_{corr}}$	$\frac{i}{\sqrt{h_{corr}}} \times 10^{-2}$	$\frac{i}{\sqrt{h_{corr}}} \times 10^{-2}$	$\frac{i}{\sqrt{h_{corr}}} \times 10^{-2}$
48.4 cm	6.957	$\frac{0.280}{6.957} = 4.02$	$\frac{0.245}{6.957} = 3.52$	$\frac{0.62}{6.957} = 8.91$
53.4	7.307	$\frac{0.290}{7.307} = 3.96$	$\frac{0.250}{7.307} = 3.42$	$\frac{0.63}{7.307} = 8.62$
58.4	7.642	$\frac{0.300}{7.642} = 3.93$	$\frac{0.250}{7.642} = 3.27$	$\frac{0.64}{7.642} = 8.37$
63.4	7.962	$\frac{0.305}{7.962} = 3.83$	$\frac{0.250}{7.962} = 3.20$	$\frac{0.65}{7.962} = 8.16$
68.4	8.270	$\frac{0.310}{8.270} = 3.75$	$\frac{0.250}{8.270} = 3.02$	$\frac{0.66}{8.27} = 7.98$
73.4	8.567	$\frac{0.320}{8.567} = 3.72$	$\frac{0.250}{8.567} = 2.92$	$\frac{0.67}{8.567} = 7.82$
78.4	8.854	$\frac{0.325}{8.856} = 3.67$	$\frac{0.255}{8.854} = 2.88$	$\frac{0.68}{8.854} = 7.68$
$\frac{i}{\sqrt{h_{corr}}}$	uncertainty	$\pm$ 2%	$\pm$ 2%	$\pm$ 1%

Experimental conditions: $Cd^{++} = 1.0 \times 10^{-3}$M, DTPA = 8.0×10^{-3}M, $\mu = 0.2$ and Gelatin = 0.002% (for pH = 3.50 only).

(g) Pb-DTPA ratio of 1:2

The Pb-DTPA solutions (ratio 1:2) also exhibited three separate reduction waves labelled A, B, and C as shown in figure 20. The halfwave potentials and wave heights were recorded in table 14. The half-wave potentials were plotted against pH in figure 21. The wave heights are compared and illustrated in figure 22. Whereas the Cd-DTPA waves disappeared at pH = 6.50, the Pb-DTPA reduction waves extend to pH = 9.00. Again the three waves (A, B, and C) will be discussed in sequence.

Wave A, at average heights ($i_d > 2.0\mu A$) was a reversible, diffusion controlled two electron reduction wave of free lead ions. This was concluded from the plot of $\log \frac{i}{(i_d - i)}$ vs. E (slope = 29 ± 2 mV and n = 2) and a half-wave potential similar to that of free lead ions. The dependence of wave height on mercury pressure ($\frac{i}{\sqrt{h_{corr}}}$ = constant) confirmed the wave to be diffusion controlled. However when wave A was small ($i < 0.50\mu A$) compared to wave B it no longer had a direct proportionality to $h_{corr}^{1/2}$ as seen from table 16. A temperature study (table 15) of wave A showed it was sensitive to a change in temperature. The temperature coefficient ($\Delta i / \Delta T$) was 4.1% / °C indicating a kinetically controlled reduction step. A plot of $E_{1/2}$ vs. pH (figure 21) gave a slope of 28 ± 2 mV / pH.

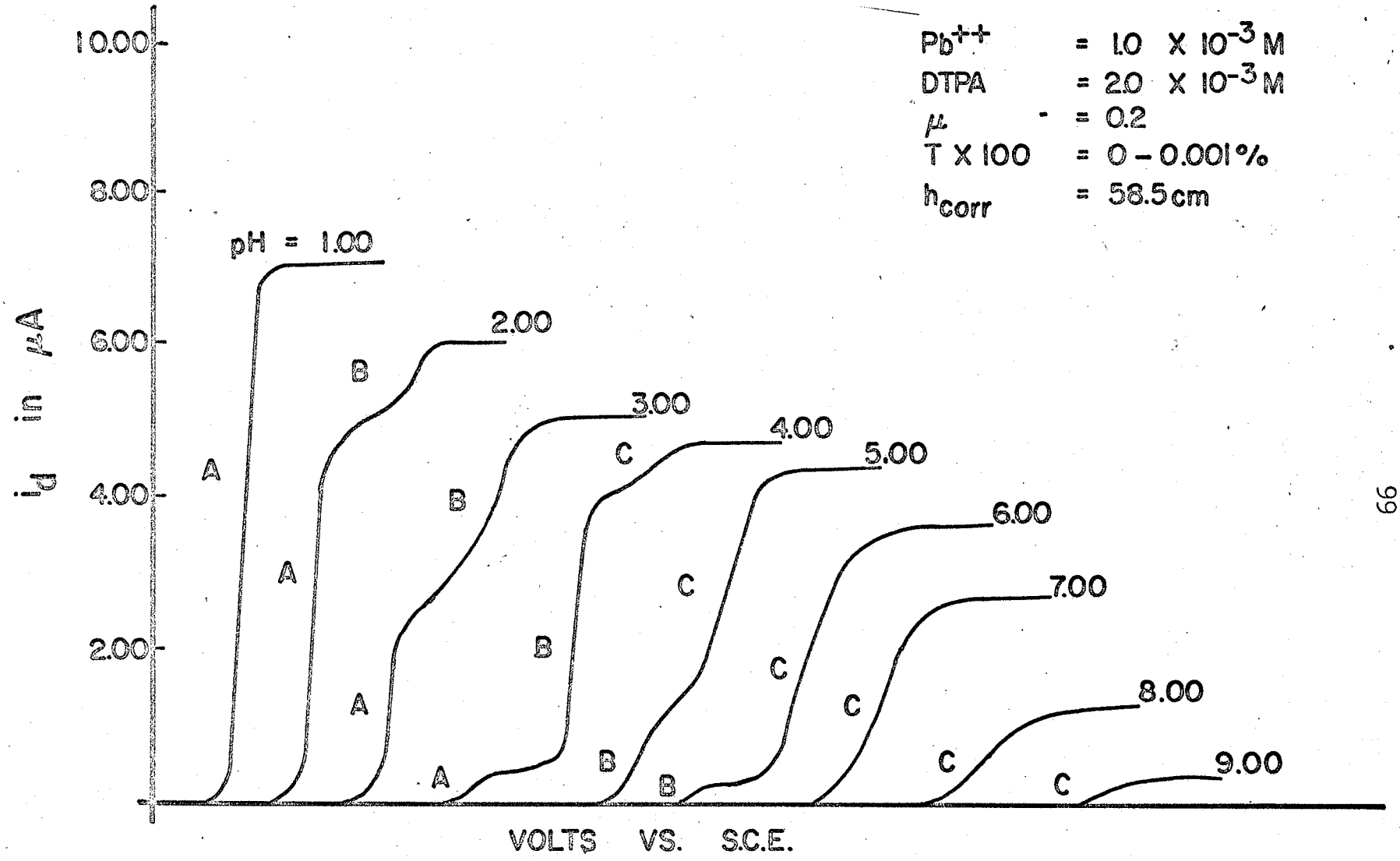

FIG. 20 A pH STUDY OF Pb – DTPA (1:2)

Table 14 $E_{1/2}$ and i_ℓ for Pb-DTPA (1:2)

	Wave A		Wave B		Wave C	
pH	$-E_{1/2}$	i_ℓ	$-E_{1/2}$	i_ℓ	$-E_{1/2}$	i_ℓ
2.00	0.47 V	4.8 μA	-	~ 1.6 μA		
2.25	0.48	4.0	-	~ 2.1		
2.50	0.49	3.6	-	~ 2.2		
2.75	0.50	3.3	-	~ 2.3		
3.00	0.51	2.5	0.62 V	2.4	0.80 V	0.25 μA
3.25	0.51	2.0	0.64	3.0	0.82	0.40
3.50	0.52	1.5	0.66	3.5	0.84	0.60
3.75	0.52	0.55	0.68	4.0	0.87	0.80
4.00	0.53	0.30	0.71	3.9	0.90	1.1
4.25	0.54	0.10	0.72	3.6	0.92	1.6
4.50	0.55	0.04	0.73	3.4	0.94	2.0
4.75	-	0.00	0.75	2.6	0.96	2.8
5.00			0.77	1.8	0.98	3.6
5.25			0.78	1.2	1.00	4.2
5.50			0.79	0.85	1.03	4.6
5.75			0.80	0.50	1.06	4.8
6.00			0.81	0.20	1.10	4.6
6.50			0.82	0.05	1.15	3.3
7.00			-	0.00	1.20	1.65
7.50					1.25	1.00
8.00					1.30	0.40
8.50					-	0.00

Experimental conditions: Pb^{++} = 1.0 x 10^{-3} M, DTPA = 2.0 x 10^{-3}M, μ = 0.2, h_{Hg} = 60 cm., temp = 25°C and TX-100 = 0.001%.

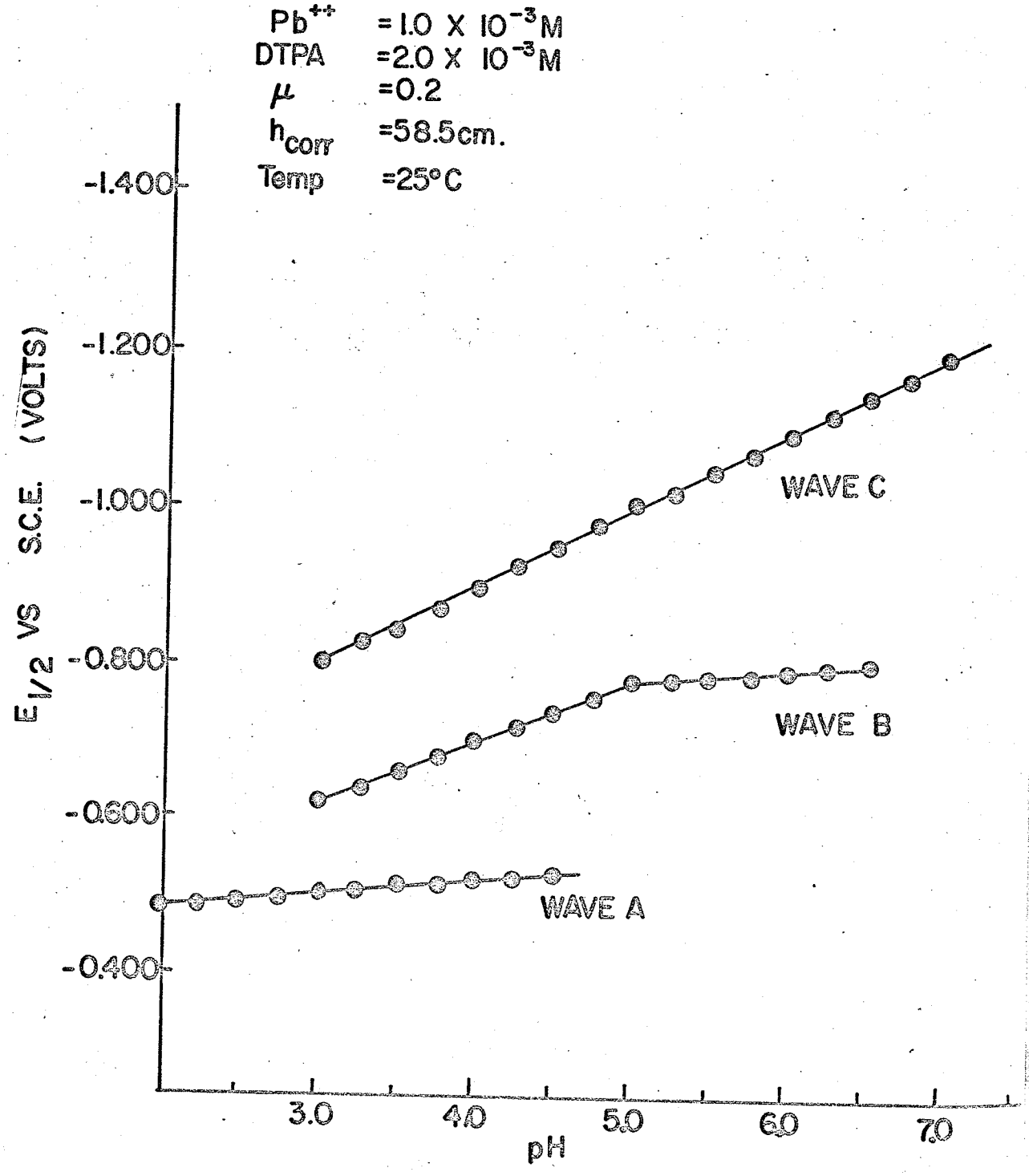

FIG. 21 $E_{1/2}$ OF Pb-DTPA VS pH.

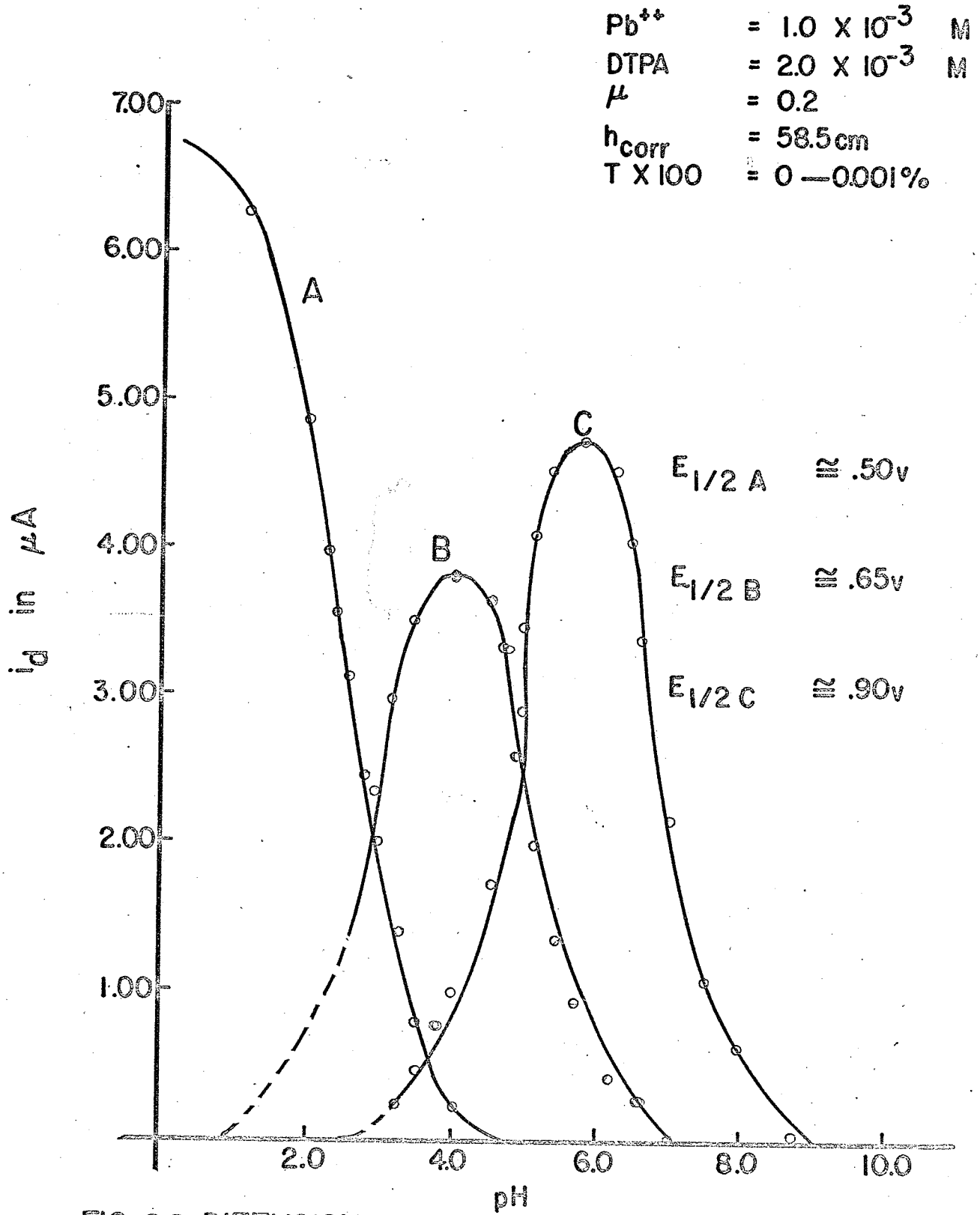

FIG. 22 DIFFUSION CURRENTS OF VARIOUS WAVES AS A FUNCTION OF pH.

Table 15 Temperature Study of Pb-DTPA (1:2)

Temp	Wave A height at pH = 4.00	Wave B height at pH = 6.00	Wave C height at pH = 7.00
20°C	0.27 ± .01μA	0.17 ± .01μA	1.35 ± .02μA
25	0.31	0.20	1.65
30	0.38	0.24	1.90
35	0.45	0.28	2.25
40	0.52	0.31	2.50
45	0.61	0.35	2.75
50	0.73	0.39	3.05
$\Delta i/\Delta T$	4.1% /°C	3.9% /°C	3.8% /°C

Experimental conditions: $Pb^{++} = 1.0 \times 10^{-3}$M
DTPA = 2.0×10^{-3}M, $\mu = 0.2$, TX-100 = 0.001%
(used for pH = 4.00 only) and h_{Hg} = 60 cm.

Table 16 Pressure Studies of Pb-DTPA (1:2)

		Wave A at pH = 4.00	Wave B at pH = 6.00	Wave C at pH = 7.50
h_{corr}	$\sqrt{h}_{corr}$	$\frac{i}{\sqrt{h}_{corr}} \times 10^{-2}$	$\frac{i}{\sqrt{h}_{corr}} \times 10^{-2}$	$\frac{i}{\sqrt{h}_{corr}} \times 10^{-1}$
48.4 cm	6.957	$\frac{0.280}{6.957} = 4.02$	$\frac{0.190}{6.057} = 2.73$	$\frac{0.97}{6.957} = 1.39$
5.34	7.307	$\frac{0.290}{7.307} = 3.96$	$\frac{0.195}{7.307} = 2.67$	$\frac{0.99}{7.307} = 1.35$
58.4	7.642	$\frac{0.300}{7.642} = 3.92$	$\frac{0.200}{7.642} = 2.62$	$\frac{1.00}{7.642} = 1.30$
63.4	7.962	$\frac{0.310}{7.962} = 3.89$	$\frac{0.205}{7.962} = 2.57$	$\frac{1.01}{7.962} = 1.26$
68.4	8.270	$\frac{0.320}{8.270} = 3.87$	$\frac{0.205}{8.270} = 2.48$	$\frac{1.03}{8.270} = 1.24$
73.4	8.567	$\frac{0.330}{8.567} = 3.85$	$\frac{0.210}{8.567} = 2.45$	$\frac{1.04}{8.567} = 1.21$
78.4	8.854	$\frac{0.340}{8.856} = 3.83$	$\frac{0.205}{8.854} = 2.32$	$\frac{1.06}{8.854} = 1.19$
$\frac{i}{\sqrt{h}_{corr}}$	uncertainty	$\pm$ 2%	$\pm$ 2%	$\pm$ 1%

Experimental conditions: $Pb^{++} = 1.0 \times 10^{-3}$ M, DTPA = 2.0×10^{-3} M, μ = 0.2 and TX-100 = 0.001% (for pH = 4.00 only).

Wave B was studied at small wave heights (pH = 6.00) just as for the Cd-DTPA case. A plot of log $i/(i_d - i)$ vs. E showed a slope of 56 ± 2 mV indicating a reversible one electron (n = 1) reduction or an irreversible two (n = 2 or higher) electron reduction. For the same reasons as outlined for the Cd-DTPA case (wave B) it was concluded that wave B was an irreversible reduction step. A pressure study (table 16) showed that wave B was not diffusion controlled ($i/\sqrt{h}_{corr} \neq$ constant). Secondly, the temperature coefficient (table 10) was 3.9% / °C indicating a kinetic wave.

Wave C proved to be irreversible (slope of log $i/(i_d - i)$ vs. E was 94 ± 4 mV) and not diffusion controlled. The value of $\frac{i}{\sqrt{h}_{corr}}$ varied beyond the limits of experimental errors as seen in table 16. The temperature coefficient (table 10) was above the normal diffusion controlled value indicating a kinetic contribution to the reduction step.

(h) Pb-DTPA ratio of 1:8

The half-wave potentials and individual wave heights for Pb-DTPA (1:8) are recorded in table 17. The data in table 17 are quite similar to the Pb-DTPA (1:2) study in table 14. Wave A, when small ($i < 0.50\mu A$) compared to wave B, was a reversible two electron reduction ($\log \frac{i}{(i_d - i)}$ vs. E_o slope = 30 ± 2 mV). It was a kinetic wave because of a large temperature coefficient (4% / °C) and not diffusion controlled from pressure studies (table 19). A plot of $E_{1/2}$ vs. pH had a slope of 32 ± 2 mV/pH.

Wave B had a slope of 62 ± 2 mV for the plot of $\log \frac{i}{(i_d - i)}$ vs. E indicating an irreversible reduction process. It also had a large temperature coefficient (4% / °C) indicating a kinetic controlled wave. It was not diffusion controlled according to pressure studies (table 19).

Wave C proved to be irreversible again, where the slope of $\log i/(i_d - i)$ vs. E was 91 ± 2 mV. The temperature coefficient (table 18) was 4% / °C showing some kinetic character to the reduction wave. The pressure studies (table 19) showed wave C was not diffusion controlled, since $\frac{i}{\sqrt{h}_{corr}}$ was not constant for the pressures (50 - 80 cm) used.

Table 17 $E_{1/2}$ and i_ℓ for Pb-DTPA (1:8).

pH	Wave A		Wave B		Wave C	
	$-E_{1/2}$	i_ℓ	$-E_{1/2}$	i_ℓ	$-E_{1/2}$	i_ℓ
2.00	0.50V	4.0 μA	-	1.4 μA		
2.25	0.50	3.6	-	1.8		
2.50	0.51	3.0	-	2.4		
2.75	0.52	2.6	-	2.7		
3.00	0.53	2.3	0.62V	2.9	0.75V	0.2 μA
3.25	0.53	1.5	0.64	3.5	0.78	0.4
3.50	0.54	0.90	0.66	3.9	0.81	0.6
3.75	0.55	0.55	0.68	4.0	0.84	0.8
4.00	0.56	0.28	0.70	3.9	0.87	1.1
4.25	0.56	0.12	0.72	3.4	0.89	1.6
4.50	0.57	0.05	0.74	3.0	0.92	2.3
4.75	-	0.00	0.76	2.4	0.95	3.2
5.00			0.78	1.7	0.98	3.9
5.25			0.79	1.20	1.01	4.1
5.50			0.80	0.85	1.05	4.3
5.75			0.81	0.40	1.09	4.4
6.00			0.82	0.18	1.12	4.3
6.50			0.83	0.04	1.18	3.1
7.00			-	0.00	1.25	1.35
7.50					1.28	0.60
8.00					1.33	0.25
8.50					-	0.00

Experimental conditions: $Pb^{++} = 1.0 \times 10^{-3}$ M, DTPA = 8.0×10^{-3} M, $\mu = 0.2$, $h_{Hg} = 60$ cm., temp = 25°C and TX-100 = 0.001%.

Table 18 Temperature Study of Pb-DTPA (1:8)

Temp	Wave A height at pH = 4.00	Wave B height at pH = 6.00	Wave C height at pH = 7.00
20°C	0.24 ± .01μA	0.13 ± .01μA	0.99 ± .02μA
25	0.29	0.18	1.35
30	0.35	0.21	1.50
35	0.42	0.25	1.75
40	0.50	0.28	2.08
45	0.59	0.32	2.35
50	0.68	0.35	2.75
$\Delta i / \Delta T$	4.2% / °C	4.0% / °C	4.0% / °C

Experimental conditions: $Pb^{++} = 1.0 \times 10^{-3}$ M
DTPA = 8.0×10^{-3} M, $\mu = 0.2$, TX-100 = 0.001%
(used for pH = 4.00 only) and h_{Hg} = 60 cm.

Table 19 Pressure Studies of Pb-DTPA (1:8)

		Wave A at pH = 4.00	Wave B at pH = 6.00	Wave C at pH = 7.50
h_{corr}	$h_{corr}^{1/2}$	$\frac{i}{\sqrt{h_{corr}}} \times 10^{-2}$	$\frac{i}{\sqrt{h_{corr}}} \times 10^{-2}$	$\frac{i}{\sqrt{h_{corr}}} \times 10^{-2}$
48.4 cm	6.957	$\frac{0.280}{6.957} = 4.02$	$\frac{0.170}{6.957} = 2.44$	$\frac{0.58}{6.957} = 8.33$
53.4	7.307	$\frac{0.285}{7.307} = 3.90$	$\frac{0.175}{7.307} = 2.39$	$\frac{0.59}{7.307} = 8.07$
58.4	7.642	$\frac{0.290}{7.642} = 3.79$	$\frac{0.180}{7.642} = 2.35$	$\frac{0.60}{7.642} = 7.85$
63.4	7.962	$\frac{0.295}{7.692} = 3.71$	$\frac{0.180}{7.962} = 2.26$	$\frac{0.61}{7.962} = 7.66$
68.4	8.270	$\frac{0.300}{8.270} = 3.62$	$\frac{0.185}{8.27} = 2.23$	$\frac{0.62}{8.27} = 7.49$
73.4	8.567	$\frac{0.305}{8.567} = 3.56$	$\frac{0.180}{8.567} = 2.10$	$\frac{0.63}{8.567} = 7.35$
78.4	8.854	$\frac{0.310}{8.856} = 3.50$	$\frac{0.185}{8.854} = 2.08$	$\frac{0.64}{8.854} = 7.22$
$\frac{i}{\sqrt{h_{corr}}}$	uncertainty	$\pm$ 2%	$\pm$ 2%	$\pm$ 2%

Experimental conditions: $Pb^{++} = 1.0 \times 10^{-3}$ M, DTPA = 8.0×10^{-3} M, $\mu = 0.2$ and TX-100 = 0.001% (for pH = 4.00 only).

CHAPTER 6

THEORETICAL CALCULATIONS AND DISCUSSION

The experimental data given in chapter 5 clearly indicated that all the reduction waves encountered for the various complexes were kinetically controlled and only Wave A was a reversible reduction process, i.e. Waves B and C were irreversible and not diffusion controlled. The polarographic method of determining formation constants of metal complexes requires a reversible equilibrium in the over-all electrode reaction.[23-26] Hence the information obtained about Waves B and C could only be used to formulate a reasonable reduction mechanism. The stability constants were all calculated using Wave A data. The Koryta and Koutecky kinetic wave treatment (see p. 45-53) was applied to each wave and gave satisfactory results for Waves A and C, when wave heights were employed. Half-wave potentials were also used to analyze the data from Wave A with reasonable success. Wave B did not fit into any one particular mechanism (as derived by Koryta and Koutecky), but seemed to be controlled by two or more competing chemical reactions preceding reduction. The waves are discussed individually.

A. Wave C

There is general agreement among investigators[39-42] that the nonprotonated metal chelates (of EDTA, DTPA, etc.) are non-reducible at the D.M.E. This accounts for the disappearance of the complex reduction wave under basic conditions (pH = 6.5 - 9.0). It seemed

logical to start analyzing Wave C results since one of the products would be the non-protonated metal-DTPA complex. Various mechanisms were proposed with the best fit obtained for the following:

$$MHA^{=} \underset{}{\overset{k_d}{\rightleftharpoons}} MA^{\equiv} + H^{+} \qquad \text{(slow)}$$

$$MHA^{\equiv} + Hg^{o} + 2e^{-} \underset{k_r}{\rightleftharpoons} M(Hg) + HA^{-4} \qquad \text{(fast)}$$

where A represents the DTPA anion, k_r is the recombination rate constant and k_d is the dissociation rate constant. Koutecky[27] has theoretically derived the kinetic equations applicable to a number of reduction mechanisms among which is one that is similar to the proposed mechanism above namely:

$$A_1 \underset{\rho\sigma}{\overset{\rho}{\rightleftharpoons}} A_2 + A_3$$

where A_2 and A_3 electroinactive, A_1 is reducible and present in small quantities, ρ is the dissociation rate constant and $\rho\sigma$ is the recombination rate constant. Restating the various terms for our metal-DTPA mechanism;

$$\text{rate} \longrightarrow = k_d [MHA] = \rho [MHA] \quad , \quad \therefore \rho = k_d$$

$$\text{rate} \longleftarrow = k_r [MA] [H^+] = \rho\sigma [MA] \quad , \quad \therefore \rho\sigma = k_r [H^+]$$

$$K^{H}_{MHA} = \frac{[MHA]}{[MA]\,[H^+]} = \frac{k_r}{k_d} \quad \text{and} \quad \sigma = \frac{k_r [H^+]}{k_d}$$

for which the following general solution is given by Koutecky, et al,[27]

$$\frac{i_k}{(i_d - i_k)} = 0.886\,\sigma\sqrt{\rho\, t} \quad \ldots\ldots\ldots 56$$

which is quite similar to equation 49 as developed in chapter 3. Upon the proper substitutions for a metal-DTPA system as proposed above, equation 56 becomes

$$\frac{i_k}{(i_d - i_k)} = 0.886 \frac{k_r}{k_d} [H^+] \sqrt{k_d t} \quad \text{and rearranging}$$

$$= 0.886 [H^+] \sqrt{k_r K^H_{MHA} t} \quad \ldots\ldots\ldots 57$$

It is evident from equation 57 that a plot of log $\frac{i_k}{(i_d - i_k)}$ vs. pH should yield a straight line plot with a slope = -1.00. (Note: $i_k = i_\ell$ in this study.) The calculations for such a plot are given in table 20 and shown graphically in figure 23 for Cd-DTPA. The slope of log $\frac{i_k}{(i_d - i_k)}$ vs. pH was approximately -1.00. Hence Wave C is associated with the equilibrium

$$CdHA^{=} \rightleftharpoons CdA^{\equiv} + H^+$$

The identical treatment was applied to the Pb-DTPA data. Table 21 gives the calculations and figure 24 shows a plot of log $i_k/(i_d - i_k)$ vs. pH. The slope of the log $\frac{i_k}{(i_d - i_k)}$ vs. pH for Pb-DTPA was approximately -1.00. Thus it was concluded that Wave C was due to the equilibrium

$$PbHA^{=} \rightleftharpoons PbA^{\equiv} + H^+$$

Equation 57 was then used to solve for k_r. In the case of Pb-DTPA at pH = 6.00, t = 4.2 sec, h_{Hg} = 60 cm, log K^H_{PbHA} = 4.52 (Schwarzenbach, p. 132) and log $\frac{i_\ell}{(i_d - i_\ell)}$ = 0.66, then

Table 20 Log $\frac{i_\ell}{i_d - i_\ell}$ vs. pH for Cd-DTPA.

	1:2			1:8			
pH	i_ℓ	$i_d - i_\ell$	log $\frac{i_\ell}{i_d - i_\ell}$	i_ℓ	$i_d - i_\ell$	log $\frac{i_\ell}{i_d - i_\ell}$	
3.50	2.5	2.5	0.00	2.1	2.9	$\bar{1}$.86	
3.75	2.2	2.8	$\bar{1}$.90	1.8	3.2	$\bar{1}$.75	Wave B
4.00	1.7	3.3	$\bar{1}$.71	1.4	3.6	$\bar{1}$.59	
4.25	1.05	3.95	$\bar{1}$.42	0.95	4.05	$\bar{1}$.37	
4.50	0.28	4.72	$\bar{2}$.77	0.25	4.70	$\bar{2}$.80	
4.75	0.10	4.90	$\bar{2}$.31	0.12	4.88	$\bar{2}$.39	
5.00	0.05	4.95	$\bar{2}$.01	0.04	4.96	$\bar{3}$.90	
4.75	2.6	2.4	0.03	3.0	2.0	0.17	
5.00	2.1	2.9	$\bar{1}$.86	2.3	2.7	$\bar{1}$.93	Wave C
5.25	1.5	3.5	$\bar{1}$.63	1.5	3.5	$\bar{1}$.63	
5.50	1.13	3.87	$\bar{1}$.46	1.1	3.9	$\bar{1}$.45	
5.75	0.54	4.46	$\bar{1}$.08	0.64	4.36	$\bar{1}$.16	
6.00	0.22	4.78	$\bar{2}$.67	0.25	4.75	$\bar{2}$.72	
6.25	0.10	4.90	$\bar{2}$.31	0.10	4.90	$\bar{2}$.31	

Experimental Conditions: i_d = 5.00μA, h_{Hg} = 60 cm and Gelatin = 0.002% (for Wave B only).

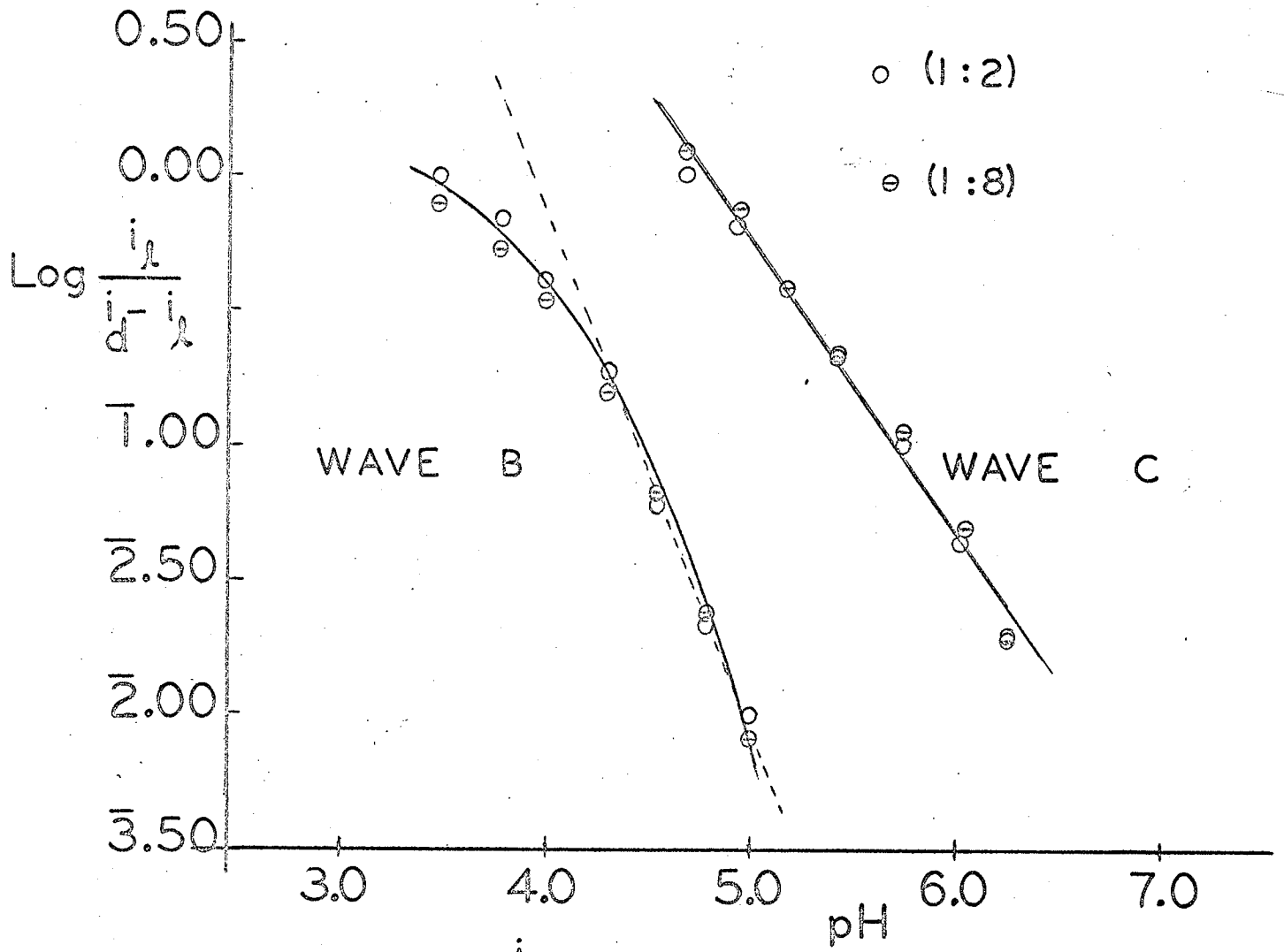

FIG. 23 Log $\frac{i_l}{i_d - i_l}$ vs. pH for Cd-DTPA.

Table 21 Log $\frac{i_\ell}{i_d - i_\ell}$ vs. pH for Pb-DTPA.

	1:2			1:8			
pH	i_ℓ	$i_d - i_\ell$	log $\frac{i_\ell}{i_d - i_\ell}$	i_ℓ	$i_d - i_\ell$	log $\frac{i_\ell}{i_d - i_\ell}$	
4.50	3.4	2.0	0.23	3.0	2.4	0.10	
4.75	2.6	2.8	$\bar{1}$.97	2.4	3.0	$\bar{1}$.90	
5.00	1.8	3.6	$\bar{1}$.70	1.7	3.7	$\bar{1}$.66	
5.25	1.2	4.2	$\bar{1}$.45	1.20	4.20	$\bar{1}$.45	
5.50	0.85	4.55	$\bar{1}$.24	0.85	4.55	$\bar{1}$.24	Wave B
5.75	0.40	5.00	$\bar{2}$.90	0.40	5.00	$\bar{2}$.90	
6.00	0.20	5.20	$\bar{2}$.58	0.18	5.22	$\bar{2}$.53	
6.25	0.12	5.28	$\bar{2}$.34	0.10	5.30	$\bar{2}$.27	
6.50	0.05	5.35	$\bar{3}$.97	0.04	5.36	$\bar{3}$.87	
6.00	4.6	0.8	0.76	4.3	1.1	0.59	
6.50	3.3	2.1	0.20	3.1	2.3	0.13	
7.00	1.65	3.75	$\bar{1}$.64	1.35	4.05	$\bar{1}$.52	Wave C
7.50	1.00	4.40	$\bar{1}$.36	0.60	4.80	$\bar{1}$.10	
8.00	0.40	5.00	$\bar{2}$.90	0.25	5.15	$\bar{2}$.69	

Experimental conditions: h_{Hg} = 60 cm, i_d = 5.40μA and no suppressor used.

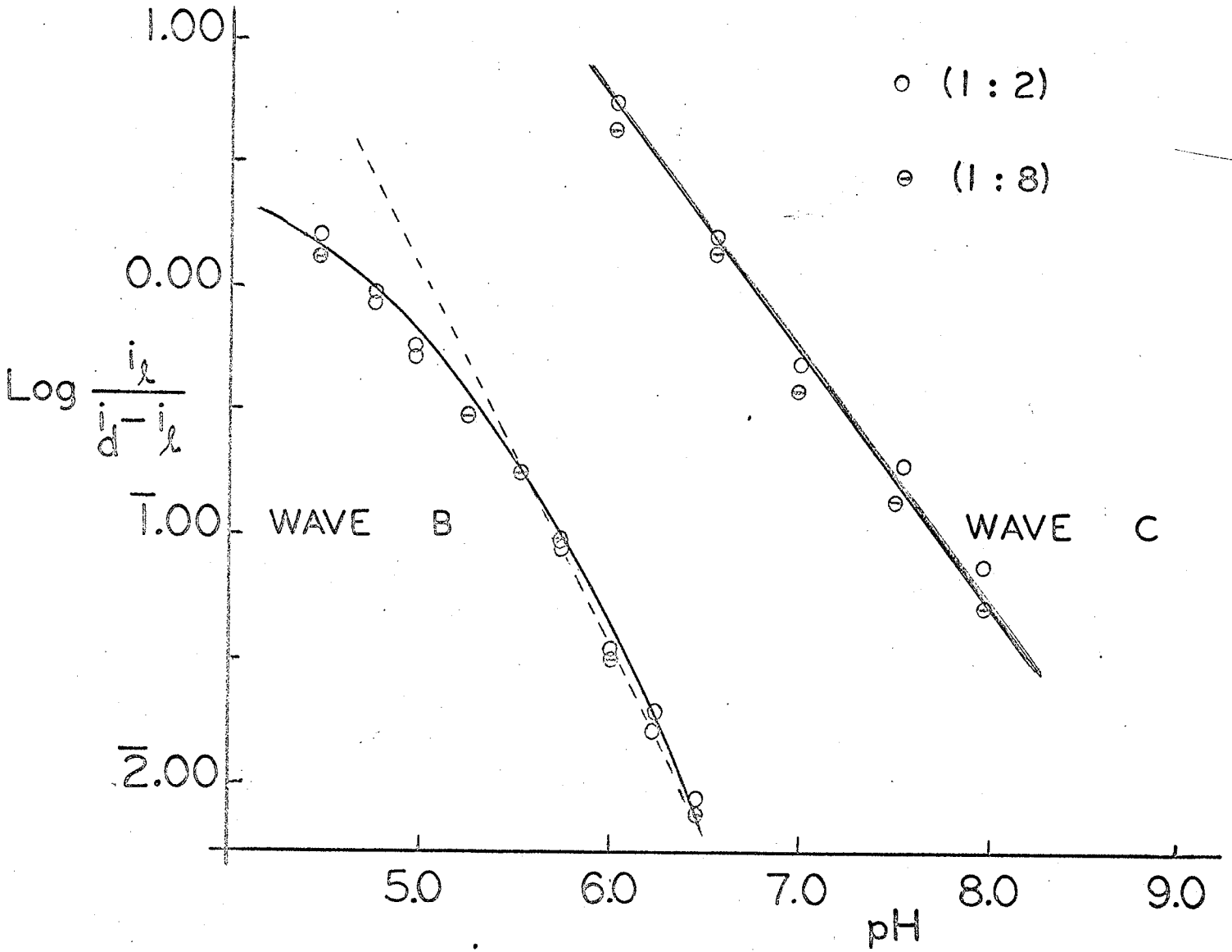

FIG. 24 Log $\frac{i_\ell}{i_d - i_\ell}$ vs. pH for Pb-DTPA.

$$0.66 = \bar{1}.91 - 6.00 + 1/2(\log k_r + 4.52 + 0.62)$$

$$6.66 = -0.09 + 1/2(\log k_r + 5.14)$$

$$\therefore \log k_r = 13.50 - 5.14 = 8.36$$

and $k_r = 2.3 \times 10^8$ liter mole^{-1} sec^{-1}

The rate constants for acid recombinations range from 10^7 to 10^{13} liter mole^{-1} sec^{-1} according to Brdicka[21]. Thus the recombination rate constant for Pb-DTPA was of a reasonable magnitude.

For Cd-DTPA at pH = 6.00, t = 4.2 sec, h_{Hg} = 60 cm, $\log K^{H}_{CdHA} = 4.17$ (Chaberek) and $\log \frac{i_l}{(i_d - i_l)} = \bar{2}.70$ (an average value), then

$$\bar{2}.70 = \bar{1}.91 - 6.00 + 1/2(\log k_r + 4.17 + 0.62)$$

and $\log k_r = 4.79$, $\therefore$ $k_r = 6.2 \times 10^4$ liter mole^{-1} sec^{-1}

This value is unusually small when compared to the Pb-DTPA case. It would appear that some steric rearrangement is necessary in the Cd-DTPA complex before protonation becomes possible.

B) Wave B

A similar theoretical treatment (as the one used for Wave C) was applied to the Wave B data for both metal complexes. The mechanism proposed was

$$MH_2A^- \underset{k_r}{\overset{k_d}{\rightleftharpoons}} MHA^= + H^+$$

where MH_2A^- was the electroactive species. The general solution is given by

$$\frac{i_\ell}{i_d - i_\ell} = 0.886\,[H^+]\sqrt{k_r\, K^H_{MH_2A}\, t} \qquad \text{.....58}$$

quite similar to equation 57. It is apparent from equation 58 that a plot of $\log\left(\frac{i_\ell}{i_d - i_\ell}\right)$ vs. pH should yield a straight line with a slope = -1.00. Figures 23 and 24 illustrate such plots for Cd-DTPA and Pb-DTPA respectively. Both metal complexes exhibited curved lines (Figures 23 and 24) with limiting slopes of approximately -1.5. Since the concentration of $MHA^=$ varies with pH in the kinetic region of Wave B, a correction was applied to $\rho\sigma$, i.e. the effective concentration of $MHA^=$ is equal to;

$$\frac{[\text{total conc. of complexes}]}{[MHA]} = \frac{[MA_T]}{[MHA]}$$

$$\therefore \rho\sigma = k_r\,[H^+]\frac{[MHA]}{[MA_T]} \quad \text{and} \quad \sigma = \frac{k_r[H^+][MHA]}{k_d\,[MA_T]}$$

Upon substitution into equation 58,

$$\frac{i_\ell}{i_d - i_\ell} = 0.886\,\frac{[H^+][MHA]}{[MA_T]}\sqrt{k_r\, K^H_{MH_2A}\, t} \qquad \text{.....59}$$

For convenience let

$$\log \text{"}\alpha\text{"}^{B} = \left[\log[MHA] - \log[MA_T] - pH \right] \quad \ldots\ldots\ldots 60$$

It is evident from equation 59 that a plot of $\log \left(\frac{i_l}{i_d - i_l}\right)$ vs. $\log \text{"}\alpha\text{"}^{B}$ should yield a straight line with a slope equal to 1.00. The experimental values for the above plots are given in table 22 and illustrated in figure 25. The slopes for the Cd-DTPA and Pb-DTPA waves were approximately 1.0 and 0.7 respectively. Again both plots showed some curvature at large wave heights ($i_l > 1.5\mu A$) which was to be expected since (the Koryta - Koutecky theory only applies to purely kinetic waves) the reduction waves only showed kinetic character at small wave heights. The large deviation from the theoretical slope for Pb-DTPA probably indicated that another mechanism was involved in the rate-determining step, though we were unsuccessful in trying to solve the problem.

Equation 59 was used to calculate k_r, i.e. for Cd-DTPA where the $\log \left(\frac{i_l}{i_d - i_l}\right) = \bar{2}.80$, pH = 4.50, $\log K^{H}_{MH_2A} = 3.32$, etc., and applying logs to equation 59;

$$-1.20 = -0.05 - pH - 0.49 + \tfrac{1}{2}(\log k_r + 3.32 + 0.62)$$

$$\text{then } k_r = 4.0, \quad \therefore k_r = 10^{4} \text{ liter mole}^{-1} \text{ sec}^{-1}$$

For Pb-DTPA at pH = 6.00, $\log \left(\frac{i_l}{i_d - i_l}\right) = \bar{2}.53$, $\log K^{H}_{PbH_2A} = 3.5$ (estimated), etc.,

$$-1.47 = -0.05 - pH - 1.51 + \tfrac{1}{2}(\log k_r + 3.5 + 0.62)$$

$$\text{then } \log k_r = 8.0, \quad \therefore k_r = 10^{8} \text{ liter mole}^{-1} \text{ sec}^{-1}$$

Hence the respective rate constants are of the same magnitude as the ones calculated for Wave C and thus indicate that the above proposed mechanism is a reasonable one.

Alternative mechanisms were proposed for Cd-DTPA with the

Table 22 $\text{Log}\left(\frac{i_\ell}{i_d - i_\ell}\right)$ and Log "α" values for Wave B.

Cd-DTPA (1:8)			Pb-DTPA (1:8)		
pH	$\text{Log}\frac{i_\ell}{i_d - i_\ell}$	Log "α" $^{B}_{\text{Cd-DTPA}}$	pH	$\text{Log}\frac{i_\ell}{i_d - i_\ell}$	Log "α" $^{B}_{\text{Pb-DTPA}}$
3.50	$\bar{1}.86$	-3.76	4.50	0.10	-4.82
3.75	$\bar{1}.75$	-3.98	4.75	$\bar{1}.90$	-5.20
4.00	$\bar{1}.59$	-4.26	5.00	$\bar{1}.66$	-5.62
4.25	$\bar{1}.37$	-4.60	5.25	$\bar{1}.45$	-6.07
4.50	$\bar{2}.80$	-4.99	5.50	$\bar{1}.24$	-6.54
4.75	$\bar{2}.39$	-5.41	5.75	$\bar{2}.90$	-7.02
5.00	$\bar{3}.90$	-5.87	6.00	$\bar{2}.53$	-7.51
-	-	-	6.25	$\bar{2}.27$	-8.00
-	-	-	6.50	$\bar{3}.87$	-8.50
Experimental Conditions: h_{Hg} = 60 cm, t = 4.2 sec., i_d = 5.0μA and Gelatin = 0.002%			Experimental Conditions: h_{Hg} = 60 cm, t = 4.2 sec, i_d = 5.4μA and no suppressor.		

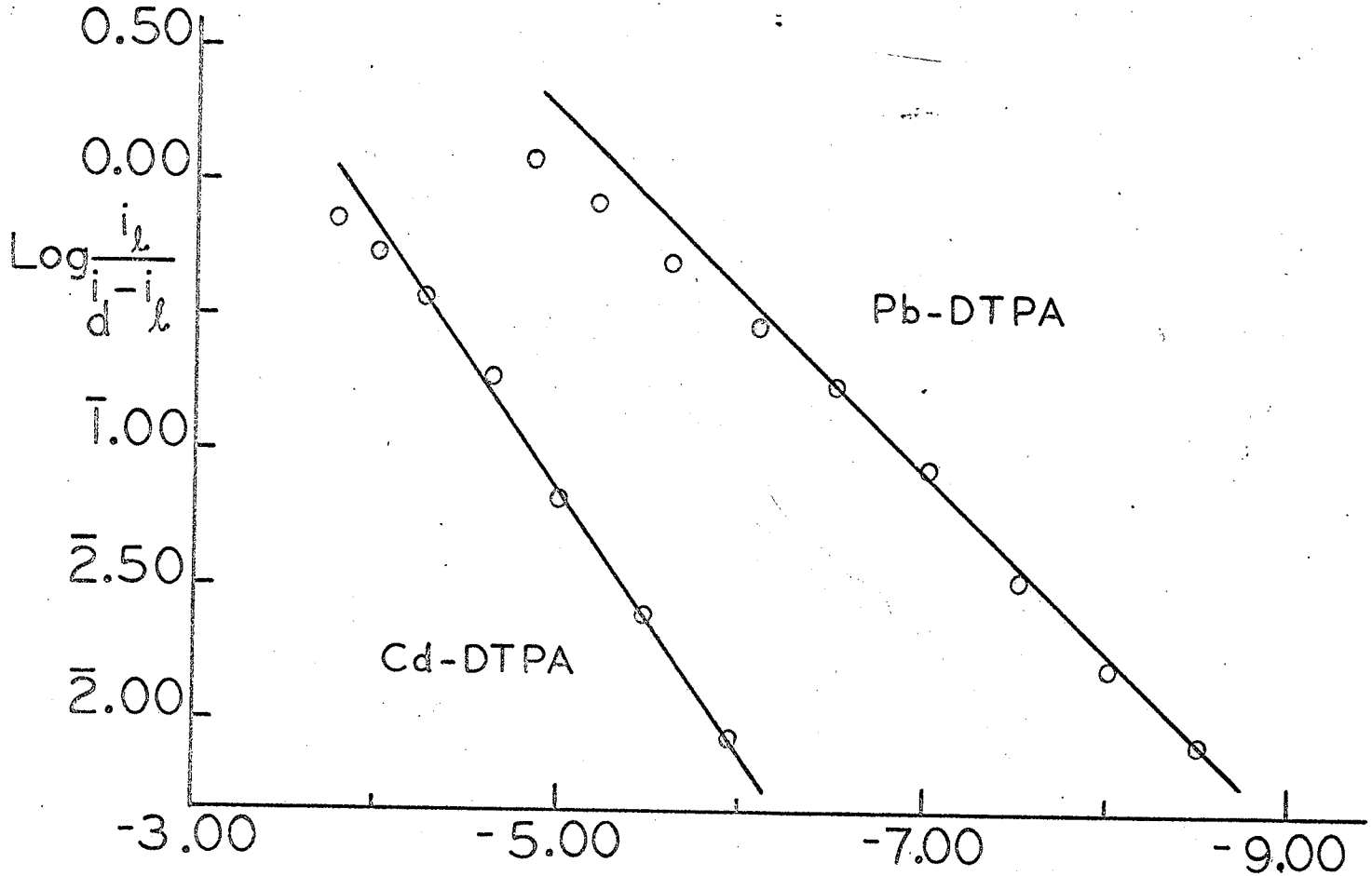

FIG. 25. $\text{Log}\frac{i_\ell}{i_d - i_\ell}$ vs. Log"α" ^{B} for WAVE B.

best fit obtained for (Note: M^{++} is the reducible species)

$$MH_2A^{=} \underset{k_r}{\overset{k_d}{\rightleftharpoons}} M^{++} + H_2A^{=}$$

when correction factors were inserted (suggested by Conradi, et. al.[22]) into the kinetic equation (equation 56) for the formation of buffer complexes, for the varying concentration of the protonated metal complex (MH_2A) and for the concentration of ligand (H_2A). The calculations for the above corrections are given in tables 23 and 24, with the theory outlined below.

Let

$[M]$ = concentration of "simple" metal ion

$[A_T]$ = total concentration of "free" DTPA

$[MA_T]$ = total concentration of metal-DTPA complexes

For protonated complexes of DTPA;

$$K_{MA} = \frac{[MA]}{[M]\,[A]}, \qquad K^{H}_{MHA} = \frac{[MHA]}{[H^+]\,[MA]}$$

$$K^{H}_{MH_2A} = \frac{[MH_2A]}{[MHA][H^+]}, \qquad K^{H}_{MH_3A} = \frac{[MH_3A]}{[MH_2A][H^+]}$$

Then

$$[MA_T] = \left[[MA] + [MHA] + [MH_2A] + [MH_3A] + \ldots \right] \quad \ldots\ldots\ldots\ldots\ldots\ldots 61$$

or

$$[MA_T] = [MA] \left[1 + K^{H}_{MHA}[H^+] + K^{H}_{MH_2A} K^{H}_{MHA} [H^+]^2 + K^{H}_{MH_3A} K^{H}_{MH_2A} K^{H}_{MHA} [H^+]^3 \ldots \right] .. 62$$

Table 23 Log "α functions" for Buffer Corrections.

pH	$\log \alpha_{Cd}$	$\log \alpha_{Pb}$	"K" values
2.00	0.10	0.18	Chloroacetic Acid Buffer
2.25	0.15	0.26	[buffer] = 0.10 M
2.50	0.21	0.35	
2.75	0.26	0.43	pK_a = 2.7
3.00	0.31	0.49	
3.25	0.35	0.54	$\log K_{CdB}$ = 1.5
3.50	0.37	0.57	
3.75	0.39	0.59	$\log K_{PbB}$ = 1.2
4.00	0.40	0.60	
4.00	0.24	0.60	Acetic Acid Buffer
4.25	0.33	0.74	[buffer] = 0.10 M
4.50	0.41	0.86	
4.75	0.48	0.95	pK_a = 4.5
5.00	0.53	1.02	
5.25	0.57	1.07	$\log K_{CdB}$ = 2.1
5.50	0.59	1.09	
5.75	0.60	1.11	$\log K_{PbB}$ = 1.5
6.00	0.61	1.12	

The various equilibrium constants were taken from "Stability Constants" by Bjerrum, J., Schwarzenbach, G. and Sillén, L. G. Chem. Soc. (London) Spec. Publ., 7(1958)

Table 24 Log "α functions" for DTPA and Metal-Complexes.

	DTPA			Cd-DTPA			Pb-DTPA		
pH	log α_{HA}	log α_{H_2A}	log α_{H_3A}	log α_{CdA}	log α_{CdHA}	log α_{CdH_2A}	log α_{PbA}	log α_{PbHA}	log α_{PbH_2A}
2.00	9.98	3.31	0.97	3.52	1.32	0.02	4.01	1.51	0.01
2.25	9.19	2.77	0.68	3.04	1.09	0.04	3.52	1.27	0.02
2.50	8.46	2.29	0.45	2.57	0.87	0.07	3.04	1.04	0.04
2.75	7.80	1.88	0.29	2.11	0.66	0.11	2.57	0.82	0.07
3.00	7.20	1.53	0.19	1.69	0.49	0.19	2.12	0.62	0.12
3.25	6.64	1.22	0.13	1.30	0.35	0.30	1.70	0.45	0.20
3.50	6.12	0.95	0.11	0.96	0.26	0.46	1.32	0.32	0.32
3.75	5.64	0.72	0.13	0.68	0.23	0.68	0.99	0.24	0.49
4.00	5.19	0.52	0.18	0.46	0.26	0.96	0.71	0.21	0.71
4.25	4.78	0.35	0.26	0.30	0.35	1.30	0.49	0.24	0.99
4.50	4.40	0.23	0.39	0.19	0.49	1.69	0.32	0.32	1.32
4.75	4.06	0.14	0.55	0.11	0.66	2.11	0.20	0.45	1.70
5.00	3.76	0.09	0.75	0.07	0.87	2.57	0.12	0.62	2.12
5.25	3.47	0.05	0.96	0.04	1.09	3.04	0.07	0.82	2.57
5.50	3.20	0.03	1.19	0.02	1.32	3.52	0.04	1.04	3.04
5.75	2.94	0.02	1.43	0.01	1.56	4.01	0.02	1.27	3.52
6.00	2.68	0.01	1.67	0.01	1.81	4.51	0.01	1.51	4.01

Constants used: DTPA - average pK's, Cd-DTPA - Chaberek's values, Pb-DTPA - Schwarzenbach's values and log $K^{H}_{PbH_2A}$ = 3.5 estimated value from this study.

with the part in parenthesis abbreviated to α_{MA} equation 62 becomes

$$[MA_T] = [MA]\alpha_{MA} \quad \ldots\ldots 63$$

It follows then that

$$\alpha_{MA} = \frac{[MA_T]}{[MA]}, \quad \alpha_{MHA} = \frac{[MA_T]}{[MHA]} \quad \text{and} \quad \alpha_{MH_2A} = \frac{[MA_T]}{[MH_2A]}$$

Secondly;

$$[A_T] = \left[[A] + [HA] + [H_2A] + [H_3A] + [H_4A] + [H_5A] \right] \quad \ldots\ldots 64$$

or

$$[A_T] = [A]\left[1 + \frac{[H^+]}{K_5} + \frac{[H^+]^2}{K_4K_5} + \frac{[H^+]^3}{K_3K_4K_5} + \frac{[H^+]^4}{K_2K_3K_4K_5} + \frac{[H^+]^5}{K_1K_2K_3K_4K_5} \right] . 65$$

with the part in parenthesis abbreviated to $\alpha_{L(H)}$ equation 65 becomes

$$[A_T] = [A]\,\alpha_{L(H)} \quad \ldots\ldots 66$$

Then

$$\alpha_{HA} = \frac{A_T}{HA} = \left[\frac{[H^+]^4}{K_1K_2K_3K_4} + \frac{[H^+]^3}{K_2K_3K_4} + \frac{[H^+]^2}{K_3K_4} + \frac{[H^+]}{K_4} + 1 + \frac{K_5}{H^+} \right] .. 67$$

$$\alpha_{H_2A} = \frac{A_T}{H_2A} = \left[\frac{[H^+]^3}{K_1K_2K_3} + \frac{[H^+]^2}{K_2K_3} + \frac{[H^+]}{K_3} + 1 + \frac{K_4}{[H^+]} + \frac{K_4K_5}{[H^+]^2} \right] .. 68$$

and

$$\alpha_{H_3A} = \frac{A_T}{H_3A} = \left[\frac{[H^+]^2}{K_1K_2} + \frac{[H^+]}{K_2} + 1 + \frac{K_3}{H^+} + \frac{K_3K_4}{[H^+]^2} + \frac{K_3K_4K_5}{[H^+]^3} \right] \ldots 69$$

Secondly for the buffer corrections;

$$\alpha_M = \frac{[M_T]}{[M]} = \frac{[M] + [MB]}{[M]} = \frac{1 + [MB]}{[M]} \quad \ldots\ldots 70$$

where [MB] is the concentration of metal-buffer complex. Since $K_{MB} = \frac{[MB]}{[M][B]}$ equation 70 becomes

$$\alpha_M = 1 + K_{MB}[B] \text{ , and } K_a = \frac{[H^+][B]}{[MB]}$$

for the buffer where $[HB] + [B] = c_T$ = total buffer concentration,

$$\therefore \alpha_M = 1 + \frac{K_{MB}\, c_T}{(1 + \frac{[H^+]}{K_a})} \quad \text{.....71}$$

Restating the proposed mechanism;

$$MH_2A^- \underset{k_r}{\overset{k_d}{\rightleftharpoons}} M^{++} + H_2A^{\equiv}$$

and writing out the rate constants, one obtains

$$\text{rate} \rightarrow = k_d[MH_2A] = \rho\sigma[MH_2A], \quad \therefore \quad k_d = \rho\sigma$$

$$\text{rate} \leftarrow = k_r[H_2A][M^{++}] = \rho[M^{++}], \therefore \rho = k_r[H_2A]$$

Recalling equations 63, 68 and 71 and applying the correction factors (α_M, α_{H_2A} and α_{MH_2A})

$$\rho\sigma = \frac{k_d}{\alpha_{MH_2A}} \text{ and } \rho = \frac{k_r[A_T]}{\alpha_{H_2A}\alpha_M}$$

$$\therefore \sigma = \frac{k_d\, \alpha_{H_2A}\, \alpha_M}{k_r\, [A_T]\, \alpha_{MH_2A}}$$

When the above corrected constants are transposed into equation 56;

$$\frac{i_\ell}{i_d - i_\ell} = 0.886 \frac{k_d \alpha_{H_2A} \alpha_M}{k_r A_T \alpha_{MH_2A}} \sqrt{\frac{k_r A_T t}{\alpha_{H_2A} \alpha_M}} \quad \text{.....72}$$

upon rearranging

$$\frac{i_\ell}{i_d - i_\ell} = \frac{0.886}{\alpha_{MH_2A}} \sqrt{\frac{k_d \alpha_{H_2A} \alpha_M t}{K^M_{MH_2A} [A_T]}} \quad \text{.....73}$$

It can be seen from equation 73 that a plot of log $\left(\frac{i_\ell}{i_d - i_\ell}\right)$ vs. $1/2(\log \alpha_{H_2A} + \log \alpha_M) - \log \alpha_{MH_2A}$ (later abbreviated to log $"\alpha"^B_{Cd\text{-}DTPA}$) should yield a straight line with a slope = 1.00. The experimental values for the above plot are given in table 22, and illustrated in figure 26. The slope was 1.00 which is in perfect agreement with the theoretical value, though some of the experimental points are off the straight line plot by ≈ 10%. Hence it appeared as though the above mechanism was a reasonable one.

Equation 73 was used to calculate the dissociation rate constant, k_d. For Cd-DTPA (1:8) at pH = 4.50, t = 4.2 sec, A_T = 7×10^{-3}M, log $K^M_{CdH_2A}$ = 7.3 (Chabarek's value), log $\left(\frac{i_\ell}{i_d - i_\ell}\right) = \bar{2}.80$ and applying logs to equation 73 one obtains;

$$-1.20 = \log 0.886 + 1/2(\log k_d + \log \alpha_{H_2A} + \log \alpha_M + \log t - \log K^M_{MH_2A} - \log A_T) - \log \alpha_{MH_2A}$$

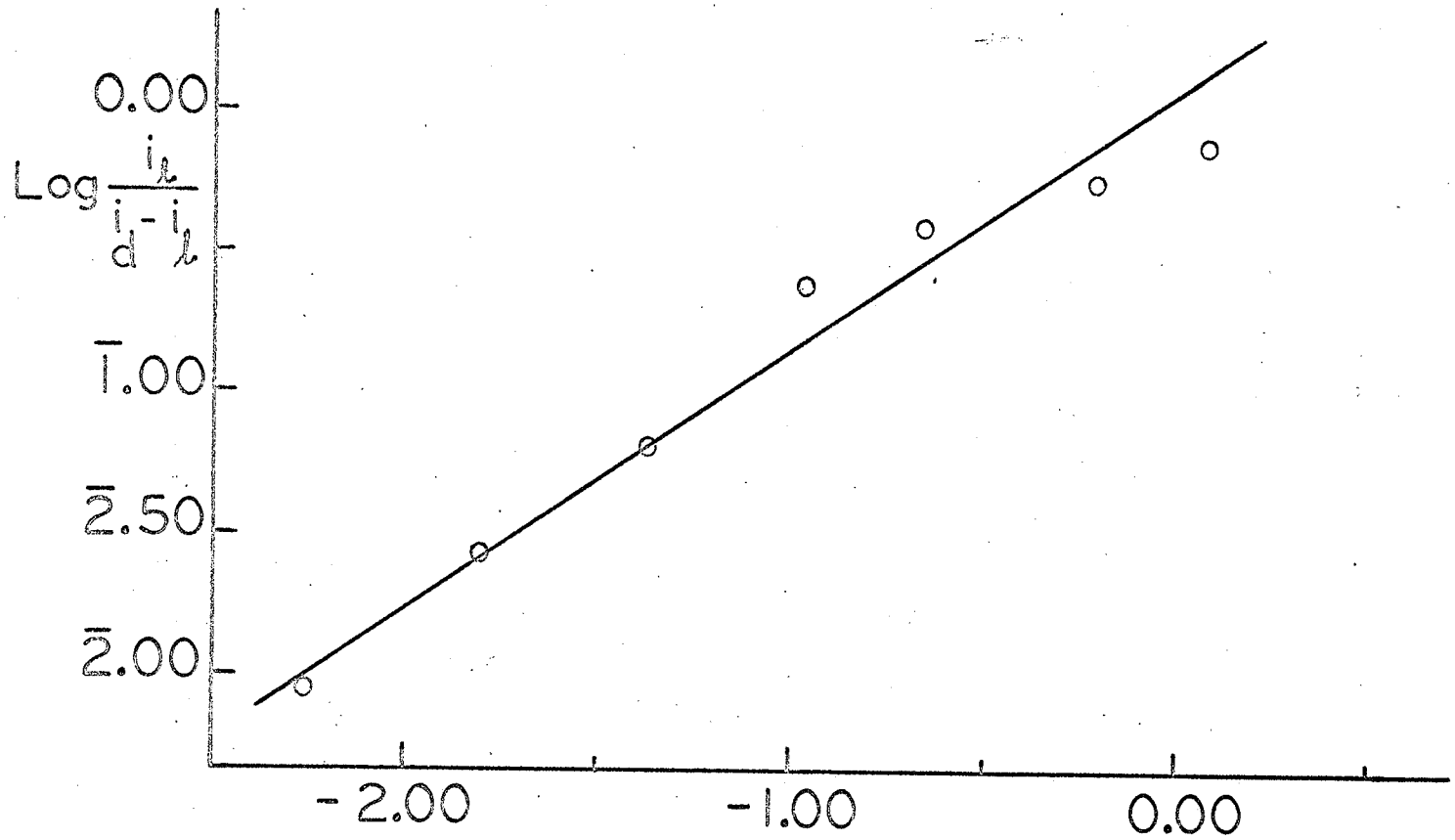

FIG. 26. Log $\frac{i_l}{i_d - i_l}$ vs. Log "α"$^{B}_{Cd\text{-}DTPA}$ for WAVE B.

where

$$\log k_d = 5.0, \quad \therefore k_d = 10^5 \text{ sec}^{-1}$$

since

$$K^M_{MH_2A} = \frac{k_r}{k_d}, \quad k_r = 2 \times 10^7 (10)^5 = 2 \times 10^{12}$$

The recombination rate constant, k_r, lies within the range of acid recombination ($10^7 - 10^{13}$) constants. However the k_r value is unreasonable for complex formation which is what it represents in the proposed mechanism above. Hence the above mechanism was discarded as an unreasonable choice.

C) Wave A

For a reversible diffusion-controlled reduction of a metal complex the half-wave potential is given by,

$$E_{\frac{1}{2}}(c) = E_{\frac{1}{2}}(s) - \frac{0.05915}{n} \log K_{eff} (C_L)_o \quad \ldots\ldots\ldots\ldots\ldots\ldots 74$$

similar to equation 29 (chapter 3), where K_{eff} is the effective stability constant and $(C_L)_o$ is the concentration of ligand at the electrode surface defined as:

$$(C_L)_o = C_L + C_M \frac{i_k}{i_d} \quad \ldots\ldots\ldots\ldots\ldots\ldots\ldots\ldots\ldots\ldots\ldots\ldots\ldots\ldots\ldots\ldots 75$$

where C_L is the concentration of free ligand and $C_M \frac{i_k}{i_d}$ is the concentration of ligand coming from the metal complex upon reduction of the metal ion at the D.M.E. Equation 35 (from chapter 3) corrects for the kinetically-controlled reduction process:

$$E_{\frac{1}{2}}(c) = E(k) + \frac{0.05915}{n} \log \frac{i_k}{i_d}$$

Equating equations 35 and 74 one obtains:

$$E_{\frac{1}{2}}(k) - E_{\frac{1}{2}}(s) = - \frac{0.05915}{n} \log K_{eff} (C_L)_o - \frac{0.05915}{n} \log \frac{i_k}{i_d} \quad \ldots 76$$

or

$$\triangle E_{\frac{1}{2}} = - \frac{0.05915}{n} \log K_{eff} (C_L)_o - \frac{0.05915}{n} \log \frac{i_k}{i_d} \quad \ldots\ldots\ldots 77$$

Solving for $\log K_{eff}$,

$$\log K_{eff} = \frac{n}{0.05195} (\triangle E_{\frac{1}{2}}) - \log \frac{i_k}{i_d} - \log (C_L)_o \quad \ldots\ldots\ldots\ldots 78$$

If one neglects the complexing effect of the buffer (since this only effects $E_{1/2(s)}$ and cancels out in solving for $\Delta E_{1/2}$), then (from $K_{eff} = \frac{[MA_T]}{[M][A_T]}$)

$$K_{eff} = \frac{[MA]\ \alpha_{MA}}{[M]\ [A]\alpha_{L(H)}} = K_{MA}\frac{\alpha_{MA}}{\alpha_{L(H)}} \quad \text{.....79}$$

where

$$\log K_{eff} = \log K_{MA} + \log \alpha_{MA} - \log \alpha_{L(H)} \quad \text{.....80}$$

or rearranging

$$\log K_{eff} + \log \alpha_{L(H)} = \log K_{MA} + \log \alpha_{MA} \quad \text{.....81}$$

Recalling equation 62, α_{MA} may be written as

$$\left[1 + 10^{\log K^H_{MHA} - pH} + 10^{\log K^H_{MH_2A} + \log K^H_{MHA} - 2pH} + 10^{\log K^H_{MH_3A} + \log K^H_{MH_2A} + \log K^H_{MHA} - 3pH} + \ldots\right] \quad \text{.....82}$$

which lends itself conveniently to a mathematical check as to how many protonated complexes are involved in the overall equilibrium.

Table 25 gives the various dissociation constants (four independent sources) of DTPA and the $\log \alpha_{L(H)}$ values based on the average pH's found in the literature. Figure 27 diagrammatically

Table 25 Dissociation and Stability Constants Information.

pH	Log $\alpha_{L_{(H)}}$	DTPA	Wänninen[6]	Durham + Ryskiewich[7]	Frost[8]	Ringbom*	Average
2.00	18.46						
2.25	17.44	pK_1	1.86	2.08	1.79	1.94	1.92
2.50	16.47						
2.75	15.55	pK_2	2.79	2.41	2.56	2.87	2.66
3.00	14.70						
3.25	13.89	pK_3	4.29	4.26	4.42	4.37	4.34
3.50	13.12						
3.75	12.39	pK_4	8.61	8.60	8.76	8.69	8.67
4.00	11.69						
4.25	11.03	pK_5	10.48	10.55	10.42	10.56	10.50
4.50	10.40						

	Chaberek, Frost et al[9]	Anderegg, ...+ Schwarzenbach**	Holloway + Reilley***	Wänninen[6]	Durham + Ryshiewich[7]
log K_{CdA}	18.9	19.31	19.0	19.06	18.93
log K_{CdHA}	4.17	-	-	-	-
log K_{CdH_2A}	3.32	-	-	-	-
log K_{PbA}	-	18.87			
log K_{PbHA}	-	4.52			
log K_{PbH_2A}	-				

*** Anal. Chem. 32 249 (1960)

** Helv. Chim. Acta 42 827 (1959)

*Complexation in Analytical Chemistry, Interscience p. 351 (1963)

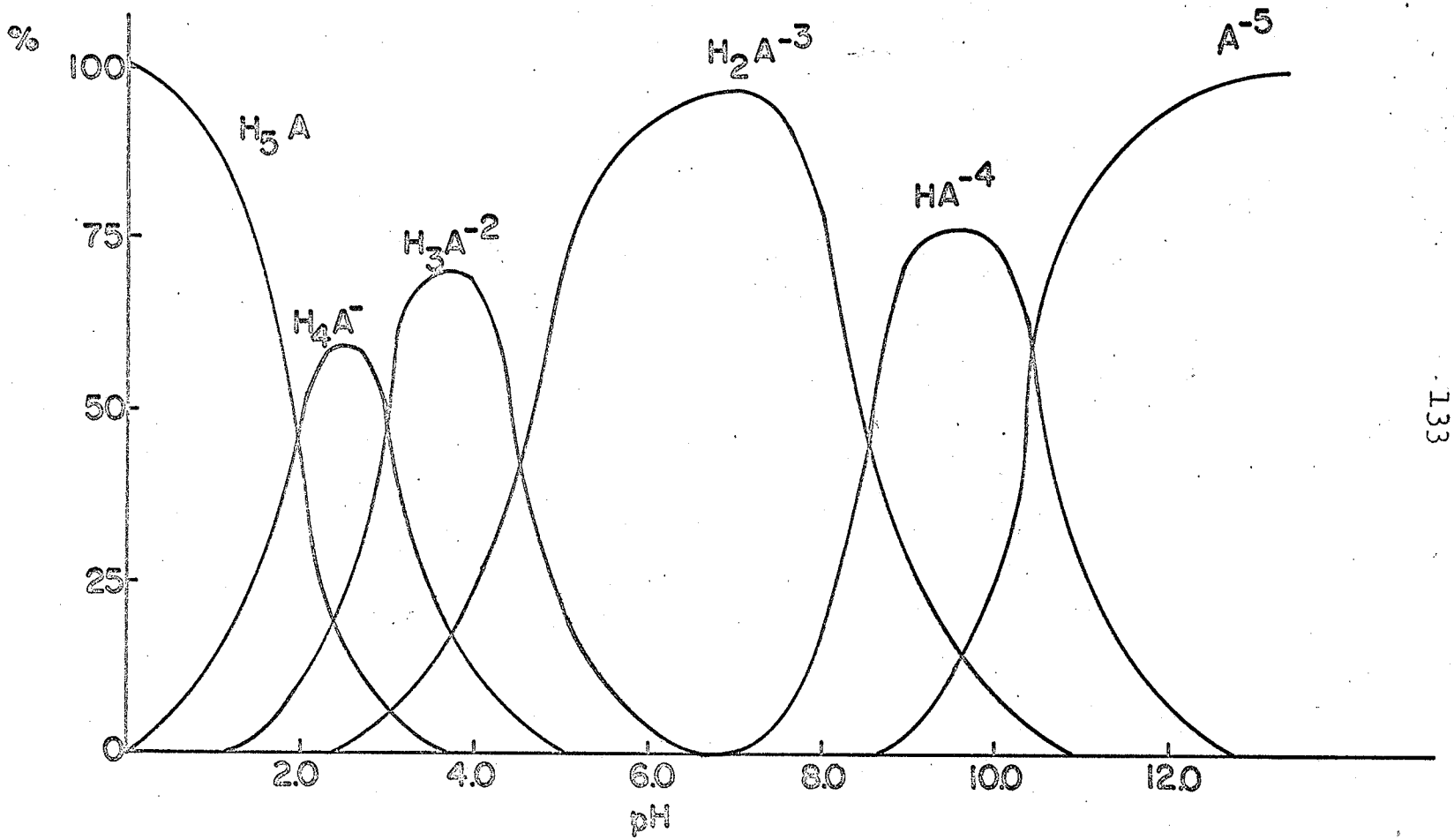

FIG.27 PERCENTAGES OF VARIOUS FORMS OF DTPA VS. pH.

shows the various forms of DTPA present at any given pH. A brief survey of this diagram (fig. 27) strongly suggests that protonated complexes would be expected in the pH range from 2.0 to 6.0. Some possible equilibria involve:

$$Cd^{++} + H_3A^{-2} \rightleftharpoons CdH_3A$$

$$Cd^{++} + H_2A^{-3} \rightleftharpoons CdH_2A^{-}$$

$$Cd^{++} + HA^{-4} \rightleftharpoons CdHA^{=}$$

The necessary calculations involved in equation 81 are recorded in tables 26_a and 26_b for Cd-DTPA. A plot of $\log K_{eff} + \log \alpha_{L(H)}$ vs. pH is shown in figure 28. Similar calculations and a graphical plot are given for Pb-DTPA in tables 27_a and 27_b and figure 29 respectively. A computer programme (least squares method) was written and applied to equation 81 to find the best theoretical fit to the experimental averages of $\log K_{eff} + \log \alpha_{L(H)}$ for both metal complexes. The inclusion of doubly ($case^a$) and triply ($case^b$) protonated complexes in α_{MA} generally gave the best fit, i.e. for Cd-DTPA,

$case^a$

$$\log K_{eff} + \log \alpha_{L(H)} = 18.81 + \log (1 + 10^{2.95-pH} + 10^{6.88-2pH})$$

$case^b$

$$\log K_{eff} + \log \alpha_{L(H)} = 19.15 + \log(1 + 10^{2.95-pH} + 10^{5.90-2pH} + 10^{8.63-3pH})$$

Table 26a Equilibrium Calculations for Cd-DTPA (Wave A)

pH	$\frac{i_l}{i_d}$	$(C_L)_o \times 10^{-3}$	$\log \frac{i_l}{i_d} + \log (C_L)_o$	$\Delta E_{1/2}$	$\log K_{eff}$	$\log K_{eff} + \log \alpha_{L_{(H)}}$	
2.00	0.88	1.88	$\bar{3}.21$	0.018	3.40	21.86	
2.25	0.80	1.80	$\bar{3}.16$	0.025	3.69	21.13	
2.50	0.68	1.68	$\bar{3}.06$	0.035	4.12	20.59	
2.75	0.53	1.53	$\bar{4}.90$	0.043	4.55	20.10	
3.00	0.36	1.36	$\bar{4}.68$	0.051	5.05	19.75	1:2
3.25	0.23	1.23	$\bar{4}.46$	0.054	5.37	19.26	
3.50	0.057	1.06	$\bar{5}.79$	0.060	6.24	19.36	
3.75	0.017	1.02	$\bar{5}.24$	0.067	7.03	19.42	
4.00	0.007	1.01	$\bar{6}.85$	0.071	7.55	19.24	
2.00	0.77	3.77	$\bar{3}.47$	0.028	3.48	21.94	
2.25	0.71	3.71	$\bar{3}.42$	0.037	3.83	21.27	
2.50	0.64	3.64	$\bar{3}.37$	0.046	4.19	20.66	
2.75	0.53	3.53	$\bar{3}.27$	0.050	4.42	19.97	1:4
3.00	0.36	3.36	$\bar{3}.08$	0.054	4.75	19.45	
3.25	0.17	3.17	$\bar{4}.73$	0.063	5.41	19.20	
3.50	0.071	3.07	$\bar{4}.34$	0.073	6.13	19.25	
3.75	0.028	3.03	$\bar{5}.93$	0.078	6.71	19.10	
4.00	0.007	3.01	$\bar{5}.33$	0.081	7.41	19.10	

Experimental Conditions: i_d = 7.00μA, h_{Hg} = 60 cm and Gelatin = 0.002%.

Table 26b Equilibrium Calculations for Cd-DTPA (Wave A)

pH	$\frac{i_\ell}{i_d}$	$(C_L)_o \times 10^{-3}$	$\log \frac{i_\ell}{i_d} + \log (C_L)_o$	$\Delta E_{1/2}$	$\log K_{eff}$	$\log K_{eff} + \log \alpha_{L_{(H)}}$	
2.00	0.70	7.70	$\bar{3}.73$	0.028	3.22	21.68	
2.25	0.64	7.64	$\bar{3}.69$	0.037	3.56	21.00	
2.50	0.60	7.60	$\bar{3}.66$	0.046	3.90	20.37	
2.75	0.47	7.47	$\bar{3}.55$	0.051	4.18	19.73	
3.00	0.28	7.28	$\bar{3}.32$	0.064	4.85	19.55	1:8
3.25	0.11	7.11	$\bar{4}.91$	0.073	5.56	19.45	
3.50	0.043	7.04	$\bar{4}.48$	0.083	6.33	19.45	
3.75	0.014	7.01	$\bar{5}.99$	0.087	6.96	19.35	
2.00	0.65	9.65	$\bar{3}.79$	0.038	3.50	21.96	
2.25	0.63	9.63	$\bar{3}.78$	0.047	3.81	21.25	
2.50	0.58	9.58	$\bar{3}.74$	0.056	4.15	20.62	
2.75	0.50	9.50	$\bar{3}.68$	0.065	4.52	20.07	1:10
3.00	0.28	9.28	$\bar{3}.42$	0.074	5.09	19.79	
3.25	0.17	9.17	$\bar{3}.19$	0.078	5.45	19.34	
3.50	0.070	9.07	$\bar{4}.81$	0.083	6.00	19.12	
3.75	0.014	9.01	$\bar{4}.10$	0.091	6.98	19.37	

Experimental Conditions: i_d = 7.00μA, h_{Hg} = 60 cm and Gelatin = 0.002%.

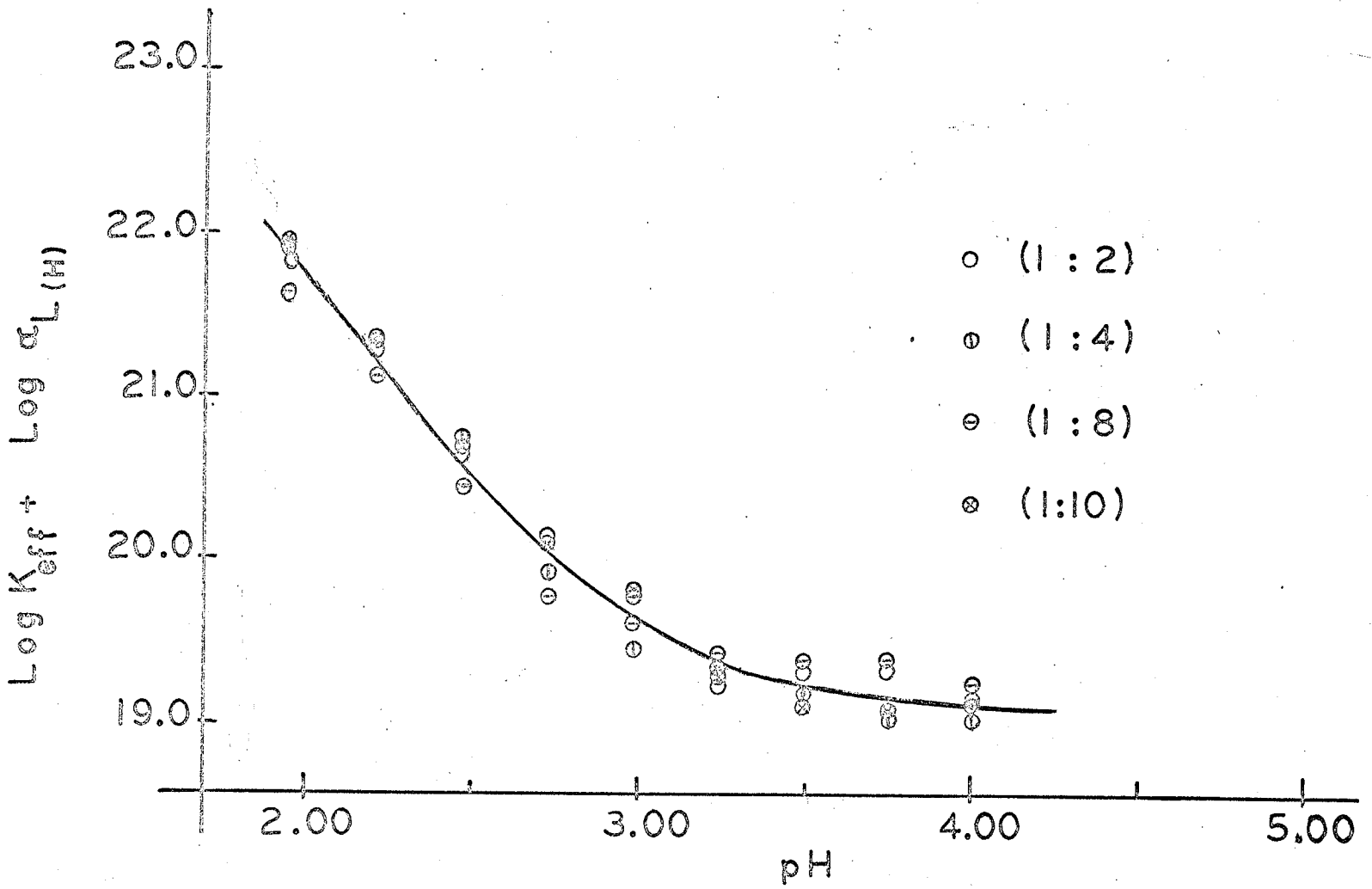

FIG. 28. Log K_{eff} + Log $\alpha_{L(H)}$ vs. pH for Cd-DTPA.

Table 27a Equilibrium Calculations for Pb-DTPA (1:2)

Wave A

pH	i_ℓ/i_d	$(C_L)_o \times 10^{-3}$	$\log i_\ell/i_d + \log (C_L)_o$	$\Delta E_{1/2}$	$\log K_{eff}$	$\log K_{eff} + \log \alpha_{L(H)}$
2.00	0.64	1.64	$\bar{3}.03$	0.053	4.76	23.22
2.25	0.54	1.54	$\bar{4}.92$	0.059	5.07	22.51
2.50	0.48	1.48	$\bar{4}.85$	0.065	5.35	21.82
2.75	0.44	1.44	$\bar{4}.80$	0.074	5.71	21.26
3.00	0.34	1.34	$\bar{4}.66$	0.081	6.08	20.78
3.25	0.27	1.27	$\bar{4}.51$	0.083	6.30	20.19
3.50	0.20	1.20	$\bar{4}.38$	0.092	6.74	19.86
3.75	0.067	1.07	$\bar{5}.86$	0.095	7.36	19.75
4.00	0.040	1.04	$\bar{5}.62$	0.100	7.77	19.46
4.25	0.013	1.01	$\bar{5}.13$	0.103	8.36	19.39
4.50	0.0054	1.005	$\bar{6}.73$	0.108	8.93	19.33

Experimental Conditions: $Pb^{++} = 1.0 \times 10^{-3}$M, DTPA = 2.0×10^{-3}M, $i_d = 7.44\mu$A, $h_{Hg} = 60$ cm, and TX - 100 = 0.001%.

Table 27b Equilibrium Calculations for Pb-DTPA (1:8)

Wave A

pH	i_ℓ/i_d	$(C_L)_o \times 10^{-3}$	$\log i_\ell/i_d + \log (C_L)_o$	$\Delta E_{1/2}$	$\log K_{eff}$	$\log K_{eff} + \log \alpha_{L(H)}$
2.00	0.54	7.54	$\bar{3}.61$	0.080	5.10	23.56
2.25	0.48	7.48	$\bar{3}.55$	0.085	5.29	22.73
2.50	0.40	7.40	$\bar{3}.47$	0.093	5.68	22.15
2.75	0.35	7.35	$\bar{3}.41$	0.100	5.98	21.53
3.00	0.31	7.31	$\bar{3}.35$	0.106	6.24	20.94
3.25	0.20	7.20	$\bar{3}.16$	0.110	6.57	20.46
3.50	0.12	7.12	$\bar{4}.90$	0.113	6.93	20.05
3.75	0.074	7.07	$\bar{4}.72$	0.120	7.35	19.74
4.00	0.039	7.04	$\bar{4}.44$	0.126	7.83	19.52
4.25	0.016	7.02	$\bar{4}.05$	0.128	8.28	19.31
4.50	0.0067	7.01	$\bar{5}.68$	0.130	8.73	19.13

Experimental Conditions: $Pb^{++} = 1.0 \times 10^{-3}$M, DTPA = 8.0×10^{-3}M, $i_d = 7.44\mu A$, $h_{Hg} = 60$ cm, and TX - 100 = 0.001%.

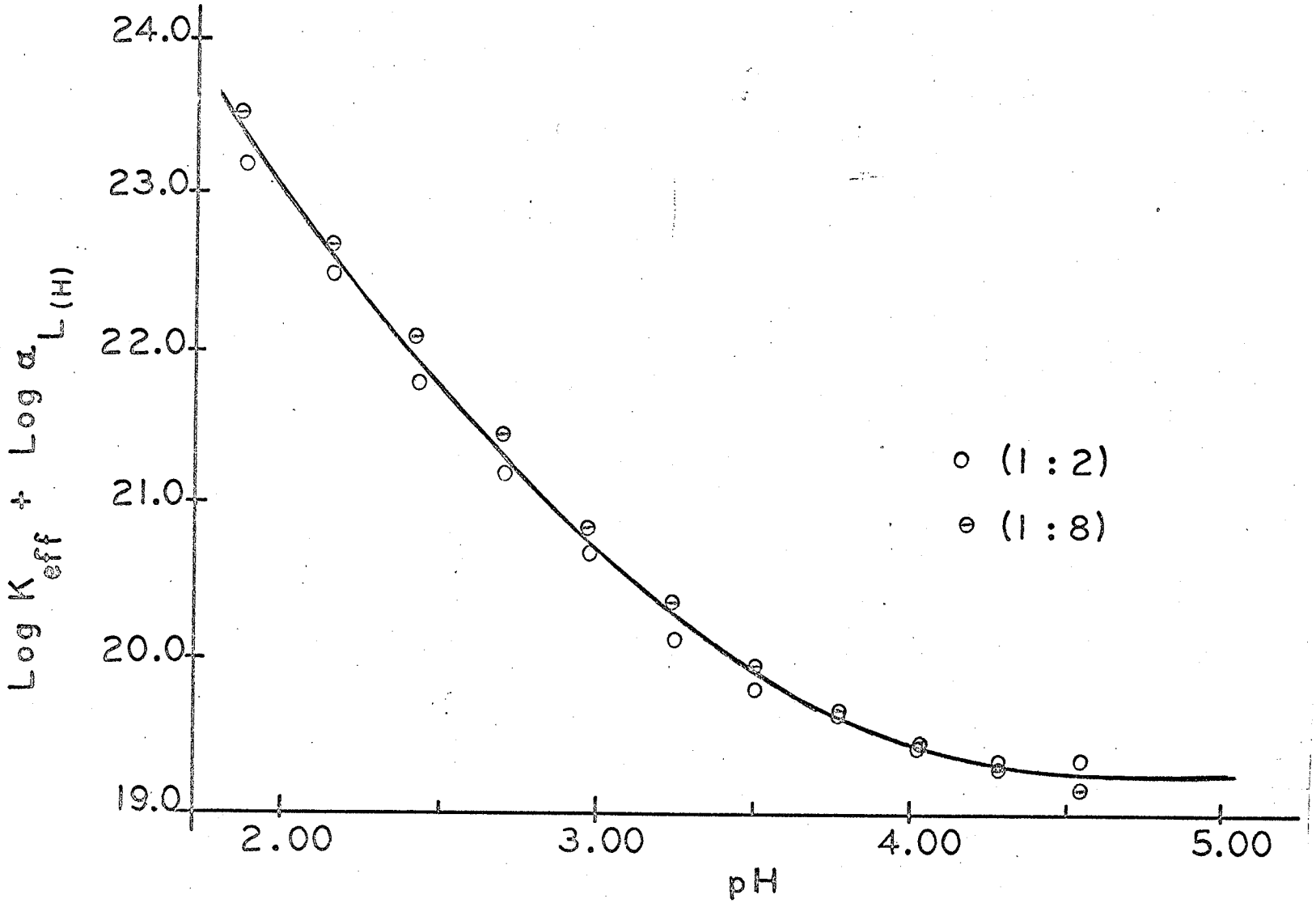

FIG. 29. Log K_{eff} + Log $\alpha_{L(H)}$ vs. pH for Pb-DTPA.

Table 28 gives the average experimental values and the calculated values of $\log K_{eff} + \log \alpha_{L(H)}$ for both cases. Close inspection of those values led to the conclusion that three protonated complexes were involved in the overall equilibrium. Thus (from equation 82) the best fit was obtained for

$$\log K_{CdA} = 19.15, \qquad \log K^{H}_{CdHA} = 2.95$$
$$\log K^{H}_{CdH_2A} = 2.95, \qquad \log K^{H}_{CdH_3A} = 2.73$$

A similar set of calculated and experimental $\log K_{eff} + \log \alpha_{L(H)}$ values for Pb-DTPA are given in table 28. The best fit (calculated to experimental) was obtained when the doubly (case^a) and triply protonated (case^b) complexes were included in α_{MA}, namely:

case^a

$$\log K_{eff} + \log \alpha_{L(H)} = 19.05 + \log(1 + 10^{3.35-pH} + 10^{7.94-2pH})$$

and

case^b

$$\log K_{eff} + \log \alpha_{L(H)} = 19.10 + \log(1 + 10^{4.05-pH} + 10^{7.45-2pH} + 10^{10.20-3pH})$$

Again case^b gave the better fit of the two. Recalling equations 81 and 82 one obtains:

$$\log K_{PbA} = 19.10, \qquad \log K^{H}_{PbHA} = 4.05$$
$$\log K^{H}_{PbH_2A} = 3.40, \qquad \log K^{H}_{PbH_3A} = 2.75$$

Table 28 Experimental and Calculated Log "K" Values.

$\text{Log } K_{eff} + \text{Log } \alpha_{L_{(H)}}$

	Cd-DTPA			Pb-DTPA		
pH	Average Exp. Value	Calculated[a]	Calculated[b]	Average Exp. Value	Calculated[a]	Calculated[b]
2.00	21.90	21.69	21.86	23.43	22.99	23.37
2.25	21.16	21.21	21.18	22.69	22.49	22.68
2.50	20.57	20.73	20.55	22.00	21.99	22.01
2.75	19.99	20.26	20.02	21.40	21.50	21.40
3.00	19.63	19.83	19.64	20.87	21.00	20.85
3.25	19.33	19.46	19.41	20.33	20.52	20.38
3.50	19.30	19.19	19.29	19.96	20.07	20.00
3.75	19.28	19.01	19.22	19.82	19.67	19.70
4.00	19.18	18.92	19.19	19.48	19.37	19.48
4.25				19.36	19.20	19.34
4.50				19.24	19.11	19.24
Case[a]		Case[b]		Case[a]		Case[b]
$\log K_{CdA} = 18.81$		$\log K_{CdA} = 19.15$		$\log K_{PbA} = 19.05$		$\log K_{PbA} = 19.10$
$\log K^{H}_{CdHA} = 3.30$		$\log K^{H}_{CdHA} = 2.95$		$\log K^{H}_{PbHA} = 3.35$		$\log K^{H}_{PbHA} = 4.05$
$\log K^{H}_{CdH_2A} = 3.58$		$\log K^{H}_{CdH_2A} = 2.95$		$\log K^{H}_{PbH_2A} = 4.59$		$\log K^{H}_{PbH_2A} = 3.40$
		$\log K^{H2}_{CdH_3A} = 2.73$				$\log K^{H2}_{PbH_3A} = 2.75$

Table 28 gives a summary of the calculated stability constants obtained from Wave A.

In table 25 are given the literature values for various Cd-DTPA and Pb-DTPA stability constants. In the case of log K_{MA}, the constants obtained in this study (for both Cd-DTPA and Pb-DTPA) compare very well with the literature values. In fact for Cd-DTPA our value falls within the range of values gives in the literature (see tables 25 and 28). In the case of Pb-DTPA our log K_{MA} value differs from the lone literature value by 0.23 log K (i.e. literature value 18.87, our value 19.10). This is considered excellent agreement for stability constants obtained by electroanalytical methods[23-26].

For log K^{H}_{MHA} the agreement was not as good. Only one (p. 132) literature value was given for each metal complex (log K^{H}_{CdHA} = 4.17, log K^{H}_{PbHA} = 4.52) differing from our values by 1.23 log K units for Cd-DTPA and 0.47 log K for Pb-DTPA. Similarly log $K^{H}_{MH_2A}$ (log $K^{H}_{CdH_2A}$ = 3.32) for Cd-DTPA differs from the literature value by 0.37 log K units. Log $K^{H}_{PbH_2A}$ has not been reported to date. No values could be found for log $K^{H}_{MH_3A}$ for either metal-DTPA complex. The relatively few literature constants determined to date (for protonated complexes of Cd or Pb) indicates a measure of the difficulty encountered in obtaining stability constants for protonated metal-DTPA complexes. It is not too surprising then to find large differences between log $K^{H}_{MH_xA}$ values which were determined by different methods and under different conditions.

A number of mechanisms (kinetically controlling Wave A) were proposed among which the best fit for Pb-DTPA was obtained with;

$$PbH_2A^- \underset{k_r}{\overset{k_d}{\rightleftharpoons}} H_2A^{-3} + Pb^{++} \qquad \text{(slow)}$$

$$Pb^{++} + Hg^{o} + 2e^- \rightleftharpoons Pb(Hg) \qquad \text{(fast)}$$

which is of the same form as the Wave C mechanism except that free Pb^{++} is the electroactive species and not the PbH_2A^- complex. Applying the Koryta and Koutecky[27] kinetic treatment (Note: the rate constant $\rho\sigma$ is always used for the reaction yielding the reducible component) one obtains:

$$\text{rate} \longrightarrow = k_d[PbH_2A] = \rho\sigma\,[PbH_2A], \therefore k_d = \rho\sigma$$

$$\text{rate} \longleftarrow = k_r[H_2A][Pb^{++}] = \rho[Pb^{++}], \therefore \rho = k_r[H_2A]$$

$$\text{and } \sigma = \frac{k_d}{k_r[H_2A]} \quad \text{with some charges omitted for simplicity.}$$

Substitution of the above constants into equation 56 yields

$$\frac{i_k}{i_d - i_k} = 0.886 \frac{k_r}{k_d\,[H_2A]} \sqrt{k_d\, t} \quad \ldots\ldots\ldots\ldots \quad 83$$

In the pH range from 2.0 to 6.0, the approximate concentration of $[H_2A]$ is,

$$[H_2A] \cong \frac{A_T K_2 K_3}{[H^+]^2 + [H^+]K_2} \quad \text{which when substituted into}$$

equation 83 yields

$$\frac{i_k}{i_d - i_k} = 0.886 \frac{k_r}{k_d} \frac{[H^+]^2 + [H^+]K_2}{A_T K_2 K_3} \sqrt{k_d\, t} \quad \ldots\ldots \quad 84$$

for which a plot of $\log\left(\frac{i_k}{i_d - i_k}\right)$ vs. pH should have a slope of approximately -2.00 depending on the relative magnitude of K_2 and $[H^+]$. However the above plot for Pb-DTPA exhibited a curved line from pH = 2.5 to 3.5 and an almost straight line (slope $\simeq$ - 1.50) between pH = 3.5 and 4.5. Conradi, et al.[22] have pointed out that under acidic conditions corrections must be applied for the concentrations of protonated complexes, for the complexing effect of the buffer used and for the concentration of ligand if not used in large excess.

Rewriting the rate constants with the above correction factors;

$$\rho = k_r \frac{[H_2A]}{\alpha_M} \qquad , \rho\sigma = \frac{k_d}{\alpha_{H_2A}}$$

$$\sigma = \frac{k_d \alpha_M}{k_r [H_2A] \alpha_{MH_2A}} \qquad \text{and } [H_2A] = \frac{[A_T]}{\alpha_{H_2A}}$$

while upon substitution into equation 56 yields;

$$\frac{i_k}{i_d - i_k} = 0.886 \frac{k_d \alpha_M}{k_r [H_2A] \alpha_{MH_2A}} \sqrt{\frac{k_r [H_2A] t}{\alpha_M}} \quad \ldots\ 85$$

rearranging

$$\frac{i_k}{i_d - i_k} = \frac{0.886}{\alpha_{MH_2A}} \sqrt{\frac{k_d^2 \alpha_M \alpha_{H_2A} t}{k_r [A_T]}} \quad \ldots\ldots\ 86$$

but

$$\frac{k_r}{k_d} = K^M_{MH_2A}$$

$$\therefore \frac{i_k}{i_d - i_k} = \frac{0.886}{\alpha_{MH_2A}} \sqrt{\frac{k_d \alpha_M \alpha_{H_2A} t}{K^M_{MH_2A} [A_T]}} \quad \ldots\ldots\ 87$$

Hence when a large excess of ligand is used (1:8, where A_T = constant) a plot of $\log \frac{i_k}{(i_d - i_k)}$ vs. $1/2(\log \alpha_M + \log \alpha_{H_2A}) - \log \alpha_{MH_2A}$ should yield a straight line with a slope = 1.00. For convenience sake, let $1/2(\log \alpha_M + \log \alpha_{H_2A}) - \log \alpha_{MH_2A} = \log \text{"}\alpha\text{"}^{A}_{Pb\text{-}DTPA}$ Figure 30 illustrates a plot of $\log \frac{i_\ell}{(i_d - i_\ell)}$ vs. $\log \text{"}\alpha\text{"}^{A}_{Pb\text{-}DTPA}$ with a slope = 0.90. This was the best fit obtained for any of the mechanisms proposed. Hence it was concluded that the Wave A equilibrium for Pb-DTPA was due mainly to

$$PbH_2A^- \rightleftharpoons Pb^{++} + H_2A \equiv$$

When the ligand concentration is not in large excess, a correction must be applied to equation 87. Koutecky, et. al.[27] have shown that the corrections for the above mechanism are

$$\frac{i_k}{i_d - i_k}\left(1 + \frac{[MA_T]}{[A_T]} \cdot \frac{i_k}{i_d}\right)^{1/2} = \frac{0.886}{\alpha_{MH_2A}} \sqrt{\frac{k_d\, \alpha_M\, \alpha_{H_2A}\, t}{K^M_{MH_2A}\, [A_T]}} \quad \ldots 88$$

where if $A_T \gg MA_T$ equation 88 reduces to equation 87. In this study the 1:8 ratio data are employed using equation 87.

In order to make use of equation 87 for the calculation of k_d, one must evaluate $K^M_{MH_2A}$. This was possible by writing

$$K^M_{MH_2A} = \frac{[MH_2A]}{[M][H_2A]} = \frac{[MH_2A]}{[H^+][MHA]} \cdot \frac{[MHA]}{[M][HA]} \cdot \frac{[H^+][HA]}{[H_2A]}$$

Table 29 $\text{Log}\frac{i_\ell}{(i_d - i_\ell)}$ + Log "α" values for Wave A.

	Cd-DTPA (1:8)		Pb-DTPA (1:8)	
pH	$\log \frac{i_\ell}{i_d - i_\ell}$	$\log \text{"}\alpha\text{"}^{A}_{\text{Cd-DTPA}}$	$\log \frac{i_\ell}{i_d - i_\ell}$	$\log \text{"}\alpha\text{"}^{A}_{\text{Pb-DTPA}}$
2.50	0.72	2.23	0.09	1.28
2.75	0.28	2.60	$\bar{1}$.97	1.08
3.00	$\bar{1}$.82	2.95	$\bar{1}$.87	0.82
3.25	$\bar{1}$.28	3.31	$\bar{1}$.58	0.58
3.50	$\bar{2}$.80	3.75	$\bar{1}$.30	0.30
3.75	$\bar{2}$.30	4.21	$\bar{1}$.05	-0.02
4.00	-	-	$\bar{2}$.74	-0.40
4.25	-	-	$\bar{2}$.36	-0.82
4.50	-	-	$\bar{3}$.97	-1.26

Experimental conditions: h_{Hg} = 60 cm, t = 4.2 sec, i_d = 5.0μA and Gelatin = 0.002%.

Note: $\text{Log "}\alpha\text{"}^{A}_{\text{Cd-DTPA}} = 1/2(\log \alpha_{H_3A} + \log \alpha_M) - \log \alpha_{CdH_2A} - pH$

Experimental conditions: h_{Hg} = 60 cm, t = 4.2 sec, i_d = 5.4μA and TX-100 = 0.001%. Note: $\text{Log "}\alpha\text{"}^{A}_{\text{Pb-DTPA}} = 1/2(\log \alpha_M + \log \alpha_{H_2A}) - \log \alpha_{MH_2A}$

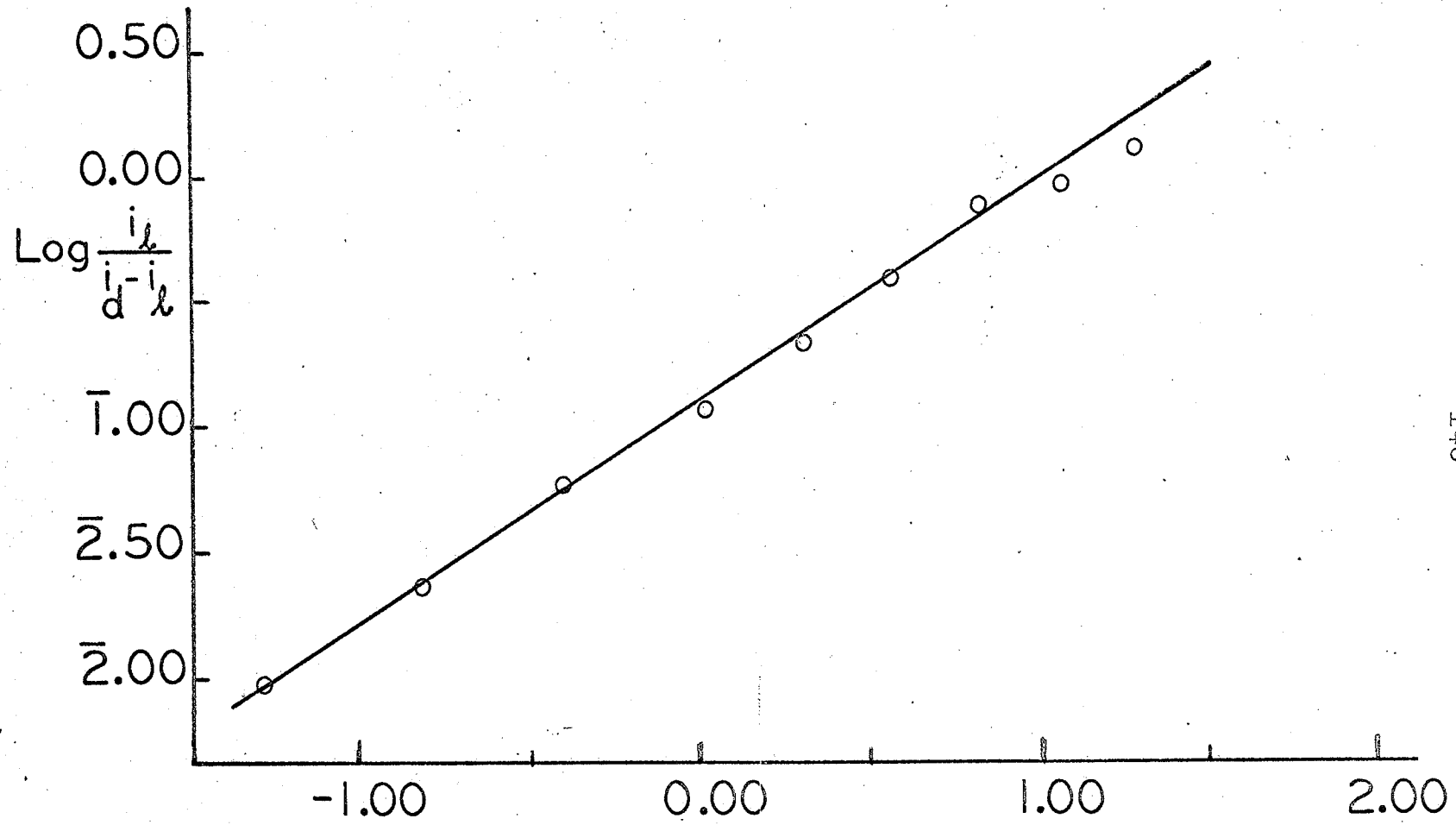

FIG. 30. Log $\frac{i_\ell}{i_d - i_\ell}$ vs. Log "a" $^{A}_{Pb\text{-}DTPA}$ for WAVE A.

applying logs,

$$\log K^{M}_{MH_2A} = \log K^{H}_{MH_2A} + \log K^{M}_{MHA} - pK_4$$

for which the r.h.s. constants are known. Chaberek's values were used except for $\log K^{H}_{PbH_2A}$ where our value of 3.5 was used.

Then $\log K^{Pb}_{PbH_2A} = 3.5 + 12.8 - 8.7 = 7.6$

and $\log K^{Cd}_{CdH_2A} = 3.3 + 12.7 - 8.7 = 7.3$

Writing out equation 87 and applying logs,

$$\log \frac{i_\ell}{(i_d - i_\ell)} = \log 0.886 + 1/2(\log k_d - \log K^{M}_{MH_2A} + \log t - \log A_T)$$
$$+ 1/2(\log \alpha_M + \log \alpha_{M_2A}) - \log \alpha_{MH_2A}$$

For the Pb-DTPA(1:8) data; $t = 4.2$ sec, $A_T = 7 \times 10^{-3}$, pH = 4.00, etc.;

$$-1.36 = -0.05 + 1/2(\log k_d - 7.6 + 0.62 + 2.15) - 0.40$$

then $\log k_d = 2.13$

$$\therefore \quad k_d = 1.14 \times 10^2 = 114 \text{ sec}^{-1}$$

since $$\frac{k_r}{k_d} = K^{M}_{MH_2A} = 4 \times 10^7$$

then $k_r \simeq 5 \times 10^9$ mole liter^{-1} sec^{-1} which is of a reasonable magnitude for an acid recombination process. The value of k_r furnishes further validity to the mechanism proposed above.

For Cd-DTPA the following mechanism gave the best fit;

$$CdH_2A^- + H^+ \underset{k_f}{\overset{k_r}{\rightleftharpoons}} Cd^{++} + H_3A^= \qquad \text{(slow)}$$

$$Cd^{++} + Hg^o + 2e^- \rightleftharpoons Cd(Hg) \qquad \text{(fast)}$$

for which;

$$\text{rate} \longrightarrow = k_r\,[CdH_2A][H^+] = \rho\sigma[CdH_2A], \quad \therefore \rho\sigma = k_r[H^+]$$

$$\text{rate} \longleftarrow = k_f\,[Cd^{++}][H_3A] = \rho[Cd^{++}], \quad \therefore \rho = k_f[H_3A]$$

$$\text{and } \sigma = \frac{k_r\,[H^+]}{k_f\,[H_3A]}$$

Upon substitution into equation 56;

$$\frac{i_\ell}{i_d - i_\ell} = 0.886\,\frac{k_r\,[H^+]}{k_f\,[H_3A]}\sqrt{k_f\,[H_3A]\,t} \qquad \ldots\ldots\ 89$$

and upon rearranging

$$\frac{i_\ell}{i_d - i_\ell} = 0.886\,k_r\,[H^+]\sqrt{\frac{t}{k_f\,[H_3A]}} \qquad \ldots\ldots\ 90$$

Rewriting the rate constants with the corrections for buffer complexes, ligand and metal-DTPA protonated complexes one obtains:

$$\rho = k_f\,\frac{[H_3A]}{\alpha_M}\,, \quad \rho\sigma = \frac{k_r\,[H^+]}{\alpha_{MH_2A}}$$

$$\sigma = \frac{k_r\,[H^+]\alpha_M}{k_d\,[H_3A]\,\alpha_{MH_3A}} \quad \text{and "K"} = \frac{k_r}{k_f}$$

where k_f is used instead of k_d because the reverse reaction is not a true dissociation reaction. When the above corrected constants are transposed into equation 56;

$$\frac{i_\ell}{i_d - i_\ell} = 0.886 \frac{k_r [H^+] \alpha_{Cd}}{k_f [H_3A] \alpha_{CdH_2A}} \sqrt{\frac{k_f [H_3A]\, t}{\alpha_M}} \quad \ldots\ldots 91$$

and rearranging $\left(H_3A = \frac{A_T}{\alpha_{H_3A}}\right)$

$$\frac{i_\ell}{i_d - i_\ell} = \frac{0.886 [H^+]}{\alpha_{CdH_2A}} \sqrt{\frac{k_r \alpha_{H_3A} \alpha_M\, t}{"K" [A_T]}} \quad \ldots\ldots\ldots 92$$

It is evident from equation 92 that a plot of $\log\left(\frac{i_\ell}{i_d - i_\ell}\right)$ vs. $1/2 (\log \alpha_{H_3A} + \log \alpha_M) - pH - \log \alpha_{CdH_2A}$ should have a slope of - 1.00. Figure 31 shows such a plot for Cd-DTPA exhibiting a slope of -1.25. A perfect mathematical fit was obtained (i.e. slope = -1.00) when $[H^+]^{3/2}$ was inserted into equation 92. This indicated that the overall equilibrium for Wave A was probably a mixture of two competing reactions. Hence it was concluded that the main mechanism responsible for Wave A was

$$CdH_2A^- + H^+ \rightleftharpoons Cd^{++} + H_3A =$$

with some contribution from

$$CdH_2A^- + 2H^+ \rightleftharpoons Cd^{++} + H_4A^-$$

which would have $[H^+]^2$ in the kinetic equation thereby giving an average $[H^+]^{3/2}$ dependence in equation 92 . Under these circumstances no attempt was made to calculate k_r.

It was evident from the experimental results and theoretical

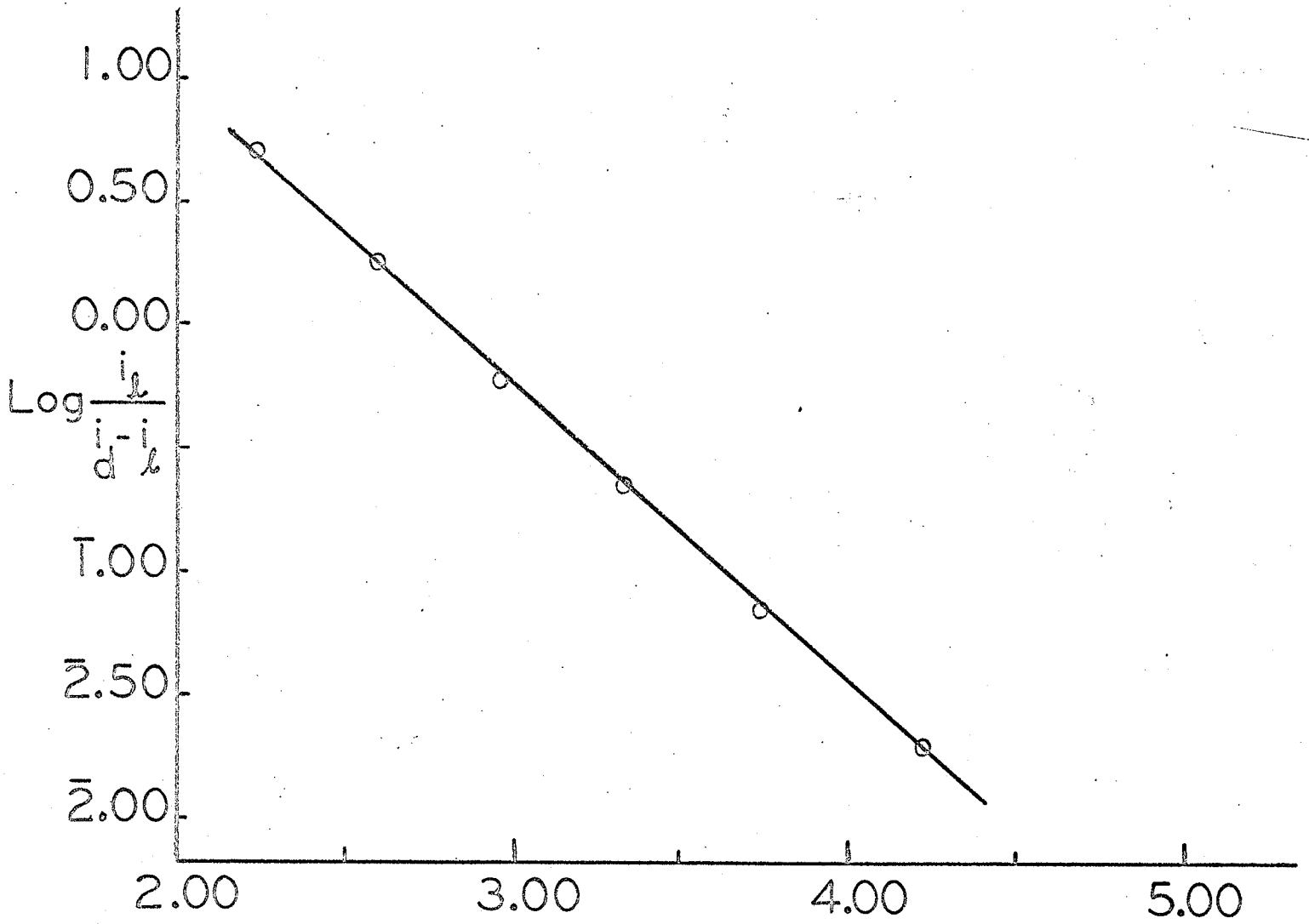

FIG. 31. Log $\frac{i_\ell}{i_d - i_\ell}$ vs. Log "a" $^{A}_{Cd\text{-}DTPA}$ for WAVE A.

considerations outlined in this chapter that the protonated complexes (CdH_xA and PbH_xA) of both metals played an important role in the polarographic investigation. Thus a supplementary study was undertaken to obtain additional information about the chemical properties and behavior of these protonated complexes, i.e. an N.M.R. study of Cd-DTPA and Pb-DTPA.

CHAPTER 7

NUCLEAR MAGNETIC RESONANCE STUDIES

A. Introduction

Early in 1946 Edward Purcell at Harvard University and Felix Bloch at Stanford University announced, almost simultaneously, that they had observed the first nuclear magnetic resonance (N.M.R.) signals of hydrogen. Purcell detected the hydrogen nuclear resonance absorption in paraffin wax, and Block observed the hydrogen signal in water. For this important discovery they received jointly the 1952 Nobel Prize in Physics.

The technique of applying nuclear magnetic resonance to inorganic complex ion studies was only begun in the 60's, although the organic chemists had employed this approach since the early 1950's. Thus the application of N.M.R. to elucidate the structure, kinetics, exchange reactions and instability constants of metal-aminopolycarboxylic acid complexes is a relatively new field of endeavor. Some of the prominent workers in this area are Reilley and Sawyer in the U.S.A., Sargeson in Australia and Shaw in England.

A nucleus with a magnetic moment can be treated as though it were a bar magnet spinning on its axis. When placed in an external field, the interaction of the magnetic moment with the external magnetic field produces a torque. This torque interacts with the angular momentum and causes the magnetic moment to precess about a fixed applied field vector. The angular frequency of the precession is referred to as the Larmor frequency, dependent on the applied field, magnetic moment and spin angular momentum of the nucleus. In an N.M.R. experiment one applies a strong

homogenous magnetic field to the sample causing the nuclei to precess. N.M.R. spectroscopy is most often concerned with nuclei having a nuclear spin quantum number of $\frac{1}{2}$, i.e. H^1, F^{19} and P^{31}. Radiation of energy comparable to the precessing frequency is then imposed with a radio frequency transmitter. When the applied frequency from the transmitter is equal to the Larmor frequency, the two are said to be in resonance, and energy can be transferred to and from the source (i.e. the transmitter) and the sample. The net result of this resonance is that some nuclei are excited from a lower energy state to a higher energy state by absorption of energy from the source at a frequency equal to the Larmor frequency. Energy will be extracted from the rf source only when this resonance condition is fulfilled. A third electronic component, namely a detector is used to observe the frequency at which the loss in energy from the transmitter occurs allowing the resonance frequency to be measured. The Larmor frequency is matched to the applied radio frequency by varying the field strength, i.e. fixed frequency probes (source and detector) are employed.

The N.M.R. phenomenon has significance to the chemist because, the energy of the resonance is dependent upon the electronic environment about the nucleus. The electrons shield the nucleus, so that the magnitude of the field seen at the nucleus, H_N, is different from the applied field, H_0:

$$H_N = H_0 (1 - \sigma) \qquad \text{..... 93}$$

where σ, the shielding constant, is a dimensionless quantity which represents the shielding of the nucleus by the electrons. The value of

the shielding constant depends on several factors, among which are the hybridization and electronegativity of the groups attached to the atom containing the nucleus being studied. Hence identical nuclei in different chemical environments absorb energy at different radiofrequencies (for a given applied field) and give different resonance signals. The separation between the various resonance frequencies is called the chemical shift. The position of the peak is a characteristic of the molecule. Since chemical shifts cannot be measured absolutely, that is, from a nucleus stripped of its electrons, the signal from a reference compound is used as an arbitrary zero. A suitable compound for H^1 resonance is tetramethylsilane (T.M.S.) for organic solvents and sodium 3-(trimethylsilyl)-1-propane sulfonate (T.M.S.*) for aqueous solutions. It is customary to quote chemical shifts in the dimensionless parameter δ (in units of parts per million p.p.m.) defined by

$$\delta = \sigma_S - \sigma_R = \left(\frac{H_S - H_R}{H_R}\right) 10^6 \qquad \text{..... 94}$$

where $\sigma_S - \sigma_R$ is the difference in shielding constants between sample and reference, being equal to $H_S - H_R$. These field measurements cannot be made with certainty hence it is more convenient to calculate δ from the expression

$$\delta = \left(\frac{\nu_s - \nu_r}{\nu_o}\right) 10^6 \qquad \text{..... 95}$$

where $\nu_s - \nu_r$ is the chemical shift difference between sample and reference in cycles sec^{-1}. Since different N.M.R. spectrometers are operated at a variety of frequencies ν_o, equation 95 gives a method of reporting δ in a consistent fashion.

Compounds having magnetic nuclei in more than one chemical environment can have absorption bands showing fine structure. This structure, known as multiplet splitting, has its origin in the coupling between magnetic nuclei taking place via bonding electrons. The magnitude of the coupling, the coupling constant J, can be determined by measuring the separation of the multiplet components providing that the chemical shift difference of the coupled nuclei is much greater than the magnitude of the multiplet splittings.

This band separation is independent of the field strength, hence J is reported in cycles sec^{-1} and not in p.p.m. The magnitudes and types of band splittings can be used to determine the relative positions of functional groups in a molecule. In the present study, N.M.R. spectra were obtained to examine the following; protonation sites of DTPA with a variation in pH, metal-ligand bond life-times, temperature and concentration effects on the complexes of DTPA and to elucidate the stereochemistry of these metal complexes. A thorough treatment of N.M.R. theory is readily available from a number of text-books.[51-55]

B. Experimental

The proton nuclear magnetic resonance (P.M.R.) spectra were recorded with a Varian A 56/60A spectrometer. Most of the spectra were recorded at 0°C, 38°C and 70°C with an accuracy of ± 1°C. The spectra were obtained first with a 500 c.p.s. span and then enlarged on a 100 c.p.s. span. The spectral data reported are average readings of several recordings with an accuracy of ± 0.4 c.p.s.

394.4 gms. of DTPA were weighed out into approximately 800 ml. of distilled water. This solution was stirred with the slow addition of potassium hydroxide pellets until the acid had completely dissolved. It required three moles of base to every mole of acid to convert the acid to a soluble potassium salt. By the addition of distilled water the solution was brought to exactly one liter. This 1.00 M stock solution of DTPA was used to prepare the N.M.R. solutions by aliquot. 1.00 M stock solutions of cadmium and lead were prepared from their nitrate salts (Reagent Grade). From these stock solutions various metal-ligand solutions were prepared, ranging in concentration from 0.10M to 0.50M with respect to both metal and ligand. Under these concentrated conditions, which were necessary to obtain a proper N.M.R. signal, no buffer was needed, i.e. DTPA served as its own buffer.

A Radiometer type PH28 pH-meter was used to determine the pH of all the solutions. The pH was adjusted by the addition of potassium hydroxide since the DTPA stock solution was quite acidic to begin with.

Pure (Fisher Scientific Co.) tertiary butyl alcohol (T.B.A.) was added to the test solutions as an internal standard reference for the N.M.R. measurements. 1% by volume of T.B.A. was sufficient to yield a good reference signal at 1.233 p.p.m. downfield from sodium trimethylsilyl-propane sulphonate (T.M.S.*). The advantage of using T.B.A. is that it is readily available and it has a single peak close to the area under investigation. The T.B.A. signal is also independent of ionic strength and pH.[61]

C. Results

(a) Free DTPA Studies

The structural formula of the DTPA pentaanion is given below. There are eight basic sites in the molecule; five carboxyl groups and three nitrogen atoms.

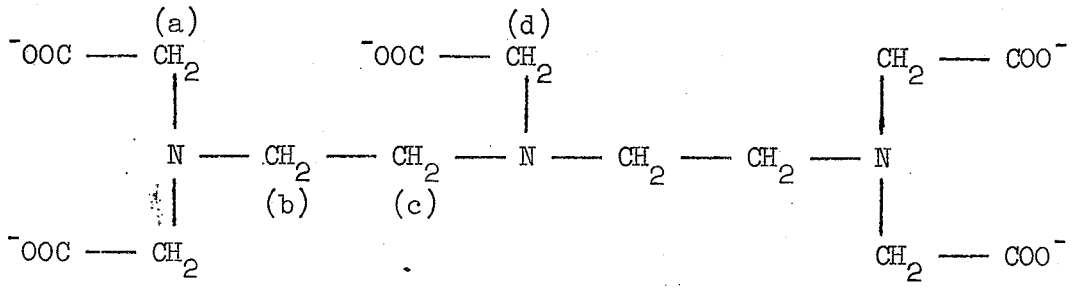

Secondly, there are four types (a, b, c, and d) of non-labile protons in DTPA. Eight acetate protons are labeled (a) and two acetate protons are labeled (d). Since neither a or d protons are appreciably spincoupled to any other nucleus, two sharp singlets containing relative areas of 4 : 1 would be expected. The two types of ethylenic protons (b) and (c) are strongly spin-coupled and should give rise to an A_2B_2 pattern when their chemical shift difference ($\Delta\delta_{bc}$) is sufficiently large.

When all sites are protonated in an acidic solution (pH = 2.0), δ_a and δ_b are nearly equal, giving rise to adjacent singlets as shown in fig. 32. δ_b and δ_c are sufficiently different to produce four distinct peaks (A_2B_2) as indicated in table30 and fig. 32. According to Anderson[56] such an A_2B_2 pattern can be realized when the ratio of coupling constant to chemical shift is approximately

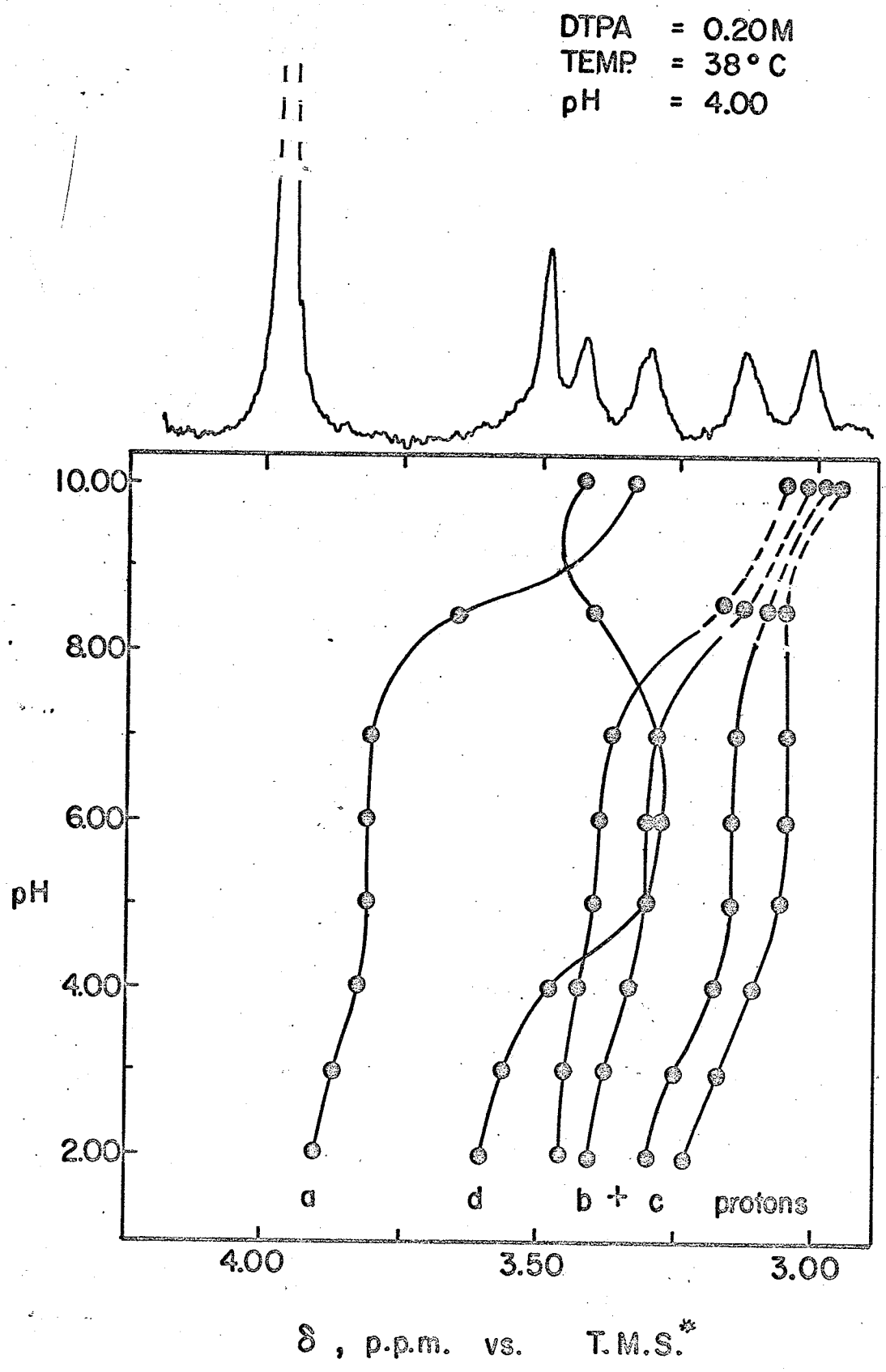

FIG. 32. CHEMICAL SHIFT OF DTPA VS. pH.

Table 30 PROTON POSITIONS OF FREE DPTA vs. T.M.S.*

pH	Temp °C	a	d		b + c		protons	
	0	237.0	217.6	-	-		-	-
2.00	38	233.5	216.5	207.5	202.5		197.0	192.0
	70	232.5	217.5	207.0	202.0		197.0	192.5
	0	233.3	215.7	208.2	203.8		195.2	190.8
3.00	38	231.3	214.1	206.8	202.8		194.6	189.6
	70	230.8	215.0	206.6	200.5		195.5	190.5
	0	232.2	211.2	207.2	203.2		189.2	180.0
4.00	38	229.5	208.5	205.7	200.5		191.5	187.1
	70	229.0	208.0	205.3	200.3		192.3	187.0
	0	231.4	207.6	207.6	200.6		192.4	179.0
4.50	38	229.3	205.8	205.0	200.0		191.3	186.2
	70	228.3	205.0	205.0	200.0		191.7	186.4
	0	230.7	199.6	204.5	199.6		183.7	179.7
5.00	38	228.8	196.4	203.3	197.8		188.5	183.2
	70	228.0	198.1	203.6	198.1		189.5	184.3
	0	230.3	197.0	203.7	198.0		182.0	179.0
6.00	38	228.8	196.4	203.3	197.8		188.5	183.2
	70	227.7	195.7	203.2	197.8		189.0	183.3
	0	230.2	197.7	203.7	197.7		188.2	179.2
7.00	38	227.7	196.7	202.0	196.7		187.7	182.5
	70	226.9	195.8	202.5	197.5		189.0	183.5
	0	214.2	209.7	-	-	189.2$^{\gamma}$	-	-
8.5	38	213.0	206.0	-	-	188.0$^{\gamma}$	-	-
	70	212.5	203.6	-	-	187.4$^{\gamma}$	-	-
	0	199.7	212.4	-	-	180.9$^{\gamma}$	-	-
10.0	38	199.0	207.3	-	-	179.3$^{\gamma}$	-	-
	70	199.0	204.0	-	-	178.5$^{\gamma}$	-	-

The proton positions are given in c.p.s. recorded at 60 MHz. The concentration of DTPA is 0.20 M.

γ The center of a broad A_2B_2 peak.

one-half. As one increases the pH, the question arises which will be the less favored protonation sites. Reilley[57] has reasoned that due to electrostatic repulsion the central nitrogen and carboxyl positions would lose their protons quite readily. For this to be the case one would expect the d protons to show a significant change in chemical shift and this is confirmed by experimental evidence. As the pH changes from 2.0 to 5.0 the d protons move upfield and remain steady until a pH of 7.0 is attained. Then the trend is reversed and at pH = 9.0 the d peak has moved downfield to almost its original acidic position. This must mean that at pH = 9.0 the central nitrogen is protonated a larger percentage of the time than the end nitrogens. Reilley[57] has computed, from NMR data, that after the addition of a single equivalent of proton to a basic solution of DTPA, the terminal acetate groups are not protonated to any detectable extent, the terminal nitrogen groups are protonated 26% of the time each, the central nitrogen is protonated 41% of the time, and the central acetate group is protonated 7% of the time. When a second equivalent of protons is added the d resonance undergoes a negative protonation shift and crosses over the a resonance position as shown in figure 32. This indicates that the two protons are spending most of their time on the terminal nitrogens leaving the central nitrogen position empty.

Simultaneously, a, b and c resonances undergo large protonation shifts as the pH changes from 2.0 to 10.0. This would indicate that

the five carboxyl groups experience similar protonation time with the pH change. In this study the A_2B_2 pattern of the ethylenic protons separated into four distinct peaks whereas Sudmeier and Reilley[58] found a broad doublet. There was perfect agreement at high pH values (8.0 - 10.0) where the A_2B_2 pattern becomes one broad peak.

Spectra of free DTPA were recorded at 0, 38 and 70° C. An increase in temperature sharpened up the peaks considerably as indicated in figure 33. There are three contributions to line width, i.e. natural line width ($1/\pi\ T_2$ dependent on temperature, viscosity), instrumental broadening ($1/\pi\ T_2'$ dependent on instrument tuning) and lifetime broadening ($1/\pi\tau$ dependent on chemical kinetics in the slow exchange limit)[54]. Sudmeier and Reilley[59] have examined the above contributions in detail for Cd-EDTA and attribute the sharpening of spectral lines to a decrease in viscosity caused by an increase in temperature. This explanation was accepted as a correct one and will be referred to later.

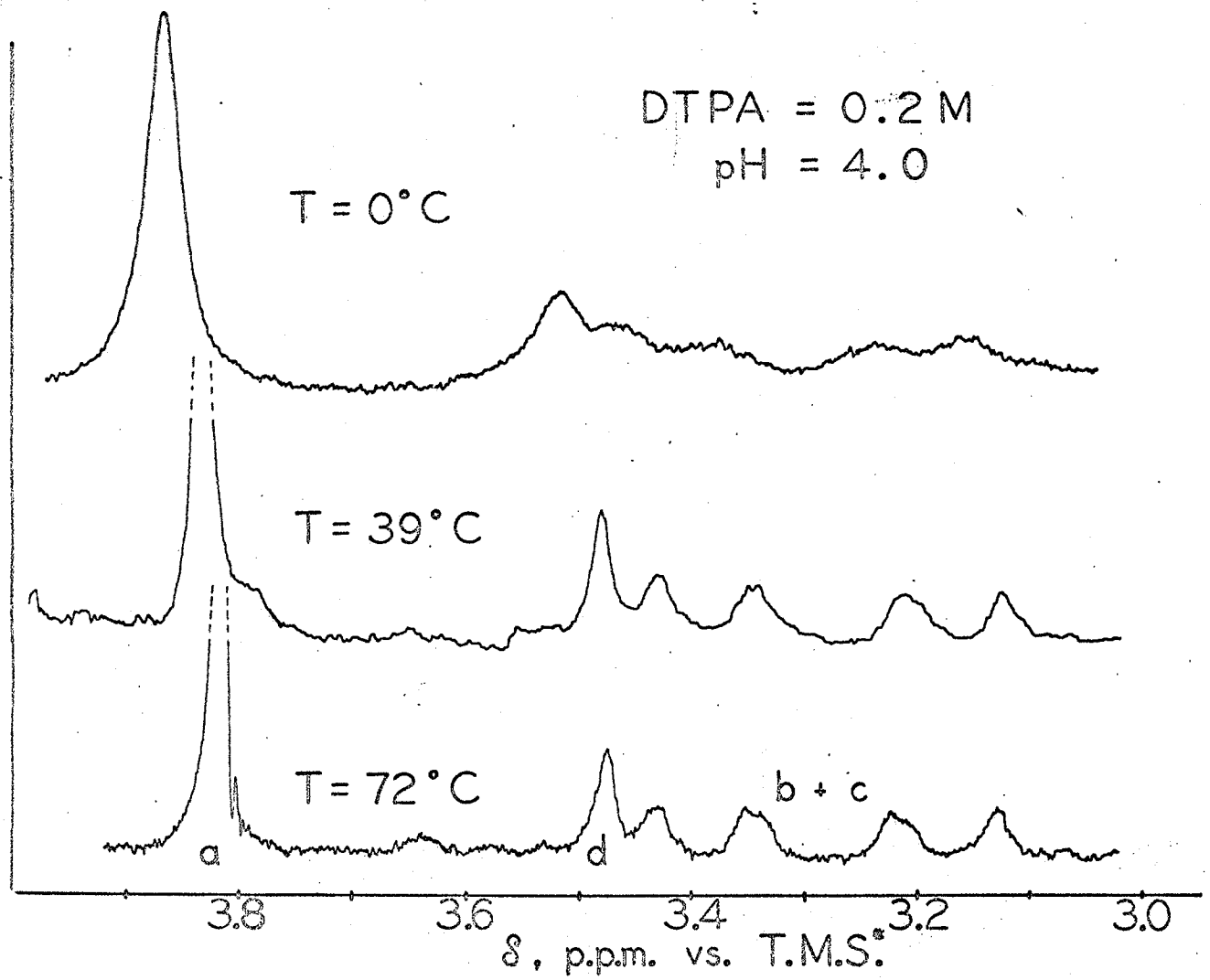

FIG.33. CHEMICAL SHIFT OF DTPA vs. TEMP.

(b) Cd-DTPA Studies

The Cd-DTPA spectra were recorded at 0, 39 and 70°C with the proton positions given in table 31. An increase in temperature again helped to sharpen up the peaks. The Cd-DTPA spectra were not as sharp as the ones for DTPA. The b and c protons yielded a broad unsymmetrical A_2B_2 pattern as shown in fig. 34. In this broadened area only a few individual quartet peaks could be measured and so the centers of the A_2B_2 peaks are given in table 31.

Spectra were obtained for Cd-DTPA solutions ranging from pH = 2.0 to pH = 10.0 and the chemical shifts plotted in figure 35. Fig. 35 shows that the a, d, b and c protons all experience a similar change in chemical shifts as the pH changes from 2.0 to 10.0. Table 31 indicates that the a proton peak breaks up into an AB spectrum after pH = 6.0 and becomes quite distinct at pH = 10.0 (Fig. 36). Actually only a doublet is seen for the AB pattern where the side peaks are lost in the noise level. Day[60] studied Cd-EDTA and found a similar spectrum for the acetate protons. He pointed out that this effect was caused by cadmium isotopes with spin zero being bound to nitrogen in the complex with a relatively long life-time when compared to the N.M.R. time scale. Cadmium isotopes (111 and 113) with spin one-half have a natural abundance of 25%, and theoretically should cause an ABX spectrum as well. This was not observed for the cadmium complexes, probably

Table 31 PROTON POSITIONS OF Cd(DTPA) vs. T.M.S.*

pH	Temp. °C	a		d			b + c	protons	
	0		221.0	211.0	-	-	186.0$^{\gamma}$	-	-
2.0	39		217.4	207.0	-	-	183.0$^{\gamma}$	-	-
	70		215.8	206.0	186.2	183.6	181.5$^{\gamma}$	180.8	178.3
	0		205.0	198.0	-	-	174.0$^{\gamma}$	-	-
3.0	39		204.0	196.0	-	-	174.0$^{\gamma}$	-	-
	70		202.1	194.0	177.3	175.2	173.5$^{\gamma}$	172.0	169.8
	0		201.0	195.5	-	-	172.0$^{\gamma}$	-	-
4.0	39		199.5	193.2	-	-	171.5$^{\gamma}$	-	-
	70		198.5	192.0	-	173.5	172.0$^{\gamma}$	-	170.5
	0		199.4	194.8	-	-	171.0$^{\gamma}$	-	167.5
5.0	39		197.5	192.5	-	-	170.0$^{\gamma}$	-	-
	70		196.6	191.0	-	-	169.4$^{\gamma}$	-	-
	0		197.8	194.0	180.5	-	171.0$^{\gamma}$	-	167.0
6.0	39	197.6		196.0 192.7	-	-	169.5$^{\gamma}$	-	-
	70		196.1	190.7	-	-	168.6$^{\gamma}$	-	-
	0		197.6	193.7	180.0	174.0	170.5$^{\gamma}$	-	167.0
7.0	39	197.6		196.0 192.5	180.2	172.5	169.0$^{\gamma}$	-	166.0
	70		195.8	190.8	-	169.0	168.0$^{\gamma}$	-	166.1
	0	200.0		197.0 193.5	180.5	174.6	170.0$^{\gamma}$	-	166.7
10.0	39	198.5		195.5 191.5	-	172.5	169.0$^{\gamma}$	-	165.2
	70	197.7		195.0 190.5	180.1	171.5	168.0$^{\gamma}$	-	164.7

The proton positions are given in c.p.s. recorded at 60 MHz. The ratio of Cd: DTPA is equimolar (1:1) at a concentration of 0.50 M.

γ The center of a broad A_2B_2 peak.

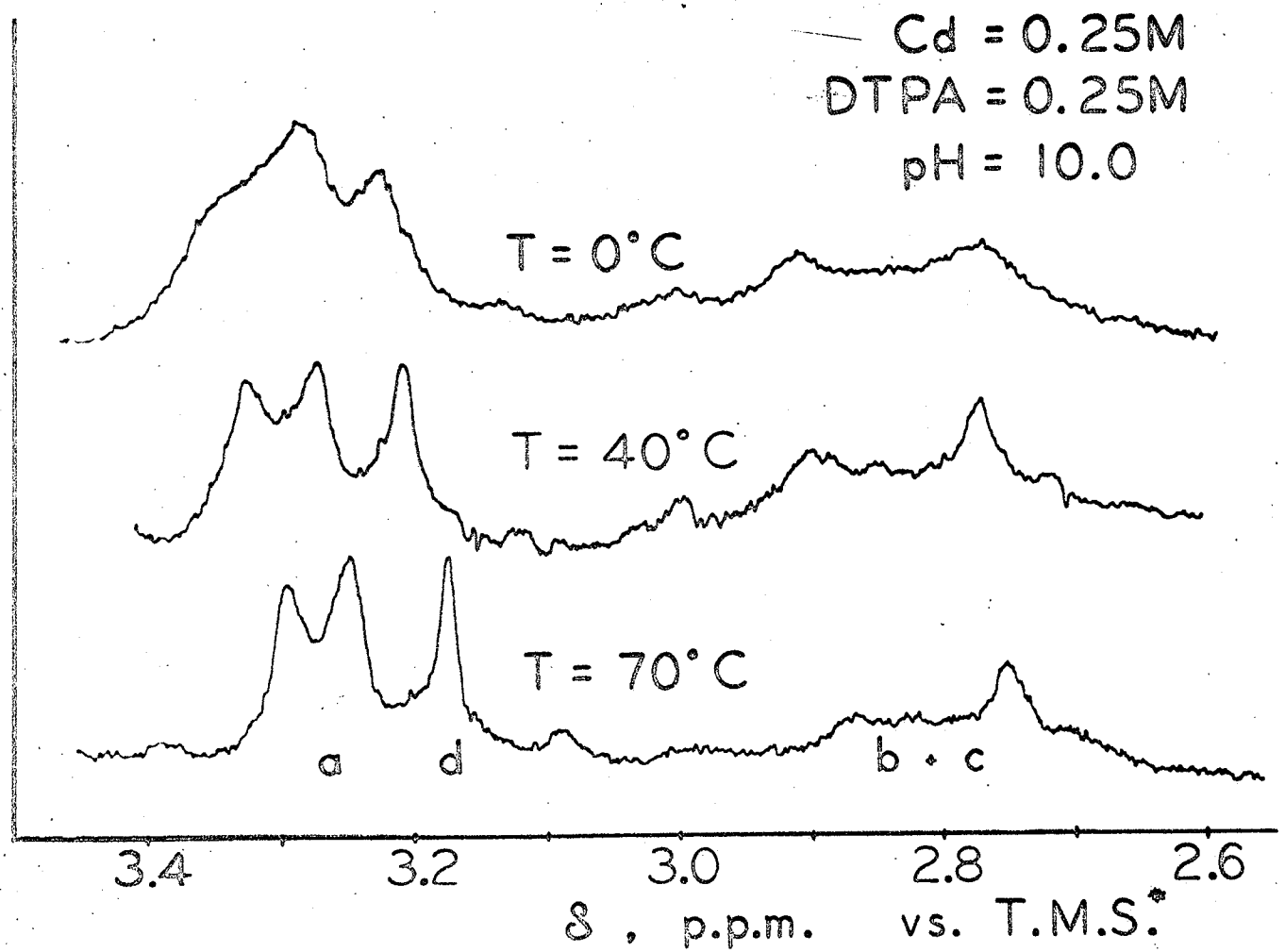

FIG. 34. CHEMICAL SHIFT OF Cd-DTPA vs. TEMP.

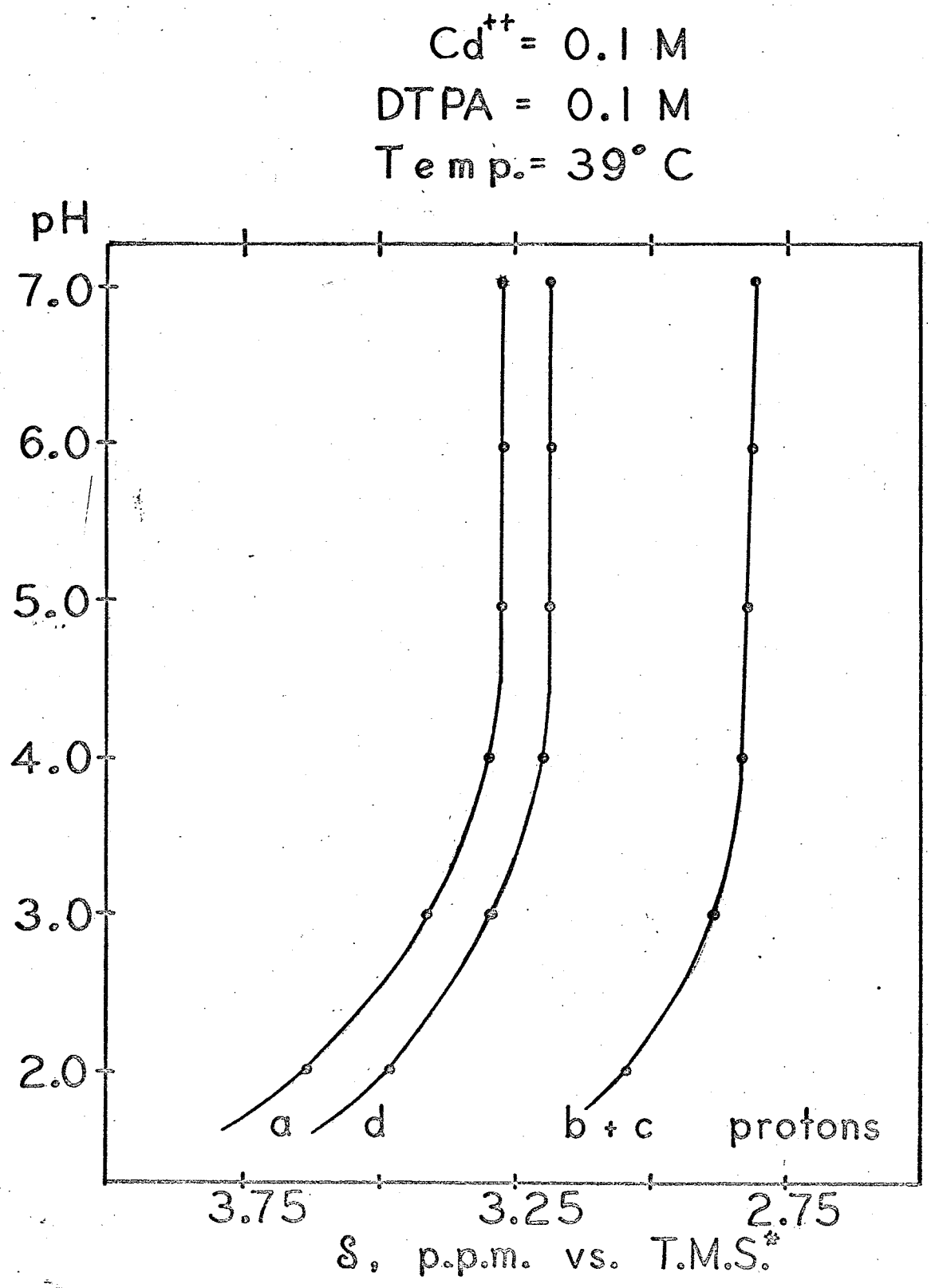

FIG. 35. CHEMICAL SHIFT OF Cd-DTPA vs. pH.

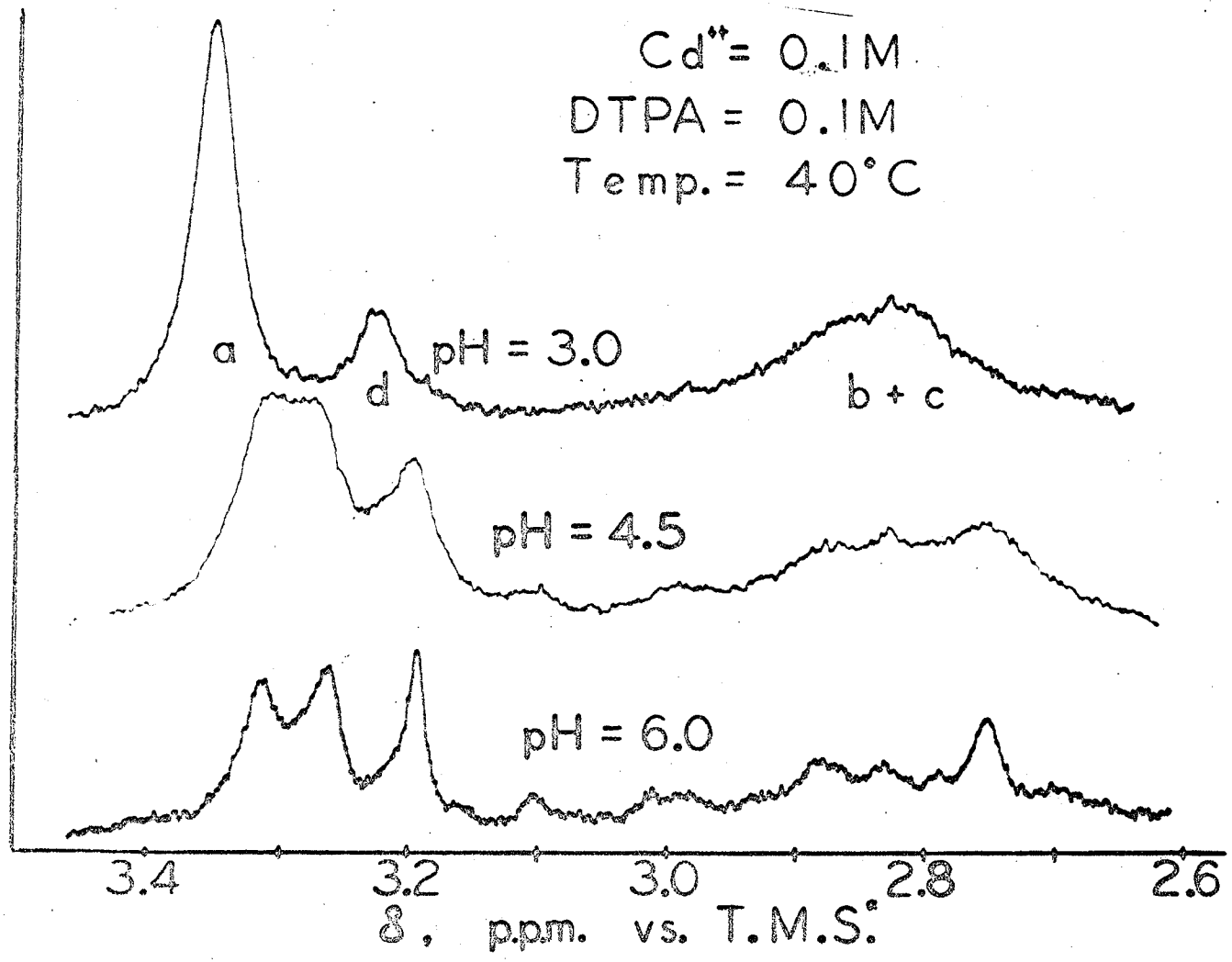

FIG. 36. CHEMICAL SHIFT OF Cd-DTPA vs. pH.

because of the generally broadened spectra obtained.

Cd-DTPA solutions with a metal-ligand ratio of 1 : 2 and 2 : 1 were also examined. In the first case (ratio 1 : 2), with an excess of DTPA, the spectra showed a free DTPA portion superimposed on the complex portion of the spectra. Both portions were generally as sharp as the individual spectra under the same conditions. Hence it was concluded that the exchange of free DTPA to complexed DTPA was minimal.

In the second case (ratio 2 : 1), with an excess of cadmium, the spectra showed a similar pattern to the equimolar Cd-DTPA solutions under the same conditions. In other words, the NMR study failed to differentiate between a 2 : 1 and 1 : 1 metal-ligand mixture.

Lastly a solution was examined containing one part of lead and one part of cadmium to two parts of DTPA at a pH of 8.5. Here one could clearly identify the Pb-DTPA complex portion and the Cd-DTPA complex portion. Both complexes exhibited AB patterns for the a protons, but the ABX part for lead was lost in the noise level of the spectrum.

(c) Pb-DTPA Studies

Pb-DTPA spectra were obtained at 0, 39 and 72°C with the proton positions given in table 32. Generally an increase in temperature sharpened up the peaks. By comparison the Pb-DTPA spectra were much sharper than the Cd-DTPA spectra. The a protons showed a poor AB spectrum at low temperature in acidic solutions and a very well defined AB and ABX pattern in basic solutions especially at high temperature. The d protons remained as a single sharp peak during the entire study. The b and c protons formed a broad peak under acidic conditions and became more clearly defined in basic solutions.

Spectra were obtained for Pb-DTPA solutions ranging from pH = 2.0 to pH = 10.00 and the chemical shifts plotted in figure 37. Figure 37 shows the a, b and c protons to undergo the same change in chemical shift with equal pH changes. However the d protons almost ignore all pH change effects. This must mean that the central acetate protons see a constant electrical environment, irrespective of the protonation taking place in the rest of the complex. As mentioned above, with an increase in pH, the a protons clearly form AB and ABX patterns. Reilley[57] studied Pb-EDTA and found the identical situation there. Lead with spin zero gives the AB spectrum and Pb^{207} (spin = 1/2) produces the ABX pattern. The relative abundance of the two isotopes is 79% and 21% respectively. The area of the two patterns (AB and ABX) is approximately 5 : 1 in good agreements with isotope concentration. The b + c protons

Table 32 PROTON POSITIONS OF Pb(DTPA) vs. T.M.S.*

pH	Temp °C	a			d	b + c			protons
	0	224.8^{p}		220.5^{p}	226.0	-		186.5$^{\gamma}$	-
2.0	39		223.3		224.8			188.8$^{\gamma}$	
	72		222.8		223.0			189.7$^{\gamma}$	
	0	224.0^{p}		219.5^{p}	226.0			186.5$^{\gamma}$	
3.0	39		223.0		225.0			189.0$^{\gamma}$	
	72		222.0		223.0			189.6$^{\gamma}$	
	0	221.4^{p}		216.6^{p}	225.0			184.5$^{\gamma}$	
4.0	39		219.5		224.0			186.5$^{\gamma}$	
	72		219.3		222.5			187.2$^{\gamma}$	
	0	215.7		210.4	224.3	-		-	
5.0	39		212.4		222.7	180.7		177.2$^{\gamma}$	-
	72		211.8		221.4	180.8		178.0$^{\gamma}$	
	0	213.8		208.2	223.8	-	181.5	-	171.0
6.0	39	212.8		208.2	222.7	185.5	181.5	173.5	171.0
	72		210.2		221.5	-	180.2	175.0	171.2
	0	213.2		207.6	223.4	-	181.5	-	170.2
7.0	39	212.1		207.4	222.4	184.4	181.0	174.0	170.0
	72	210.5		207.5	221.0	-	180.0	173.2	170.2
	0	213.8		208.2	223.3	-	181.5	-	170.5
8.0	39	212.0		207.6	222.3	185.0	181.0	174.4	170.0
	72	211.4		207.6	221.6	184.5	181.5	174.1	170.7
	0	213.6		208.1	223.6	-	181.6	-	170.3
9.0	39	212.1		207.5	222.5	185.1	181.0	174.5	170.1
	72	211.0		207.1	221.2	184.2	181.1	174.6	170.4
	0	213.5		208.1	223.6	-	181.4	-	170.1
10.0	39	212.0		207.2	222.2	184.7	181.0	174.0	170.2
	72	211.0		207.0	221.1	184.3	181.0	174.2	170.0

The proton positions are given in c.p.s. recorded at 60 MHz. The ratio of Pb: DTPA is equimolar (1:1) at a concentration of 0.50 M.

γ The center of a broad A_2B_2 peak.

p Approximate positions from a poorly defined AB pattern.

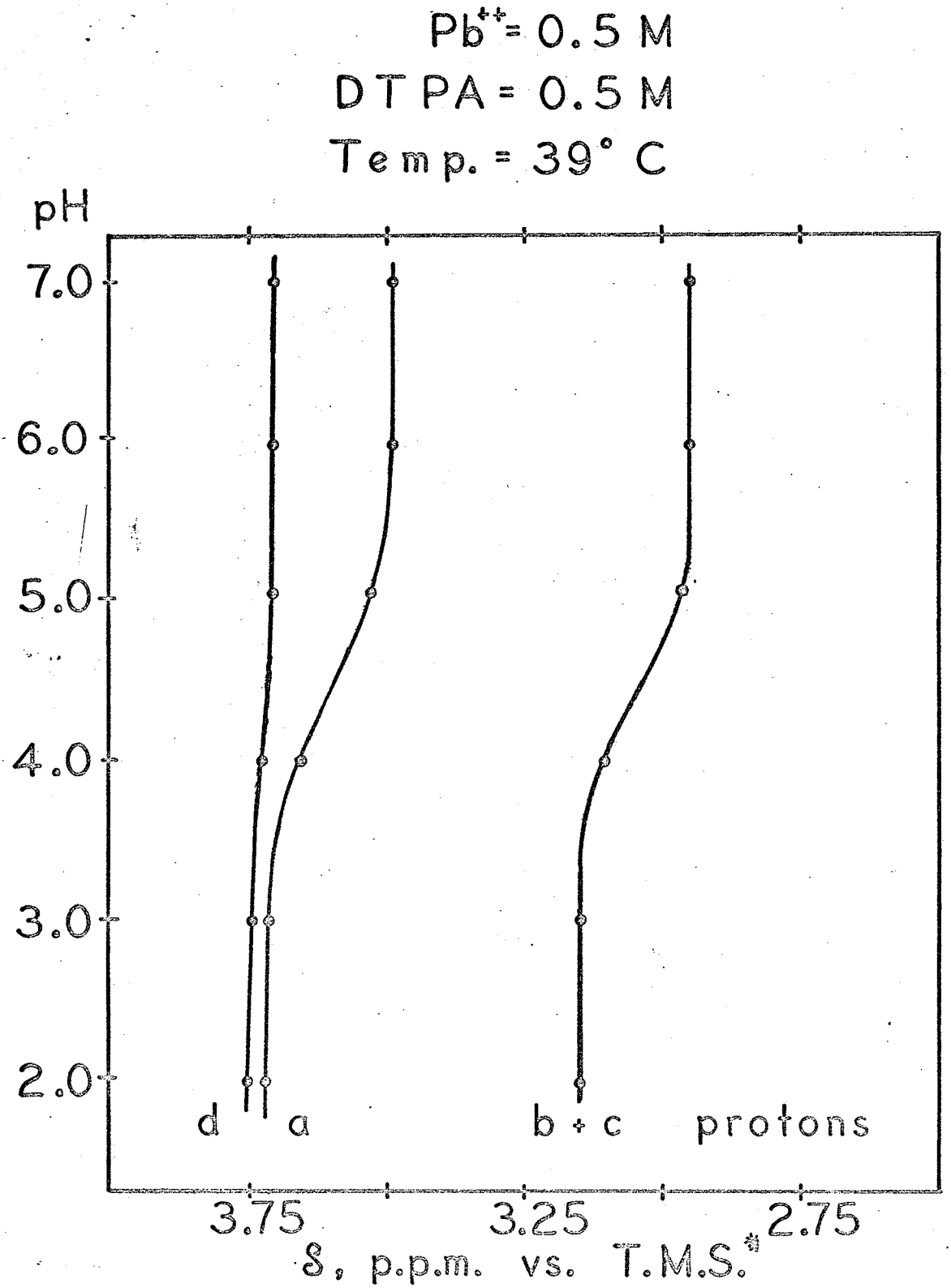

FIG. 37. CHEMICAL SHIFT OF Pb-DTPA vs. pH.

form an A_2B_2 pattern which becomes sharper as the pH increases. At pH = 10 the spectrum is a fairly sharp quartet but unsymmetrical as shown in figure 38.

Pb-DTPA solutions with a metal-ligand ratio of 1 : 2 and 2 : 1 were also examined. With an excess of DTPA (ratio 1 : 2), the free DTPA spectrum was superimposed on the complex (Pb-DTPA) portion. Both NMR portions were as sharp as the individual spectra run under the same conditions. This indicated that the exchange between free DTPA and complexed DTPA was insignificant.

In the second instance (ratio 2 : 1) with an excess of lead, spectra could only be obtained at pH = 1.5. The reason for this was that $Pb(OH)_2$ was insoluble (above pH = 1.5) in the concentrated solutions used. At this low pH free DTPA began precipitating as well. Hence a poor spectrum of free DTPA portion could be detected similar to a free DTPA spectrum taken at pH = 2.0.

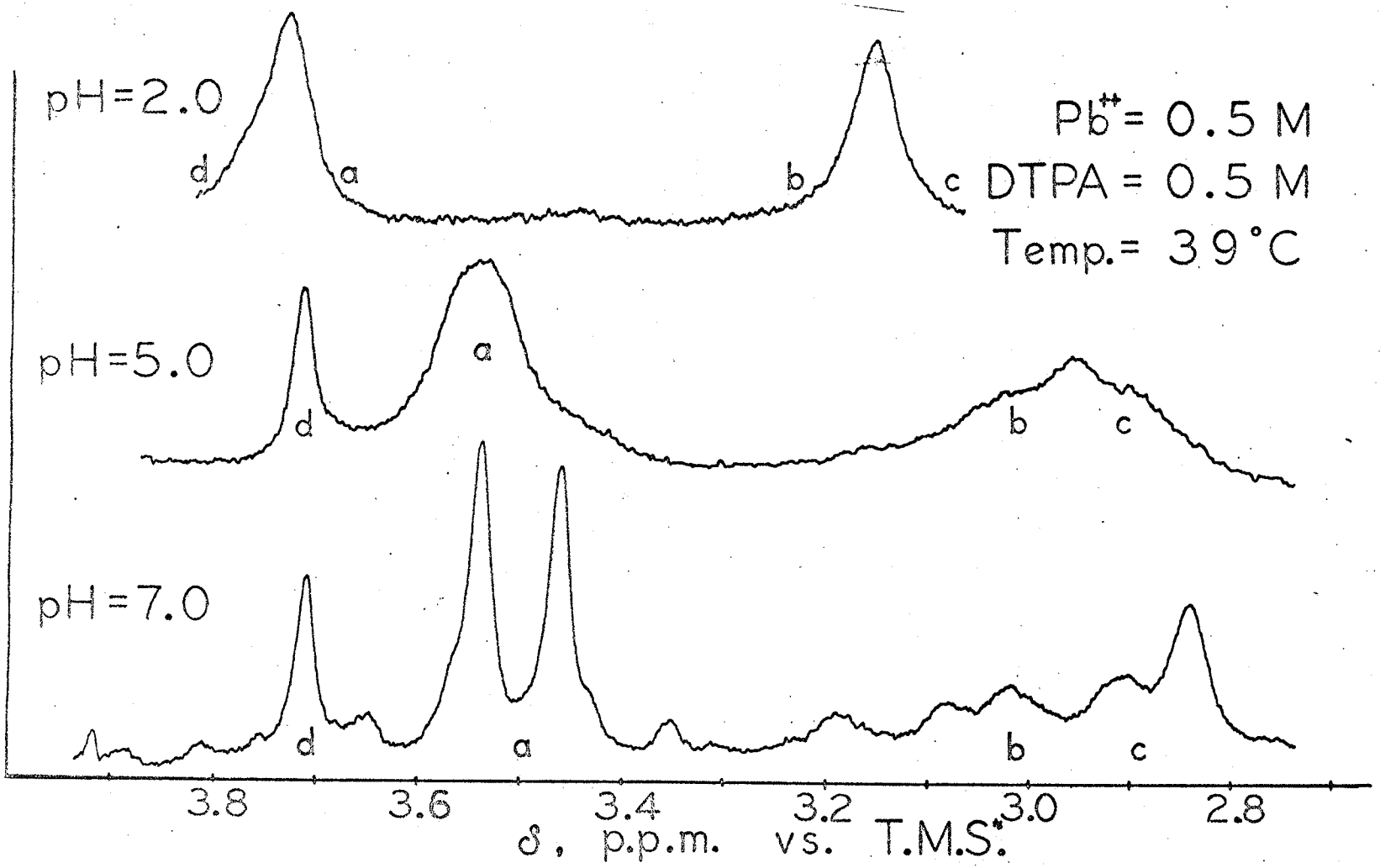

FIG. 38. CHEMICAL SHIFT OF Pb-DTPA vs. pH.

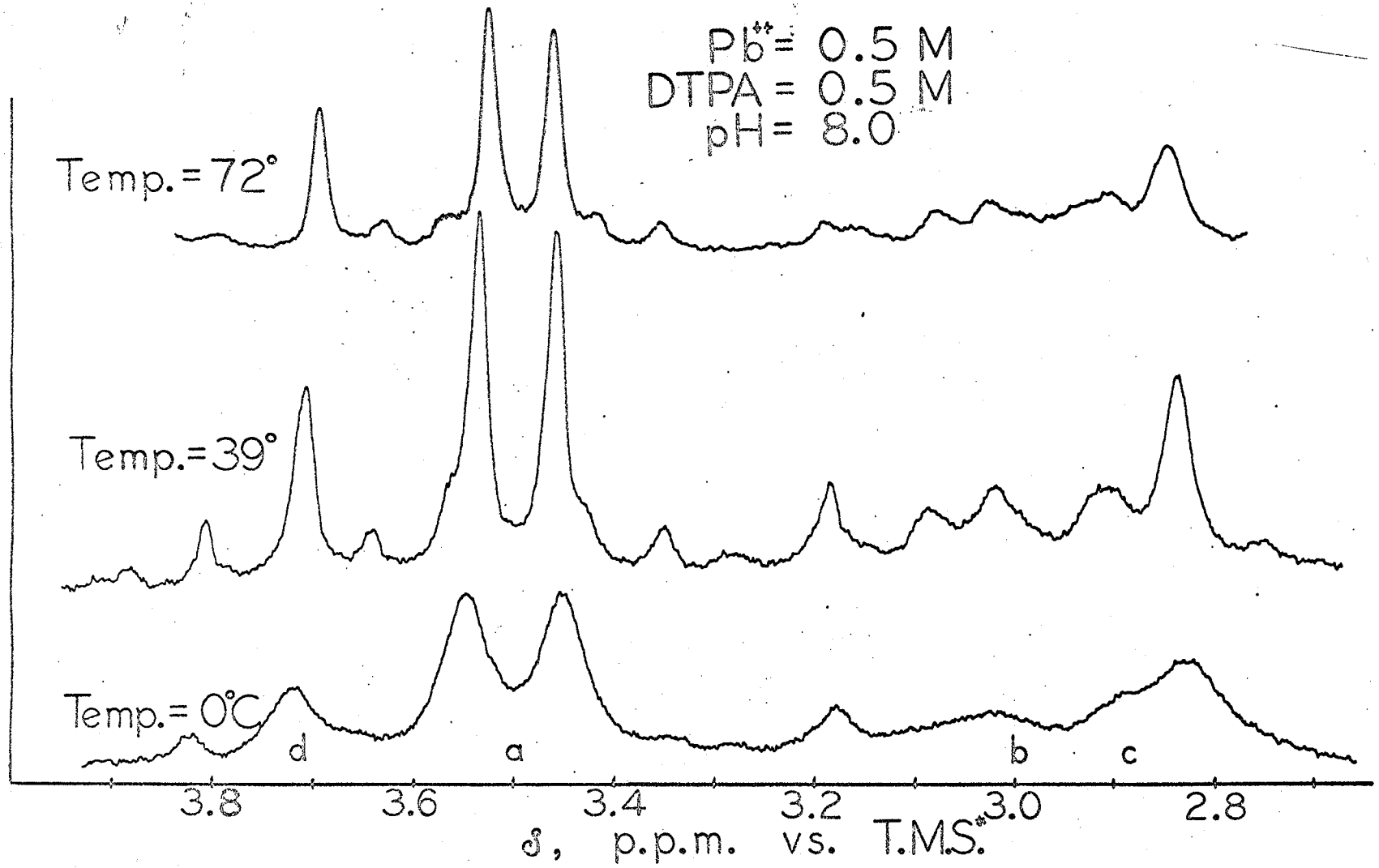

FIG. 39. CHEMICAL SHIFT OF Pb-DTPA vs. TEMPERATURE.

D. Theoretical Discussion

NMR measurements can be very useful in elucidating the lability of the individual bonds of a multidentate complexing agent attached to a metal ion. DTPA contains both oxygen (acetate) and nitrogen donor atoms and depending on the lability of the various metal-ligand bonds, four clearly defined possibilities can arise. The lifetimes of both the metal-oxygen and metal-nitrogen bonds are short or long; and on the other hand, the lifetime of the metal-oxygen bond is long while that of the metal-nitrogen bond is short, or vice versa. All of the above possibilities will be examined with the aid of the following octahedral configurations for both metal-EDTA and metal-DTPA complexes.

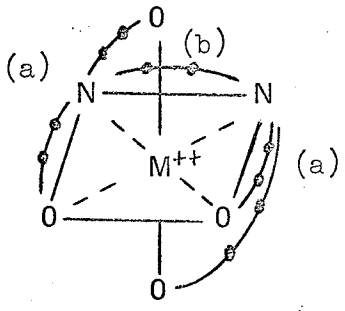

Metal-EDTA complex

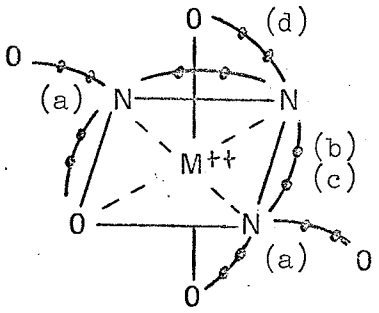

Metal-DTPA complex

Note: The curved lines with large dots represent C - C linkages, where the C - H and C - O bonds are omitted. The protons are labelled as previously outlined on page 161.

First, the lifetime of both metal-oxygen and metal-nitrogen bonds may be short. EDTA complexes of diamagnetic metal ions (and having negligible amounts of isotopes with spin one half) should have simple NMR spectra exhibiting two sharp peaks corresponding to the ethylenic and acetate protons, as has been reported for a number of such chelates[61]. The reason for this is that the complex should exist in various stages of unwrapping of the EDTA molecule, and although the rates of unwrapping and wrapping may be fast, the lifetime of a given EDTA molecule on a given metal ion may be long. Thus the ethylenic or acetate protons are made equivalent by internal exchange caused by rapid umbrella inversion of the nitrogen atoms thereby collapsing any possibly multiplets caused by proton-proton splitting. If the metal ion has appreciable abundance of isotopes with spin one half and a high degree of covalent bonding, metal-proton splitting occurs because the isotopes can couple to the EDTA protons so long as the chelate does not exchange rapidly with free metal ion or free EDTA. This metal-proton splitting persists despite the short lifetime of the metal-nitrogen bonds and rapid inversion of the nitrogen because the nitrogen-metal bond always reforms to the same metal ion; hense all nuclei are still in the same spin states as present prior to the bond rupture and the coupling is not relaxed. An example of this system is Pb-EDTA[60], where each ethylenic and acetate proton peak is split into doublets corresponding in size to the concentration of lead

with spin one half. For a DTPA complex one would expect the identical situation for the acetate protons and a very complex pattern for the ethylenic A_2B_2 portion. In this study the A_2B_2 pattern was a broad quartet for free DTPA and it would have been very difficult to detect a further metal-proton splitting in the complex for isotopes of spin one half.

In the second situation, where both the nitrogen-metal and oxygen-metal bonds have long lifetimes, rather complex spectra would be expected because the acetate groups would not be equivalent and, depending on the stereochemistry of the complex, even the ethylenic protons may be non-equivalent. In the case of an octahedral DTPA complex where all nitrogen atoms are bound and two acetate groups are free, various possibilities can be imagined. If one assumes the case above with a central acetate bound, then in a given optical form (dextro or levo), the free acetate groups would differ from the bound, and the central acetate would be different from either of the terminal acetate groups. The two methylene protons on a given acetate group are in different magnetic environments giving an AB pattern. Therefore the four types of acetate protons may exhibit four different AB patterns. Secondly the rigidity of such a structure may affect the two sets of ethylenic protons so that they no longer would be equivalent A_2B_2 components. The overall spectrum could be a very complex one indeed. An example of a relatively simple case is Co-EDTA[60].

Here the acetates exhibit two different AB patterns, where two acetate groups are in the plane and, two out of the plane with respect to the metal-nitrogen bonding plane. An interesting study of Co(III)-EDTA with one coordinating position taken up by a nitro group was undertaken by Smith[62]. He found three distinctly different acetate protons; one type for the free acetate group and the other two for in plane and out of plane bonding.

In the third case, where the lifetime of the metal-oxygen bond is short and the metal-nitrogen bond is long, the acetate and ethylenic protons exhibit different NMR spectra for EDTA complexes. The ethylenic carbons have two highly probably "gauche" conformations where the CH protons exist as two equivalent axial-equatorial pairs. These two conformations can rapidly interconvert and thus average out any difference of the two protons on a given ethylenic carbon. The symmetry of the chelate makes the two carbons equivalent so that all four ethylenic protons are equivalent even if the metal-nitrogen bond has a long lifetime. Hence only one resonance peak is expected under these conditions. For DTPA an A_2B_2 pattern would be expected for the ethylenic protons because of their unsymmetrical environment. For both EDTA and DTPA complexes the methylene protons on a given terminal acetate are not equivalent. If the acetate group is free to rotate about the acetate-carbon-nitrogen bond, then various rotational staggered configurations are possible. Many of these are non-equivalent just as in the case where the carbon is bound to an asymmetric carbon

atom[51]. Any one acetate group sees an asymmetric quaternary nitrogen atom. Hence the inherent dissymmetry or the different amount of time the proton spends in various rotational conformations leads to an AB splitting pattern for the acetate protons. An example of this type is Cd-EDTA[60]. The ethylenic single peak is split into a doublet by isotopes of spin one half. The acetate protons exhibit an AB pattern which is split into two doublets (ABX) by isotopes of cadmium with spin one half. For a DTPA complex one would theoretically expect the A_2B_2 ethylenic portion to be undisturbed except for isotopes of spin one half, and the acetate protons should each yield their own AB pattern.

The last case where the nitrogen-metal lifetime is short and the metal-oxygen lifetime is long seems highly unlikely. If the structure of a DTPA complex is examined, it is unlikely that the metal-nitrogen bond could be broken without prior rupture of the metal-oxygen bonds on its associated acetate groups. Investigations so far have not provided any evidence of this type of complex bonding[60]. Thus the first three cases are the most probable ones to encounter.

In this investigation, Cd-DTPA spectra gave the following information. At a pH below 4.0 the a and d protons gave singlets and the ethylenic protons (b + c) showed a broad single peak. At a pH of 5.0 the a singlet began to split into a doublet and became an AB pattern at pH = 10.0. Similarly the b and c protons slowly

separated into an A_2B_2 pattern as the solution became more basic. These trends are shown in figure 36, where the A_2B_2 pattern also becomes slightly unsymmetrical with an increase of pH. This would indicate that at low pH (below 4.5) the metal-nitrogen bonds are short-lived, allowing free rotation of the acetate groups whose protons can then average out any non-equivalence and yield singlets. Under basic conditions (pH above 7.0) the metal-nitrogen bond lifetime becomes longer and the acetate protons no longer experience a single average magnetic environment due to an asymmetric quaternary nitrogen atom. Thus the dissymmetry or different amounts of time the proton spends in various rotational conformations leads to an AB pattern for the a protons. The d protons remain as a singlet throughout the entire study. This means that the central acetate group has a symmetrical environment (similar to free DTPA) so that the two d protons are equivalent. From figure 35 it is obvious that all the DTPA protons are affected similarly upon protonation, since they all experience the same chemical shift with a change in pH. The chemical shift moves upfield below pH = 4.0, and remains constant thereafter. Thus various protonated Cd-DTPA complexes exist below pH = 4.0. It seems reasonable to predict protonated species in this pH range, since there is a steady upfield protonation shift from pH = 1.0 to pH = 4.0. The unsymmetrical A_2B_2 portion could be attributed to the time it takes the DTPA molecule to wrap or unwrap itself around the metal

ion, during which time the individual ethylenic protons experience an unsymmetrical magnetic environment.

Thus, the predicted structure for the Cd-DTPA complex is an octahedral one, where under acidic conditions (pH < 4.0) the metal-ligand bonds are relatively short-lived with some of the acetate groups and nitrogen atoms protonated to various degrees. In basic solution the metal-nitrogen bond lifetime is relatively long-lived compared to the metal-oxygen bonds. The five acetate groups are competing for three remaining co-ordinating positions on the octahedral complex, with at least two acetate groups left free at any given instant. The reasons for the choice of an octahedral structure will be outlined later.

The Pb-DTPA spectra were different from those of Cd-DTPA. First the d protons completely ignored all protonation changes as shown in figure 37. An explanation for this would be that the central acetate group was bound to the metal a large percentage of the time, and so could not be protonated. The a, d, b and c protons exhibited broad singlets at low pH similar to the Cd-DTPA complex. Under neutral conditions the a protons showed a poor AB pattern which became very well defined at pH = 9.0 as shown in fig. 40. In fact the ABX pattern from Pb^{207} with spin one half was clearly visible under basic conditions. The ethylenic protons similarily split into an A_2B_2 pattern in basic solutions. Again the A_2B_2 pattern became slightly unsymmetrical at high pH. The a and b + c protons experience similar chemical shifts with

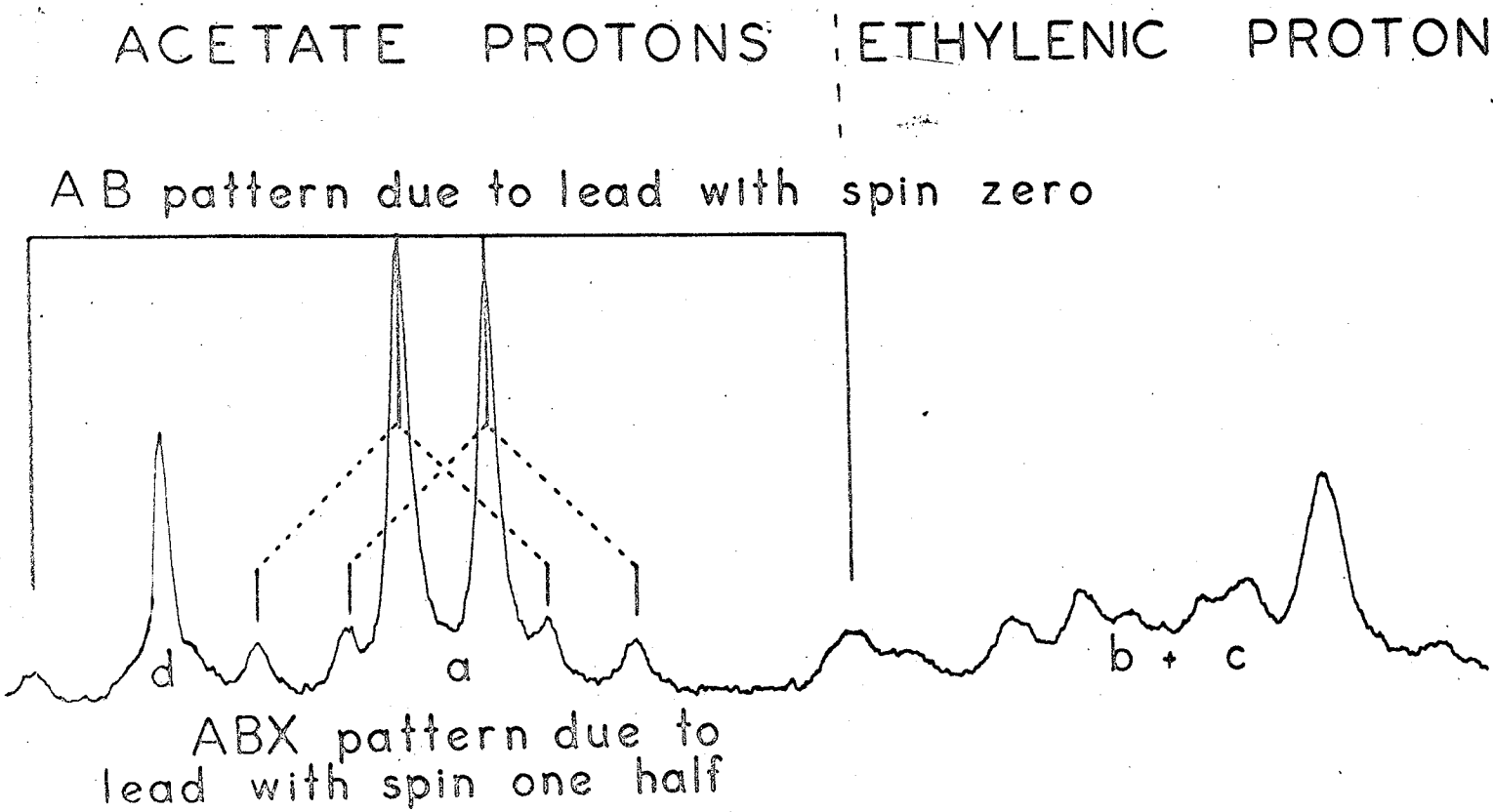

FIG. 40. NMR SPECTRUM OF Pb-DTPA AT pH 9.0.

pH (fig. 37), which move upfield from pH = 3.5 to 6.0. This points to the fact that deprotonation begins at pH = 3.5 and is complete by pH = 6.0. Hence the Pb-DTPA complex below pH = 3.5 is a stable protonated species, then loses the protons between pH 3.5 to 6.0 and finally forms a stable non-protonated species in neutral or basic solution.

A reasonable structure for the Pb-DTPA complex is an octahedral one, where in acidic medium (pH < 6.0) the free acetate groups and the nitrogen atoms are protonated to various degrees depending on the pH, and in basic medium (pH > 6.0) they are not. In basic media the metal-nitrogen bond lifetime is long and the metal-oxygen bond lifetime is short, except for the central acetate group which is bound to the metal ion most of the time.

A survey of the coordination chemistry of divalent metal-aminopolycarboxylate complexes revealed ample evidence for octahedral chelation[63-67], especially for lead and cadmium. However DTPA, being an octadentate ligand, could wrap around a metal ion in many different ways and still exhibit an octahedral configuration. A number of possibilities are shown on the next page. The arguments and experimental evidence used in predicting a particular structure in neutral or basic media for Cd-DTPA and Pb-DTPA follow.

STRUCTURE I

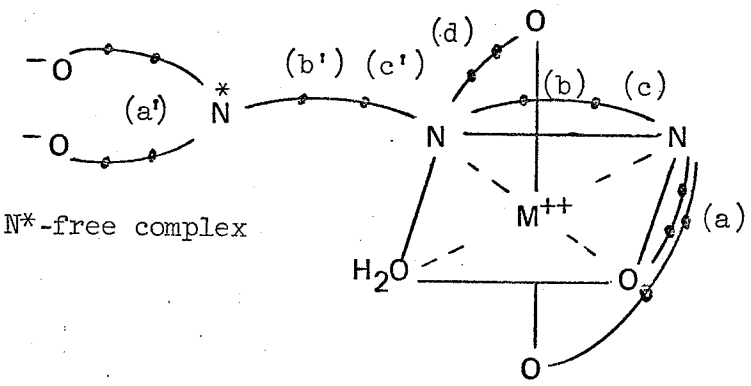

N*-free complex

STRUCTURE II

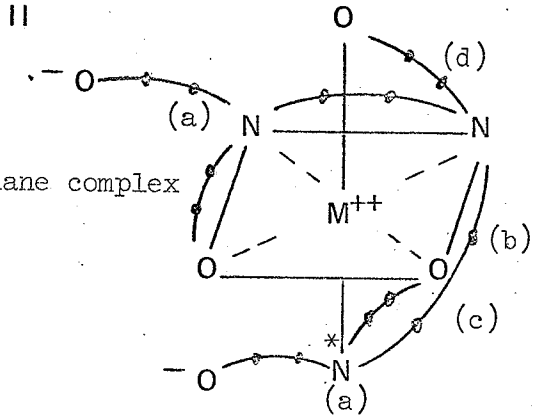

N*-out-of-plane complex

STRUCTURE III

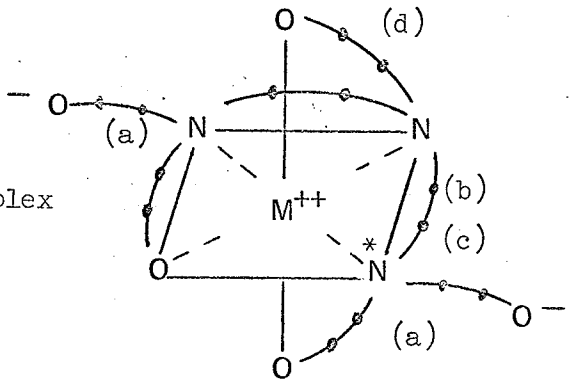

N*-in-plane complex

In Structure I one of the end nitrogen atoms with two accompanying acetate groups is free a large percentage of the time. One can readily imagine numerous isomers of Structure I that would yield similar NMR spectra. In all cases separate spectra would be expected for bound and free acetate or ethylenic protons. This behaviour was reported by Smith[62] for Co(III)-DTPA, where the in-plane and out-of-plane acetate groups were also identified from different NMR signals. The Cd-DTPA and Pb-DTPA spectra obtained in this investigation did not show different spectra for the terminal acetate protons at any given pH. Hence Structure I can be eliminated as a possible model, except for the case when the terminal nitrogen and carboxyl groups are rapidly bonding to and coming free from the metal ion. Even this possibility is only consistent with experimental evidence under acidic conditions ($pH < 5.0$) where only a singlet is observed for the a protons. Since these metal-DTPA complexes are quite labile at low pH no definite structure was assigned to them under those conditions.

In Structure II a terminal nitrogen atom is bonded to the metal ion out of plane with respect to the other two nitrogen-metal bonds. Stereo-models show a plane of symmetry through the metal ion-center nitrogen bond, which would indicate similar spectra for the a protons. This is consistent with the

NMR data obtained. However a Fischer-Hirchfelder metal-DTPA model reveals that Structure II is favored for large metal ions ($r > 1$ Å) and shows considerable strain and congestion for small ions ($r < .75$ Å). The ion radius of Pb^{++} is 1.20 Å and for Cd^{++} is 0.97 Å. Thus Structure II is a possibility except for considerable steric hinderance of the terminal acetate groups.

Structure III has all the nitrogen atoms bonded to the metal ion in one plane. Such a structure eliminates the steric hindrance of the end acetate groups. Stereo-models show that there is some strain on the chelate rings in the nitrogen-metal plane for large ions ($r > 1.10$ Å). Thus the information from stereo-models indicates that Cd^{++} would favor Structure III and Pb^{++} would have a slight preference for Structure II to eliminate the strain produced when all nitrogens bond in one plane. The stereo-models also show that for very large ions ($r > 1.30$ Å) both Structure II and III experience considerable strain in the chelate rings, and would be highly unlikely to exist as such.

CHAPTER 8

CONCLUSION

The polarograms and NMR spectra for the Cd-DTPA solutions were not as well defined as those for Pb-DTPA. This made the experimental measurements quite difficult and reduced the accuracy of these measurements as well, especially in the polarographic study. Inspection of table 28 reveals that the protonated CdH_xA stability constants range from $\log K^{H}_{CdHA} = 2.95$ to $\log K^{H}_{CdH_3A} = 2.73$. These values are somewhat unreasonable in that (on purely statistical grounds) one would expect that the probability of protonating a CdHA complex in successive steps should decrease by approximately 0.6 log K units (probability of 4 to 1). However the Pb-DTPA (table 28) stability constants were quite reasonable from this standpoint.

On examining the NMR spectra of both Cd-DTPA and Pb-DTPA solutions as a function of pH (Figures 35 and 37), one would conclude that the protonation of CdA began at pH = 4.5 and at pH = 5.5 for PbA. Thus an estimated $\log K^{H}_{CdHA}$ would be approximately 4.0 and $\log K^{H}_{PbHA}$ would be approximately 5.0. Chaberek's value [9] then for $\log K^{H}_{CdHA} = 4.17$ would seem to be a reasonable one, and Schwarzenbach's $\log K^{H}_{PbHA} = 4.52$ might seem somewhat low. However, the difference in concentrations and ionic strengths employed in the two independent studies (NMR and polarography) could account for the discrepancy. By comparison, our values of the Pb-DTPA protonated complexes (table 28) are also low, yet exhibiting a decrease in stability with each proton added to the complex. Our values for the stability constants of CdHA, CdH_2A and CdH_3A were low and failed to

show a marked decrease in the stability of the complexes upon successive protonation. Thus it was concluded that the polarographic technique was not the best technique available to study Cd-DTPA, but could be used with reasonable success for Pb-DTPA.

The NMR spectra pointed out that the protonation of the complexes occurred mainly at the basic nitrogen sites rather than on the carboxyl groups. Secondly, the Pb-DTPA complex seemed to be more labile than the Cd-DTPA complex, i.e. the Pb-DTPA spectra were sharper than the Cd-DTPA ones (NMR), and the Pb-DTPA complex unwrapped and reduced faster at the D.M.E. than the Cd-DTPA complex (polarography).

An interesting extention to the polarographic study would be to use a vibrating dropping mercury electrode (V.D.M.E.). Recently Cover and Connery [68] have demonstrated that a V.D.M.E. has certain advantages over the conventional D.M.E. since it can suppress maxima of the first and second kind without the addition of surfactants. Secondly, kinetic currents can be minimized or eliminated at the V.D.M.E. A natural extention to both the NMR and polarography would be to use TTHA and TPHA. These ligands, which were difficult to obtain in a pure state, have recently been prepared (apparently without difficulty) by Site and Baybarz [69] who used them to complex Am^{+3}. The higher homologs of EDTA (TTHA and TPHA) open up new areas of investigation in the co-ordination chemistry of metal-aminopolycarboxylic acid complexes.

BIBLIOGRAPHY

REFERENCES

1. Schwarzenbach, G. and Ackermann, H., Helv. Chim, Acta 30 1798 (1947)

2. Welcher, F., J., The Analytical Uses of Ethylenediaminetetraacetic Acid, Van Nostrand New York, 1957.

3. Pribil, R., Chelometry - Basic Determination Chemapol, Prague, Czech. (1961).

4. Flaschka, H.A., EDTA Titrations 2nd Ed. Pergamon Press (1964).

5. Schwarzenbach, G., Complexiometric Titrations Methuen & Co. Ltd., London 1957).

6. Wänninen, E. Svomen Kemistilehti B. 28 146 (1955).

7. Durham, E.J. Ryskiewich, D.P., J. Am. Chem. Soc. 80 4812 (1958).

8. Frost, A.E., Nature 178 322 (1956).

9. Chaberek, S. Frost, A.E., Doran, M.A., Bicknell, N.J., J. of Inorg. and Nucl. Chem. II 184 (1959).

10. Chaberek, S., and Harder, R., ibid 11 197 (1959)

11. Chaberek, S., Vandegaer, J., and Frost, A.E., ibid 11 210 (1959).

12. Přibil, R. and Veselý, V., Talanta 9 939 (1962).

13. Bailer, J.C. Jr., and Sievers, R.E., Inorg. Chem. 1 174 (1962).

14. Grimes, J.H., Huggard, A.J., and Wilford, S.P., J. Inorg. Nucl. Chem. 25 1225 (1963).

15. Martell, A.E., and Bohigan T.A., Inorg. Chem. 4 1264 (1965).

16. Catch, A., and Jordan, S., Experentia 17 205 (1961).

17. Koryta, J. and Koessler, I., Coll. Czech. Chem. Comm. 15 241 (1950).

18. Pecsok, R. J., Chem. Educ. 29 597 (1952).

19. Heyrovsky, J. and Matyas, M., Coll Czech. Chem. Comm. 16 455 (1951).

20. Tanaka, N., Oiwa, I.T. and Kodama, M., Anal. Chem. 28 1555 (1956).

21. Schmid, R.W. and Reilley, C.N., J. Am. Chem. Soc. 80 2101 (1958).

22. Conradi, G., Kopanica, M., and Koryta, J. Coll. Czech. Chem. Comm. 30 2029 (1965).

23. Heyrovsky, J. and Kůta, J., Principles of Polarography, Academic Press, New York p. 24 (1966).

24. Meites, L., Polarographic Techniques, 2nd Ed. Interscience Pub. Inc. p. 321 (1965).

25. Lingane, J.J., Electroanalytical Chemistry, 2nd Ed., Interscience Pub. Inc. New York (1958).

26. Kolthoff, I.M. and Lingane, J.J., Polarography, 2nd Ed. Vol. I, II, Interscience Pub. Inc. N.Y. (1952).

27. Zuman, P. and Kolthoff, I.M., Progress in Polarography, Vol. I, II, Interscience Pub. Inc. New York (1962).

28. Milner, G.W.C., The Principles and Applications of Polarography and other Electroanalytical Processes, Longmans London (1957).

29. Müller, O.H., The Polarographic Method of Analysis, 2nd Ed., Chem. Ed. Pub. Co. Easton Pa. (1951).

30. Longmuir, I.S., editor Advances in Polarography, Vol. I, II, III Pergamon Press, N.Y. (1960).

31. Delahay, P., New Instrumental Methods in Electrochemistry, Interscience Pub. Inc. New York (1954).

32. Ilkovic, D., Coll. Czech. Chem. Comm. 6 498 (1934).

33. Antweiler, H.J., Z. Electrochem. 44 719, 831, 888 (1938).

34. Lingane, J.J., Loveridge, B.A., J. Am. Chem. Soc. 72 438 (1950).

35. Strehlov, H. and von Stackelberg, M., Z. Electrochem. 54 51 (1950).

36. Reilley, C.M., editor Advances in Analytical Chemistry and Instrumentation, Vol. I 241-292 (1960).

37. Markowitz, J.M., and Elving, P.J., Chem. Revs. 58 1047 (1957).

38. Meites, J. and Meites, T., J. Am. Chem. Soc., 73 395, 1581 (1951).

39. Hume, D.M., and Deford, D.D., J. Am. Chem. Soc. 73 5321 (1951).

40. Delahay, P., and Tobias, C.W. editors Advances in Electrochemistry and Electrochemical Engineering Vol. 6 289-327 (1967).

41. Schmid, R.W., and Reilley, C.N., J. Am. Chem. Soc. 80 2087, 2101 (1958).

42. Koike, Y. and Hamaguchi, H.J., Inorg. Nucl. Chem. 29 473 (1967).

43. Wiesner, K., Z. Elektrochem. 49 164 (1943).

44. Brdička, R., and Wiesner, K., Coll. Szech. Chem. Comm. 12 139 (1947).

45. Koutecky, J., Coll. Czech. Chem. Comm. 18 11 (1953).

46. " " " " " " 183 (1953).

47. " " " " " " 311 (1953).

48. " " " " " " 597 (1953).

49. Cotton, F.A., editor Progress in Inorganic Chemistry Interscience Pub., N. Y. 211-384 (1963).

50. Koryta, J., Coll. Czech. Chem. Comm. 24 3057 (1959).

51. Pople, J.A., Schneider, W.G. and Bernstein, H.J., High Resolution Nuclear Magnetic Resonance McGraw-Hill New York (1959).

52. Roberts, J.D., Nuclear Magnetic Resonance Applications to Organic Chemistry McGraw-Hill, New York (1959).

53. Bible, R.H., Interpretation of NMR Spectra, Plenum Press, New York (1965).

54. Emsley, J.W., Feeney, J. and Sutcliffe, L.H., High Resolution Nuclear Magnetic Resonance Spectroscopy Vols. I and II, Pergamon Press, New York (1965).

55. Aleksndrov, I.V., The Theory of Nuclear Magnetic Resonance Academic Press, New York (1966).

56. Anderson, W.A., NMR and EPR Spectroscopy, Pergamon Press, Oxford p. 162 (1960).

57. Reilley, C.N., Anal. Chem. 37 1298 (1965).

58. Sudmeier, J.L., Reilley, C.N., Anal. Chem. 36 1698 (1964).

59. " " , Inorganic Chem. 5 1047 (1966).

60. Day, R.J., Reilley, C.N., Anal. Chem. 36 1073 (1964).

61. Kula, R.J., Sawyer, D.T., Chan, S.I., Finley, C.M., J. Am. Chem. Soc. 85 2930 (1963).

62. Smith, B.B., Post-doctoral fellow at the U. of Man., Wpg., Canada (private communication).

63. Cotton, J.A. and Wilkinson, G., Advanced Inorganic Chemistry 2nd Ed. Interscience Pub. New York (1968).

64. Kirschner, S.,editor Advances in the Chemistry of the Coordination Compounds Macmillan, New York (1961).

65. Lewis, J. and Wilkins, R.G., editors Modern Coordination Chemistry Interscience New York (1960).

66. Basolo, J. and Pearson, R.G., Mechanisms of Inorganic Reactions 2nd Ed. John Wiley N.Y. (1968).

67. Martell, A.E. and Calvin, M., Chemistry of the Metal Chelate Compounds Prentice-Hall Inc., Englewood Cliffs, N.J. (1952).

68. Cover, R.E. and Connery, J.G., Anal. Chem. 41 918 (1969).

69. Site, A.D. and Baybarz, R.D., J. Inorg. Nucl. Chem. 31 2201 (1969).